

NASA TECHNICAL MEMORANDUM

(NASA-TM-78237) RESULTS OF CORONAL HOLE
RESEARCH: AN UPDATE (NASA) 96 P
HC A05/MF A01

N79-32146

CSCL 03B

G3/92 35776
Unclas

NASA TM 78237

RESULTS OF CORONAL HOLE RESEARCH: AN UPDATE

By Robert M. Wilson
Space Sciences Laboratory

July 1979



NASA

*George C. Marshall Space Flight Center
Marshall Space Flight Center, Alabama*

TABLE OF CONTENTS

	Page
INTRODUCTION.	1
DISCUSSION	2
Results from 1975	4
Results from 1976	5
Results from 1977	19
Results from 1978	41
Miscellaneous	58
REFERENCES	59
APPENDIX A.	85

RESULTS OF CORONAL HOLE RESEARCH: AN UPDATE

INTRODUCTION

In a previous report, Wilson [1] described the general features of coronal holes and presented an overview of scientific results, particularly for the period since 1970 (i.e., 1970-76). In the present report, Wilson continues his overview of reported findings dealing with coronal holes, thereby essentially updating the previous report to include the papers published from 1976-78. As before, the author has relied heavily on several primary journals; supplementing them with those articles contained in books, IAU symposia, etc., that were easily accessible. The main journals employed in this literature search include Solar Physics, Astrophysical Journal, Astronomy and Astrophysics, Journal of Geophysical Research, Astrophysical Journal Supplement Series, Astronomy and Astrophysics Supplement, and Bulletin of the American Astronomical Society. In addition, the author has incorporated articles found in The Solar Output and Its Variation (ed., O. R. White); Contributed Papers to the Study of Travelling Interplanetary Phenomena/1977 (Proceedings of COSPAR Symposium B, Tel Aviv, Israel, June 1977) (eds., M. A. Shea, D. F. Smart, and S. T. Wu); Study of Travelling Interplanetary Phenomena 1977 (Proceedings of the L. D. de Feiter Memorial Symposium held in Tel Aviv, Israel, June 7-10, 1977) (eds., M. A. Shea, D. F. Smart, and S. T. Wu), Astrophysics and Space Science Library, vol. 71; Proceedings of the November 7-10, 1977, OSO-8 Workshop (eds., E. Hansen and S. Schaffner); Physics of Solar Planetary Environments (Proceedings of the International Symposium on Solar-Terrestrial Physics) (ed., D. J. Williams); Basic Mechanisms of Solar Activity (eds., V. Bumba and J. Kleczek); Scientific Investigations on the Skylab Satellite (eds., M. I. Kent, E. Stuhlinger, and S. T. Wu), Progress in Astronautics and Aeronautics, vol. 48; Annual Review of Astronomy and Astrophysics (eds., G. R. Burbidge, D. Layzer, and J. G. Phillips); Solar Gamma-, X-, and EUV Radiation (ed., S. R. Kane); and Coronal Disturbances (ed., G. Newkirk, Jr.). Also, the author has drawn, where possible, from other scientific journals. The present overview contains annotated accounts of some 220 articles. To give the reader a complete record of those articles dealing with coronal holes which are summarized in the previous and present reports, the author includes as an Appendix a listing of the pertinent articles which were referenced in the previous report.

DISCUSSION

With the completion of the Skylab Solar Workshop on Coronal Holes and publication of its monograph [2], solar physicists gained new insight into the coronal hole phenomenon. We know that coronal holes are regions of abnormally low density and temperature in the solar corona, that they are most prominent in the two or three years just before sunspot minimum, that they are large-scale coronal regions with open magnetic-field lines, and that they are associated with recurrent high-speed streams in the solar wind and with geomagnetic storms on Earth. (Orrall [3] and Zirker [4,5] have provided current reviews of coronal hole physical properties, models, etc.). The succeeding pages recount the results of analyses by coronal hole solar physicists, in particular since 1976. As in the previous report, the results are presented chronologically; however, in this report they are also presented alphabetically (by author) within each year with the exception of those articles contained in Coronal Disturbances, Annual Review of Astronomy and Astrophysics, and Solar Gamma-, X-, and EUV Radiation.¹

In Coronal Disturbances (1974, ed. G. Newkirk, Jr., IAU Symp. No. 57, D. Reidel Publ. Co.), four articles appear which briefly discuss coronal holes. The first by Bumba and Šýkora [6] concerns large-scale magnetic structures responsible for coronal disturbances, and the authors establish the existence of one heliographic longitude which was associated with coronal holes and the positive polarity large-scale pattern. In a second paper, Tousey et al. [7] discuss preliminary results from the NRL instruments aboard Skylab, and they note that coronal holes can be discerned by their He II (304 Å) and He I (584 Å) emissions which also show that coronal holes extend well down into the chromosphere. A third paper by Pneuman [8] discusses the theoretical magnetic structure responsible for coronal disturbances; Pneuman addresses the association of recurrent, high-speed solar wind streams with coronal holes. In the fourth paper, Altschuler [9] takes a look at the observations relevant to magnetic structure responsible for coronal disturbances.

The first discussion of coronal holes in Annual Review of Astronomy and Astrophysics (Annual Reviews, Inc., Palo Alto, CA) appears to be one by Culhane and Acton [10], who summarize certain aspects of the X-ray solar spectrum. In their discussion, the authors briefly mention that coronal holes were first specifically identified on the basis of EUV spectroheliograms, that they are associated with weak unipolar magnetic regions having open field lines,

1. The author has combined two references [73,74] in the same paragraph, which then places reference [74] out of alphabetical order.

and that solar wind streams emanate from these features and, hence, their density and X-ray emission are reduced.

Another paper by Parker [11] concerns the origin of solar activity. In it he addresses the implications of solar activity, the origin, behavior and dissipation of the magnetic fields, magnetic buoyancy, twisted fluxtubes, and other particular topics. Concerning coronal holes, the author merely mentions the association of macrospicules and coronal holes and between coronal holes and weak-field regions.

A third paper by Withbroe and Noyes [12] discusses some results of investigations into the mass and energy flow in the solar chromosphere and corona. Concerning coronal holes, the authors point out that, in most spectral lines and continua, there is little difference in the appearance and intensity of the chromosphere observed in coronal holes and quiet regions. Also, a unique feature — macrospicules — appears solely associated with coronal holes. Coronal holes appear to be associated with weak-field magnetic structures that have an open diverging configuration, and there is strong evidence supporting the view that coronal holes are the major source of the solar wind, certainly the recurrent high-speed streams responsible for recurrent geomagnetic disturbances. The authors also present empirical and theoretical models for coronal holes.

A fourth paper by Howard [13] concerns large-scale solar magnetic fields. Related to coronal holes, the author notes that potential-field calculations based on Skylab-period observations show that a coronal hole is the locus of open-field lines. Additional remarks include that coronal holes appear to be the origin of high-speed solar wind streams and that they may be seen in X-ray observations, in many far ultraviolet lines, and in the 10830-Å line observations from the ground.

In the book *Solar Gamma-, X-, and EUV Radiation* (1975, ed. S. R. Kane, IAU Symp. No. 68, D. Reidel Publ. Co.), two articles appear which briefly discuss coronal holes. The first by Noyes et al. [14] gives preliminary results obtained by the Harvard College Observatory (HCO) EUV spectroheliometer aboard Skylab, and the authors note that coronal holes manifest themselves in all layers of the Sun's upper atmosphere. In the second paper by Golub et al. [15], while the intent of the paper is time variations of solar X-ray bright points, the authors show X-ray imagery containing a coronal hole. (A third paper by Glencross [16] discusses X-ray filaments and suggests that they may be formed by a mechanism similar to coronal holes.)

Results from 1975

Cavallini and Righini [17], based on observations obtained during the solar eclipse of 20 July 1963, have modeled a relatively cool coronal region. Their model explains the presence of abnormal Ca II H- and K-line emissions and the large amount of F corona present in the spectrum. A temperature of 10^5 K is deduced for this coronal hole area-like region.

Kanno and Tanaka [18] have considered three composite models of the chromosphere-corona transition region, taking account of the orientation of spicules. The three models include the spicule-sheath model, the hot plagette model, and the platelet region model. The authors show that a comparison of 3-cm and 21-cm observations with hypothetical predictions based on the first two aforementioned models, yield results which are incompatible; only the platelet model is in accord with observations. The authors note that, in the platelet model, the effective transition region corresponds to thin platelet media which are placed on the top of the chromosphere and scattered between the network boundaries below the spicules. The authors briefly discuss the limb darkening effects at centimeter and decimeter wavelengths in the vicinity of polar coronal holes.

Kopp et al. [19], using carefully chosen blocking filters to isolate broad regions of the faint continuous spectrum of spicules from their much stronger chromospheric line emissions, have observed chromospheric spicules near 4700 \AA during the solar eclipse of 30 June 1973. Analysis of these observations indicates that spicules may extend to substantially greater heights in the corona than one infers from filtergrams and spectra of only the stronger spicule emission lines. Further, their analysis indicates that the derived densities are in approximate agreement (perhaps slightly higher) with those found by others. The authors note that their data may contain some broadband emission features corresponding to the so-called "superspicules" (i.e., macrospicules) which are recorded in certain strong EUV lines and occur within the chromospheric boundaries of coronal holes, since the eclipse frames were positioned at one edge of a large coronal hole overlying the north solar pole.

Liebenberg et al. [20], using deconvolution techniques that preserve the line intensity versus wavelength profile-shape, have investigated the Fe XIV (5303 \AA) coronal green-line emission of the 30 May 1965 total solar eclipse. The authors determine that a west limb coronal enhancement has temperatures $< 3 \times 10^6$ K and turbulent velocities of $\sim 25 \text{ km s}^{-1}$, decreasing with altitude. The authors note that temperature gradients provide evidence for marginal solar wind flow from this enhancement and that, above the quiet photosphere

in the southwest quadrant, the comparison of line and continuum intensities and consideration of line width suggest that the coronal region is filled with inhomogeneous plasma, dense enough in localized regions to maintain collisional excitation. The authors interpret this region to be a coronal hole and suggest that coronal material is heated by the quiet photosphere below.

Straka et al. [21], using the 36.58-m Haystack antenna at 3.8 cm, have studied the left and right circularly polarized emission during a very quiet solar period (22-26 September 1974). The authors note the existence of two regions in the southern hemisphere of the Sun with brightness temperatures ~ 10 percent below the surrounding solar disk temperature. They show that one region was associated with a large filament, while the other had no $H\alpha$ or magnetic-field counterpart. The authors suggest that this second depression may be associated with a coronal hole.

Svalgaard et al. [22], using 454 sector boundary observations recorded at Mt. Wilson during the period 1959-73, study the synoptic appearance of solar magnetic sectors. The authors note that sector boundaries can be clearly identified at north-south running demarcation lines between regions of persistent magnetic polarity imbalances, where these regions extend up to about 35° latitude of both sides of the equator. Further, they note that these regions generally do not extend into the polar caps and that the polar cap boundary can be identified as an east-west demarcation line marking the poleward extent of the sectors. The authors determine the typical flux imbalance for a magnetic sector to be about 4×10^{21} Mx. Some discussion is given to the relation of ephemeral regions and coronal holes.

Results from 1976

Adams [23,24] has investigated the differential rotation aspects of the photospheric magnetic fields underlying coronal holes. He performs his study by measuring the daily positions of filaments and plages surrounding a large coronal hole that lasted for several disk passages and comparing their rotational rates with that of the coronal hole. He notes that the resulting differential rotation curve was considerably flatter than the standard curve for long-lived filaments and was in remarkably good agreement with the curve found for the overlying coronal hole itself.

Akasofu [25] has reviewed the solar cycle and its many manifestations. Regarding coronal holes, the author notes that coronal holes are associated with high-speed solar wind streams and represent the source region for the

recurrent geomagnetic storms. He also discusses cosmic ray modulation, solar cycle effects on the outer planets and the terrestrial atmosphere. He further notes that recent intensive studies of magnetospheric substorms have revealed that geomagnetic activity is controlled by the north-south component of the interplanetary magnetic field, which modulates the efficiency of the solar wind-magnetosphere dynamo.

Axford [26] has briefly reviewed the basic aspects of mass and energy transport in the solar corona, solar wind and the Earth's magnetosphere. The author notes that the corona may be divided into regions of closed and open magnetic fields, where open magnetic regions occupy ~16 percent of the solar surface. He also addresses the question whether the characteristics of coronal holes are the result of reduced coronal temperatures and/or densities in the lower corona.

Bame et al. [27], based on solar wind observations from Mariner 2, Vela 2-6, Pioneer 6 and 7, and IMP 6-8, have found large-amplitude, high-speed solar wind streams and streams with maximum speeds in excess of 700 km s^{-1} are far more common in years of declining and minimum solar activity than near solar maximum. Further, they find that the broadest solar wind streams observed during 1962-74 occurred near solar minimum in 1974. They report that changes in the frequency and nature of solar wind stream structures at the orbit of Earth appear to be directly related to the long-term evolution of regions of low density (coronal holes) in the solar corona.

Beckers [28] has reviewed the topic "magnetic fields in the solar atmosphere." Concerning coronal holes, the author points out their near-rigid rotation characteristic, their apparent association with high-speed streams in the solar wind, their magnetic field being open to the interplanetary medium, their emissivity being very low, and their relation to geomagnetic M regions.

Behannon [29] has summarized Mariner 10 interplanetary magnetic-field results, especially for the period November 1973 through March 1974 and for heliocentric distances between 0.46 and 1.0 AU. The author reports that large variations in the field due to the effects of high-speed streams and stream-stream interactions were observed. Further, he notes that Mariner 10 results suggest roughly constant relative magnitude fluctuation levels on average between 1.0 and 0.46 AU and perhaps a weak decrease in transverse fluctuations with increasing heliocentric distance. Additionally, a close correspondence is reported by the author between the magnetic-field stream signatures and persistent but evolving coronal hole regions on the Sun. Also, he notes that a clear pattern of large southward fields in stream interaction regions and high levels of field fluctuations within the high-speed streams were seen.

Bell and Noci [30] have determined, by the method of superposed epochs, the average solar wind velocity (from Pioneer 6 and 9) and the level of geomagnetic activity (Kp) following central meridian passage of coronal weak (coronal holes) and bright features (active regions) identified from OSO 7 isophotes of Fe XV (284 Å) for the period 29 April 1972 through 30 August 1973. They report that their results are consistent with the concept that bright regions possess magnetic fields of closed configuration, thereby reducing particle escape, while coronal holes possess open magnetic-field lines favorable to particle escape or enhanced outflow of the solar wind. The authors note that coronal holes are identified with Bartel's M regions, not only statistically, but by linking specific long-lived holes with individual sequences of geomagnetic storms. In the study of bright regions, the authors find a subdivision by radio brightness temperature (9.1 cm radiation) to be significant, with regions of higher brightness temperature having a stronger inhibiting power on the outflow of the solar wind when the regions were located in the solar hemisphere on the same side of the solar equator as the Earth. They also note that regions of highest brightness temperature most strongly depress the outflow of solar wind but are also the most likely to produce flare-associated great storms.

Bohlin [31] has reviewed the physical properties of coronal holes. The author notes that, with the exception of the lines from helium, the photosphere and the low chromosphere do not show distinct evidence that a large-scale depression of coronal temperature and density may lie overhead. The author also discusses three other basic phenomena of holes: macrospicules, Ne VII (465 Å) limb brightening, and polar plumes. He addresses the evolution of coronal holes, stressing areas covered by holes (~20 percent of the Skylab-period Sun was covered by holes; ~15 percent contained at the poles), lifetimes (all but two Skylab-period holes had lifetimes in excess of 3 solar rotations), and differential rotation (coronal holes appear to be near-rigid rotators). He also examines the association of coronal holes to other solar phenomena; e.g., large-scale magnetic fields (coronal holes occur only within large, unipolar cells; holes only form in cells that have the same polarity as the polar caps in the same hemisphere; and there exists a generally well-defined "boundary zone" between the edges of a coronal hole and the adjacent neutral lines of the magnetic cell in which it lies) and disk activity and origin of holes (i.e., holes develop as a consequence of the emergence of disk activity).

Bridge [32] has briefly reviewed the present experimental evidence for changes in the properties of the solar wind during solar cycle 20. The author notes that it is evident that the average properties of the solar wind do not show large changes during the cycle, although there are significant changes of the order of 25 percent in the speed and, perhaps, similar changes in the number

density and flux density. Further, he points out the association of recurrent, high-speed solar wind streams with coronal holes.

Chiuderi-Drago and Noci [33], following the hypotheses of constant pressure and conductive flux in the transition region and of constant temperature and hydrostatic equilibrium in the corona, have derived simple formulae yielding radio brightness temperature. Using three solar minimum, radio-brightness temperature observations, they deduce a model of the transition region and corona which results in parameters that are similar to coronal holes. Thus, the radio quiet Sun (solar minimum condition) can be better identified with coronal holes than with UV quiet corona.

Cushman and Rense [34, 35] (see also Cushman et al. [36]), based on a study of the solar spectrum in the range 200–700 Å which was photographed with a rocket grazing-incidence spectrograph on 30 August 1972, have investigated the Doppler shifts of the three coronal lines Si XI (303 Å), Mg X (610 Å), and Mg IX (368 Å) for a coronal hole. From the relative shifts of the three lines, the authors deduce an average outward flow velocity of 16 km s^{-1} for the plasma in the coronal hole. They also note that the FWHM for each of the three lines was appreciably less in the coronal hole than in a quiet region, indicating a lower temperature in the hole.

Doschek et al. [37] have investigated the emission-line spectrum above the limb of the quiet Sun in the wavelength band of 1175–1940 Å on 27 August 1973. The authors note that the slit of their instrument at 12 arcs inside the limb was partially within a coronal hole. They present relative line intensities and line profiles as a function of height above the limb. They also deduce random mass-motion velocities, and they show a wavelength list with identifications for the spectrum obtained at 4 arcs above the white-light limb.

Dürst [38] has investigated the polarigraphic observations of the 7 March 1970 eclipse. In particular, he has analyzed the coronal hole which was located in the southwest quadrant, explaining the low intensity and polarization by a hole with an extent in longitude between 1 and 2 times its extent in latitude and with a minimum electron density between 0 and 0.3 of that outside the hole.

Feldman et al. [39] have investigated the emission-line spectrum (1175–1940 Å) above the limb of the north polar coronal hole on 14 August 1973. They present relative line intensities and line profiles, and they compare coronal hole line intensities with corresponding intensities obtained from quiet-Sun spectra. Likewise, they deduce random mass-motion velocities from the coronal hole lines and compare them with those deduced from quiet-Sun spectra.

Feldman et al. [40], based on Skylab NRL spectrograph observations recorded on 13 August 1973, have discussed spectra between 1200 and 1560 Å of a supergranulation cell interior and cell boundary. They give absolute intensities for selected lines of chromospheric and transition-region ions, including C II (1334, 1335 Å), C IV (1548 Å), N V (1239 Å), O I (1356 Å), O IV (1401 Å), Si II (1304 Å), Si III (1207 Å), Si IV (1394 Å), and S I (1473 Å). They find the width of the cell boundary to be ~10 arcs in lines of low-temperature ions and ~6 arcs in lines of high-temperature ions. They note that the brightness contrast between cell interior and boundary is an increasing function of the characteristics emitting temperature of the observed lines between $\sim 8 \times 10^3$ K and 1.3×10^6 K, with the maximum contrast being observed in O IV (about a factor of 5). The contrast, above and below the temperature of O IV, falls and is about 1.5 for lines of O I and S I. The FWHM of the optically-thin lines are the same over cell interiors and cell boundaries, and agree with the widths observed in limb spectra. The authors deduce, from the FWHM of the Si III line, optical depths at line center of 5.8 and 1.6 for the cell boundary and cell interior, respectively. Also, they determine that the electron density in the cell boundary appears to be nearly equal to the cell interior density, and, from the intensities of the O IV intersystem lines measured above the quiet-Sun limb, they deduce an electron density of $4.6 \times 10^9 \text{ cm}^{-3}$, a density that does not change within the first 8000 km above the limb and which is about a factor of 1.6 lower in the north solar, polar coronal hole. Furthermore, they deduce, assuming a constant pressure, that the characteristic height of the Si III emitting region is ~840 km in the boundary and ~380 km in the cell interior.

On the basis of mass, momentum and energy, Flower and Pineau des Forêts [41] have computed spherically symmetric models of the solar transition region and corona. They suppose heating to be caused by the periodic passage of shock waves and include conduction and radiation in their computations (terms relating to shock wave dissipation were neglected, as was the presence of magnetic field). They develop a boundary condition which they call "the choking condition," which ensures the continuity of the flow at the critical Mach number. (High Mach numbers were noted as being attainable, perhaps, in coronal holes, far above the limb.) Comparison to non-coronal hole EUV-line observations is found to be unsatisfactory.

Golub et al. [42] have reported observations of X-ray bright points (XBP) over a six-month interval in 1973 which show significant variations in both the number density of XBP as a function of heliographic longitude and in the full-Sun average number of XBP from one rotation to the next. The authors note that the observed increases in XBP emergence are estimated to be equivalent to several large active regions per day for several months. They also note

that the number of XBP emerging at high latitudes varies in phase with the low-latitude variation and reaches a maximum approximately simultaneous with a major outbreak of active regions. Further, the authors report that the quantity of magnetic flux emerging in the form of XBP at high latitudes alone is estimated to be as large as the contribution from all active regions. Concerning coronal holes, the authors note that the visibility of XBP in coronal holes on long exposure images is much higher than that of XBP against background structures.

Golub et al. [43] have measured the lifetimes of all compact emission features visible on the Skylab AS&E X-ray images. Based on a study of 300 XBP, they determine the time rate of change of the number of XBP visible at any one time. The authors note that the spectrum of lifetimes is found to be heavily weighted toward short lifetimes, with the number of features present on the disk which live 2-48 h being at least ten times as great as the number living more than 48 h. The authors report that a four-parameter function is necessary to fit the data. They show that features living two days or less have a very broad latitude distribution, whereas nearly all longer-lived versus short-lived points are the same to within ~ 20 percent, with the major difference being that long-lived points continue to grow and generally reach larger sizes. The authors note that the mean lifetime of XBP in coronal holes is found to be consistent with that of the XBP observed on the entire solar disk.

Holzer [44] has reviewed the current (as of 1976) state of quantitative understanding of the coronal expansion. He emphasizes the problem of supplying the mass and energy fluxes observed in high-speed solar wind streams from the low-density, rapidly diverging coronal hole regions. Also, he indicates future directions for theoretical research on this problem.

Kopp and Holzer [45] have explored the hydromagnetic properties of a steadily expanding corona for situations in which departures from spherically symmetric outflow are large (i.e., the geometrical cross-section of a given flow tube increases outward from the Sun faster than r^2 in some regions, where r is distance from the Sun). Assuming polytropic flow, the authors show that in certain cases the flow may contain more than one critical point, and they derive the criterion for determining which of these critical points is the correct one. Applying the theory to geometries which exhibit rapid spreading of the flow tubes in the inner corona, followed by more or less radial divergence at large distances (i.e., like coronal holes), the authors show that, if the initial divergence is sufficiently large, the outflow becomes supersonic at all greater heights in the corona. This feature strongly suggests that coronal hole regions differ from other open-field regions of the corona in that they are in a fast, low-density expansion state over much of their extent; i.e., they have low

values of electron density, yet large particle fluxes in their associated high-speed streams in the solar wind.

Kopp and Orrall [46] have developed a practical methodology for the calculation of numerical models of the solar corona, from the 3×10^5 K transition-region level to the 3 solar radii level for regions where the magnetic field is open (i.e., coronal holes). Their methodology takes into account radiative, conductive, and solar wind energy losses, and an analytic expression containing two adjustable parameters is used to approximate the coronal heating function. Using EUV-line intensities, electron densities in the middle corona, and solar wind observations, they compute appropriate values for the model boundary conditions and heat input and then derive temperature and density distributions for the quiet Sun and a coronal hole. The typical coronal hole is observed to be slightly cooler than, and less than half as dense as, the background corona. The temperature gradient in the coronal hole transition region is a factor of 5 less than that for the quiet Sun. They note that less than one-fourth of the mechanical energy which heats the quiet corona is required to maintain a coronal hole, and that in the coronal hole, this reduced energy flux is dissipated over a region more than twice as broad as in the quiet Sun, resulting in a temperature distribution which peaks much more sharply and at a lower height in quiet coronal regions than in coronal holes.

Koutchmy and Stellmacher [47] have performed a photometric and colorimetric analysis of a color picture of the very inner solar corona near the south pole region, obtained during the total solar eclipse of 30 June 1973. They report the existence of coronal spikes and deduce a halfwidth of 1.67 arcs and an electron density of 10^{10} cm^{-3} . They discuss the possibility that the spikes may be associated with a "disappearing coronal hole." The authors note that their observations support the concept of a "striated" corona.

Kundu and Liu [48] have investigated coronal holes at radio wavelengths. They note the presence of a coronal hole on 24 November 1970 observed at 85 GHz (3.5 mm). The authors report the mm counterpart of the coronal hole to be much weaker and less widespread than observed in X rays. The brightness temperature inside the hole is reported by the authors to be, in most places, about 100-200 K lower than the mean brightness temperature of the Sun at 85 GHz.

Levy [49], based on a study of the so-called "20-year wave" in the diurnal variation of energetic cosmic rays, has proposed that it is a consequence of the likely average odd symmetry of the interplanetary magnetic field about the solar equatorial plane. Assuming that the magnetic field in each hemisphere

of the solar magnetic cavity has the same average sense as the polar magnetic field at the corresponding solar pole and by considering the motion of energetic particles near the average plane of symmetry, the author finds that the direction, period, and phase of the 20-year wave in the diurnal anisotropy are implied, implications which agree with the observed variation of the diurnal anisotropy over a period of the full solar magnetic cycle. The author then gives a simplified, analytic computational model of the proposed mechanism and uses it to calculate some further properties of the wave; e.g., he calculates the energy dependence of the anisotropy and finds that it agrees with observations.

Liu and Kundu [50], using 8.6-mm La Posta radiospectroheliogram data, have studied the rotation of the solar atmosphere during the period 6-30 March 1972. The authors observe regions both in emission and absorption. They note that the rotational rate is larger for absorption regions than for emission regions at all latitudes and shows smaller differential rotation. The authors attribute this apparent difference to the difference in height of formation of the emission and absorption regions. The authors also compare their results with those based on sunspots, photospheric magnetic field, K-corona, EUV emission, $H\alpha$ filament, Ca II K-line emission, spectroscopic velocity in the photosphere, and coronal holes.

McIntosh [51] has derived an empirical model for the origin and evolution of coronal holes, based on OSO-7 Fe XV (284 Å) images, Skylab coronal hole data, and an atlas of $H\alpha$ synoptic charts covering 1972-73. He notes that coronal holes first form within especially large, unipolar magnetic cells centered near the solar equator, at a time just prior to that cell merging with a low-latitude extension of one of the polar regions. The author notes that the polarity of the polar region represents a gap in the polar-crown filament, the highest latitude magnetic neutral line. Further, the author finds that the differing rates of rotation for the equatorial cells and the polar-crown gaps cause a sequential realignment of the polar-crown gap with equatorial cells and that there is motion of the pole-equator connection toward the east, from one equatorial cell to the next. The author reports that there were only four such large equatorial cells of like-polarity during 1972-73, where in each of these four north pole-to-equator unipolar zones a coronal hole formed east of a previous hole within the next cell, forming just prior to the demise of the previous coronal hole.

McIntosh et al. [52] have compared daily maps of magnetic neutral lines derived from $H\alpha$ observations with solar X-ray images for the period 15-30 June 1973 (Carrington rotation 1602). The authors note that nearly all X-ray-emitting structures consist of systems of arches covering chromospheric

neutral lines. Areas of low emissivity (coronal holes) appear as the areas between arcades of arches. Thus, the presence of a coronal hole is determined by the spacing between neutral lines and the scale of the arches over those neutral lines. X-ray emissivity on the solar disk extends from neutral lines in proportion to the vertical and horizontal scale of the arches over those neutral lines. The authors note that increasing scale of arches corresponds with increasing age of magnetic fields associated with the neutral line, and that all X-ray filament cavities coincided with neutral lines, but filaments appeared under cavities for only part of their length and for only a fraction of the disk passage.

Montgomery [53] has reviewed results of outward going spacecraft, especially Pioneer 10 and 11, concerning solar wind observations throughout the solar system. His review emphasizes a comparison of spacecraft results with predictions of models and he uses this comparison as a basis for the discussion of those physical processes that appear to be important. About coronal holes, the author notes that the coronal hole is the source of the long-lived, well-developed streams of the 1973-75 period, and that coronal holes show divergent fields.

Neupert [54] has examined the evolution of coronal holes based on synoptic observations of Fe XV (284 \AA) emission from OSO 7. The author states that his compilation of 1972 synoptic maps conveniently shows the evolution of large-scale features with time. He notes that during this period new active regions frequently appeared within coronal holes at sunspot latitudes with the consequence that the remnant hole either shifted in solar longitude or was restricted to higher solar latitudes. Thus, the author concludes that frequent emergence of such activity within holes may serve to disrupt patterns of recurrent solar wind streams, which then become more evident as solar activity subsides.

Nolte et al. [55], based on Skylab AS&E X-ray observations, have compiled an atlas of coronal hole boundary positions for the period 28 May-21 November 1973. The authors present the data as tracings of the soft X-ray boundaries as they appeared when the holes were near central meridian. They identify six coronal holes, denoted CH1-6.

Nolte et al. [56] have investigated the association of high-speed solar wind with coronal holes during the Skylab mission by direct comparison of solar wind and coronal X-ray data, comparison of near-equatorial coronal hole area with maximum solar wind velocity in the associated streams, and examination of the correlation between solar and interplanetary magnetic polarities. The authors find that all large near-equatorial coronal holes seen during the Skylab

mission period were associated with high-velocity solar wind streams observed at 1 AU. This result is consistent with the hypotheses that coronal holes are open magnetic structures and that they are solar wind stream sources.

Öhman [57] has discussed the possible solar origin of submicron particles, based on the evidence of a red shift in the Fraunhofer lines of the F-component corona and the existence of a faint negative polarization of the F-component corona. The author suggests that the faint X-ray clouds which are sometimes found to surround point X-ray sources in coronal holes may be due to scattering by submicron particles.

Parker [58] has reviewed the outstanding puzzles still besetting solar physicists today. He lists these fundamental problems as (1) the convection and circulation in the ionization of the Sun; (2) the generation of magnetic fields; (3) the properties of the emerging fields, forming active regions; (4) the frequent solar eruptions; (5) the coronal hole and the high-speed wind streams, and the suppression of the coronal hole by magnetic fields; and (6) the complicated climatological effects of the solar luminosity and solar activity.

Pneuman [59] has examined the influence of coronal magnetic fields on the solar wind. He points out that the geometry of coronal magnetic fields has a profound effect on the temperature and density structure of the corona and interplanetary medium, as well as on the gross properties of the solar wind. The author notes that the identification of coronal holes as the source of recurrent high-speed streams, the observed heliographic latitude dependence of the solar wind speed and variations in the bulk properties of the solar wind can all be easily understood in terms of magnetic geometrical effects occurring in the solar corona. He discusses the basic physical mechanisms controlling this gas magnetic-field interaction and he describes a three-dimensional model of the solar atmosphere and interplanetary medium intended to interconnect observations of physical quantities in the inner corona with observations of solar wind at 1 AU. He also presents and compares quantitative calculations for a selected test period with observations.

Reeves [60] has investigated the EUV structure and intensity of the chromospheric network from quiet solar regions. He notes that the distribution of intensities within supergranulation cell interiors follows a near normal function, and that the intensities from the centers of supergranulation cells appear to be the same in both quiet regions and coronal holes, although the network is significantly different in the two types of regions. The author reports that the average halfwidth of the network elements was measured as 10 arcs, and was independent of the temperature of formation of the observing line for

$3.8 < \log T_e < 5.8$ (T_e is the electron temperature). Further, the author notes that the contrast between the network and the centers of cells is greatest for lines with $\log T_e \approx 5.2$, where the network contributes approximately 75 percent of the intensity of quiet solar regions. He also notes that the contrast and fractional intensity contributions decrease to higher and lower temperatures characteristic of the corona and chromosphere. Concerning coronal holes, the author reports that coronal holes are especially visible in the EUV lines of Mg X and Si XII.

Rhodes and Smith [61] have studied the large-scale gradient in the bulk solar wind velocity by means of data obtained from Mariner 5 and Explorers 33-35 during mid-1967, and interpret it as a heliographic latitude gradient. The authors note that data indicate the existence of a latitude gradient in the radial component of the solar wind velocity during 1964-67. During this epoch the gradient between 0° and 7.25° N heliographic latitude apparently varied between 10 and $15 \text{ km s}^{-1} \text{ deg}^{-1}$, and the authors note that this dependence on latitude has now been seen in all spacecraft data that they have investigated, including those of Vela 2-4. Additionally, the authors report reasonable agreement between this gradient derived from satellite data near the ecliptic plane and the gradient implied by the interplanetary scintillation (IPS) data, covering a much larger latitude range. They note that the IPS gradients appear to be at most a factor of 3 smaller than the spacecraft gradients, but are definitely nonzero. Thus, while there are several competing explanations of the spacecraft and IPS gradients (e.g., existence coronal holes) and while no one explanation is as yet sufficient, the authors note that the evidence favors the existence of a gradient at high, as well as at low, heliographic latitudes during at least some portions of the solar cycle.

Rickett et al. [62], using IPS observations to reveal the presence of corotating high-speed solar wind streams and Skylab XUV solar images to reveal coronal holes, have mapped streams of heliographic latitudes from $+40^\circ$ to -60° back to the vicinity of the Sun during the period mid-1973 to early-1974. They find some evidence that the high-speed streams are preferentially associated with coronal holes and that they can spread out from the hole boundaries up to about 20° in latitude. However the authors note that this association is not one to one; i.e., streams are observed which do not map back to coronal holes, and holes are observed which do not lie at the base of streams. The authors conclude that, to the extent that a statistical interpretation is possible, the association is not highly significant, but individual consideration of streams and holes suggests that the statistical result is biased against a strong correlation.

Roelof [63] has analyzed a variety of flare-associated and recurrent solar particle events by means of the technique of "mapping" the fluxes back

to the estimated high coronal longitude of the interplanetary-field line passing through the spacecraft. He reports clear associations in 1973 among energetic injection profiles, solar wind stream sources, and low-coronal magnetic structure. In particular, the author notes that the recurrent region around 0° longitude for Carrington rotations 1601-04 of helium-rich and enhanced medium nuclei is a coronal hole (CH1) which is associated with a solar wind stream.

Rosenbauer et al. [64] have presented preliminary results of the Helios Sunprobes. The authors describe the interplanetary "weather" as quiet during the period December 1974 to April 1975. They note the existence of two, very pronounced and steady fast streams with velocities ranging up to 800 km s^{-1} , each stream being associated with a coronal hole. The authors observe that changes of plasma velocity with solar longitude are more abrupt not only at the trailing edges but also at the front side of fast streams at smaller distances from the Sun.

Sheeley [65] has extended his original study of the numbers of faculae at the solar poles, during the period 1906-64, to include the period 1964-75. This information is used to estimate the strengths of the polar magnetic fields and, as the author notes, should be useful for coronal hole studies. The author finds that the polar fields are stronger now than they have been for a decade, with most of the strength increase occurring in 1973 for the south solar pole and gradually during 1972 and 1973 for the north solar pole. He also notes that, except for a relatively brief interval during 1959, the south polar field has been weaker during the last magnetic cycle than it has been during any cycle since 1906, the beginning of the Mt. Wilson observational record. A plot of sunspot number versus time is superposed on the faculae number versus time, and the author notes an apparent $\sim 90^\circ$ lag of solar polar fields with sunspot number, consistent with the hypothesis that the polar magnetic fields are produced by the transport of flux that originates in bipolar magnetic regions of the sunspot belts on the Sun.

Sheeley et al. [66] have compared observations of coronal holes, solar wind streams, and geomagnetic disturbances (C9 index) during 1973-76 by means of a 27-day pictorial format which shows their long-term evolution. They note that their results leave little doubt that coronal holes are related to the high-speed streams and their associated recurrent geomagnetic disturbances, that these observations strongly support the hypothesis that coronal holes are the origin of the high-speed streams observed in the solar wind near the ecliptic plane, and that coronal hole observations can be used to forecast the occurrence of solar wind streams and geomagnetic disturbances at the Earth (on the basis of 10830-Å observations).

Smerd [67] has reviewed radio observations of coronal phenomena and solar flares. Concerning radio "dark" regions or coronal holes, the author notes that at 80 and 160 MHz and 10.7 GHz, radio dark regions correspond in size, shape, and position with X-ray and EUV coronal holes. He also notes the existence of coronal holes in the 1420-MHz solar maps from Fleurs (Australia) and at 169 and 408 MHz from Nançay. Additional remarks, concerning the faster-than-radial field expansion and the inconsistency of EUV and radio modeling, are also given.

Sofue et al. [68] have observed Faraday rotation of linearly polarized radio waves from the Crab Nebula (Tau A) at 4170 MHz during solar coronal occultations in June 1971-75. The authors note that mean amplitudes of the variations of position angle are larger in an active phase of the solar cycle than in a quiet phase. Also, in occultations in 1971 and 1973, the position angle of the polarization varied oscillatory by 20-50 degrees due to local magnetic structures in the corona with a typical variation of position angle of polarization which is expected from a Y-shaped field configuration in coronal streamers. The authors remark that the Faraday rotation is enhanced when the line-of-sight to Tau A passes through strong coronal magnetic fields, while the rotation is suppressed when the line-of-sight passes through large coronal holes. Short-time oscillation of the rotation angle observed in 1971 and 1973 suggests that neutral sheets in coronal streams oscillate at a period of 3 hours with an amplitude of ~ 1 solar radius at a distance of ~ 10 solar radii from the Sun.

Stenflo [69] has examined the observed properties of small-scale magnetic fields. In his discussion, the author addresses rotation rates on the Sun. He notes that the angular velocity of the quiet-Sun magnetic fields is systematically higher than for active region fields, indicating that the quiet-Sun fields are related to layers deeper than those associated with active region fields. Thus, the quiet-Sun regions (including coronal holes) may be more directly linked to the subsurface sources, thereby, accounting for the apparent rigid-body rotation properties.

Stix [70] has explored the relationship of dynamo theory and the solar cycle. A part of his investigation deals with magnetic sectors and the existence of coronal holes.

Suess [71] has investigated latitudinal variations in the solar wind. He emphasizes an axisymmetric description to isolate those variations which are an imprint of coronal processes and those which are internally generated within the solar wind from the otherwise already understood variations associated with stream interaction between the Sun and 1 AU. He gives and discusses an example

of a large polar coronal hole to illustrate the physics of several important processes: directed meridional flow in the corona out to 5 solar radii, temperature and density characteristics in a coronal hole and beyond, temperature effects in the interplanetary medium, internally generated meridional flow in the interplanetary medium, and how one can see polar hole material in the ecliptic at 1 AU.

Svalgaard and Wilcox [72] have discussed the Hale solar sector boundary. They define a Hale sector boundary as the half (northern or southern hemisphere) of a sector boundary in which the change of sector magnetic-field polarity is the same as the change of polarity from a preceding spot to a following spot. The authors note that sectorial structures include magnetic sectors and, at least some, coronal holes. Above a Hale sector boundary, the green-line corona has maximum brightness, while above the non-Hale boundary the green-line corona has a minimum brightness. The Hale portion of a photospheric sector boundary tends to have maximum magnetic-field strength, while the non-Hale portion has minimum strength.

Tousey [73] has summarized initial results of the NRL XUV spectrographic instrument aboard Skylab, and Reeves et al. [74] have similarly described initial results of the HCO EUV spectroheliometer aboard Skylab. Both papers show coronal hole imagery and briefly discuss some of the first studies of those Skylab-obtained data.

Van Tend and Zwaan [75] have summarized published data on the mean sidereal rotation rates as a function of heliographic latitude. One particular finding is that coronal holes show very little change in rotation rate versus latitude, implying near-rigid rotation.

Wagner [76] has examined the rotational characteristics of coronal holes. The author finds, using an autocorrelation technique, that coronal holes show almost rigid rotation. At low latitudes during the period May 1972–October 1973, the author observes four orthogonal "inactive longitudes" which show coronal holes. He further notes that coronal hole rotation periods at high latitudes best compare with inferred interplanetary field rotation periods.

Wefer and Bleiweiss [77] have discussed observations of coronal hole-associated features at 2-cm and 8.6-mm wavelengths. The authors construct "differenced maps" which show deviations from the background and find examples of coronal hole-associated features which manifest themselves as enhancements.

Weisberg et al. [78], by measuring the dispersion of radio-frequency pulses from pulsar NP 0532 during the June 1973 occultation, have determined

the mean electron density of the solar corona. The authors report a redistribution of coronal density from 1969-70 levels, such that at 17 solar radii east and west of the Sun, integrated densities were 50 percent greater in 1971 than in 1969-70, and by 1973 the corresponding densities had increased a further 30 percent; but, at 5 solar radii south of the Sun, integrated densities in 1971 and 1973 had declined to approximately one-half its 1969-70 value. The authors note that model-fitting results suggest that the corona was even more concentrated toward the equator in 1973 than in 1971. Further, they report that in 1973 the equatorial electron number density at 10 solar radii was approximately the same as in previous years ($7500 \text{ electrons cm}^{-3}$), while the electron density at higher latitudes decreased. The authors state that the radial density gradient was less steep in 1973 than in 1971, and markedly less than in 1969-70, and the coronal multipath scattering delay, an index of coronal inhomogeneity, remained near its 1971 level, approximately one-tenth of the value in 1969-70. The authors suggest that a local density decrease and scattering increase observed on 12 June may correspond to a coronal hole-like structure.

Wibberenz [79] has reviewed the topic energetic particles throughout the solar system. In his review, instead of using coronal holes as the source for the M-region phenomenon, the author suggests that corotating events are due to interactions of the solar wind itself.

Wilcox [80] has reviewed the history of solar-terrestrial relations as deduced from spacecraft and geomagnetic data. He begins with a discussion of the observation of a white-light flare by Carrington on 1 September 1859 and moves on to a discussion of solar M regions by Bartels in 1932. He also reports the apparent association of M regions with coronal holes.

Results from 1977

Ahmad [81] has performed a two-dimensional Fourier analysis of the EUV chromospheric network and a coronal hole. He finds that the network shows no signs of regularity to the cellular structure and that the transform within coronal holes does not differ significantly from that outside them.

Ahmad and Withbroe [82] (see also Ahmad [83]), based on Skylab EUV Mg X (625 \AA) and O VI (1032 \AA) data, have investigated three polar plumes lying within the boundaries of a polar coronal hole. They report that the mean temperature of the plumes is about $1.1 \times 10^6 \text{ K}$ and that they have a small vertical temperature gradient. Further, they determine that densities within these plumes are consistent with white-light analyses, and the variation of density with height in the plumes is comparable to that expected for hydrostatic

equilibrium. The authors also note that polar plumes will be a source of solar wind if the magnetic-field lines are open. They determine that polar plumes contain about 15 percent of the mass in a typical polar hole and occupy about 10 percent of the volume.

Altschuler et al. [84], using high-resolution KPNO magnetograph measurements of the line-of-sight photospheric magnetic field, have performed an analysis of the photospheric and coronal magnetic-field distributions. The authors average the daily magnetograph measurements collected over a solar rotation onto a 180×360 synoptic grid of equal-area elements, and they determine a unique solution for the global magnetic field under the assumption that there are no electric currents above the photospheric level of measurement. Because the solution is in terms of an expansion in spherical harmonics to principal index $n = 90$, the authors note that the global photospheric magnetic-energy distribution can be analyzed in terms of contributions of different scale-size and geometric pattern. They construct different types of maps for the coronal magnetic field to show the strong field at different resolutions, to trace the field lines which open into interplanetary space and to locate their photospheric origins (e.g., coronal holes), and to map in detail coronal regions above (specified) limited photospheric areas.

Antonucci et al. [85] have examined the chromospheric rotational rate, based on Ca II K_3 -line observations during 1972-73, years of declining solar activity. The authors report that the time series of the daily chromospheric data detected at central meridian, relative to 30 consecutive latitude zones, are analyzed to determine the recurrence tendency due to the rotation of long-lived chromospheric features. They note that the computed rotation is independent of latitude, in agreement with the results obtained for the green-line corona during the years before sunspot minimum; namely, both chromospheric and coronal features, with lifetimes exceeding one solar rotation, are almost not affected by differential rotation before sunspot minimum.

Antonucci and Doderio [86] have detected a coronal rotation dependence on the solar cycle phase. Based on a study of the Fe XIV (5303 Å) green-line emission of the coronal rotation rate during 1970-74, they confirm that the differential rotation degree varies systematically through a solar cycle and that the corona rotates in an almost rigid manner before sunspot minimum. Further, they note that, during 1970-71, the differential rotation degree, characteristic of high solar activity periods is detected, while during 1972-74 a drastic decrease of the differential rotation degree occurs and the green-line corona rotates almost rigidly, as the coronal holes observed in the same period.

Axford [87] has reviewed the general structure of the interplanetary medium, especially in three-dimensions, with special emphasis being given to the solar wind, the interplanetary magnetic field, the modulation of galactic cosmic rays, and the propagation of energetic solar particles. In his review, he contrasts three different models: the completely open magnetic-field model, the two-component stationary model with open (coronal holes) and closed magnetic-field regions, and the three-component model of the solar magnetic field, containing long-lasting open and closed regions and regions which are open but connected to sources of strong photospheric fields rather than coronal holes and also transiently open and closed regions from which coronal plasma escapes.

Benz and Gold [88] have considered a corona in which diffusive separation of the atomic species can take place, leading to a two-stream solar wind model in which escaping proton flux is generated at each level, able to penetrate the overburden, and at the same time a lower energy collisional plasma partakes of an essentially hydrodynamic flow. The authors find that for low temperatures the solar wind hydrogen acceleration is more of an evaporative nature and, for higher temperatures ($T \gtrsim 1.2 \times 10^6$ K), it is more hydrodynamical. They note that the changeover from one extreme mechanism to the other would make it possible to temporarily change the solar wind He/H ratio by a very large amount. Further, the authors find that, even when the acceleration process is nearly hydrodynamical, proton evaporation leads to an enhanced proton energy flux (typically a factor of 4) which reduces the requirements for extended coronal heating that seem to be inherent to hydrodynamic models. The resulting proton thermal anisotropy then probably becomes unstable towards magnetosonic whistlers at about 10 solar radii, the stability perhaps being responsible for locking the different fluxes to each other and producing the common stream observed in interplanetary space. The authors note that, since low-density and temperature coronal holes are now believed to be a major source of solar wind outflow and since they appear to expand to higher coronal heights in a non-radial way, coronal holes (non-radial flows) will generally enhance the total evaporative escape from a region beyond that which the same sector would supply in the case of strict radial symmetry.

Bohlin [89] has compiled an atlas of disk boundaries of coronal holes for the Skylab mission period. Using this atlas, he finds their sizes, global distributions, differential rotation rates, growth/decay rates, and lifetimes. The author notes that the polar cap holes together covered ~ 15 percent of the Sun's total surface area, a number which remained surprisingly constant throughout Skylab despite the fact that each pole independently evolved in time,

and that lower latitude holes contributed another 2 to 5 percent. The author also confirms the anomalous differential rotation law that had been reported in the literature. Further, he determines the average growth/decay rate for coronal holes to be $1.5 \times 10^4 \text{ km}^2 \text{ s}^{-1}$, and that the lifetimes of lower latitude holes to regularly exceed 5 solar rotations, in good agreement with the lifetimes of recurrent geomagnetic storms.

Chiuderi-Drago et al. [90] have investigated the coronal hole observed on 31 May 1973 using EUV Fe XV (284 Å) line emission and radio observations (169 and 408 MHz). They report an unsuccessful attempt to deduce an homogeneous model of the hole from these observations, and, therefore, suggest the existence of inhomogeneities in both the EUV and radio data to account for the observation. Their model consists of hot ($2 \times 10^6 \text{ K}$) elements covering 10 percent of the hole surface surrounded by regions of colder gas ($8 \times 10^5 \text{ K}$).

Chiuderi-Drago and Poletto [91] have developed a dynamical, homogeneous model of coronal holes which considers a more than radially divergent magnetic field, constant temperature at coronal levels, and a constant ratio of the square of the pressure to the conductive flux in the transition region. Using radio observations of the brightness temperature at 80, 160, 169, and 408 MHz, they deduce the above ratio and the temperature and density at the base of the corona. They find that their model gives correct values of the EUV-line intensities arising from the transition region, but still yields computed values which for Mg X (625 Å), are lower by about one order of magnitude with observed values. Thus, it is still not possible to reproduce at the same time EUV and radio observations, assuming an hydrodynamic or hydrostatic atmosphere.

Covington [92] (see also, Covington [93]) has explored the 2800-MHz radio emission of the Sun. He finds that radio cool regions are associated with X-ray coronal holes and he derives lower envelopes which are similar to spotless Sun drift curves. He determines that the flux for CH1 with central meridian passage on 25 July 1973 is 66.5 s.f.u., a level which is identified as that observed during sunspot minimum by comparison with the flux of 67.2 observed in July 1964 and with the low daily values of 67.5 and 67.1 observed in April 1975 and January 1976. The author states that the ratio enhancement of the quiet Sun of 3.0 s.f.u. for the optically inactive hemisphere of 20 May 1974 suggests that the radio quiet Sun may vary during the sunspot cycle.

Cuperman [94] has reviewed a number of the theoretical contributions to solar wind research. Concerning coronal holes, the author addresses many of their known characteristics and the association of high-speed solar wind flows with high-latitude coronal holes. He recounts that coronal holes are regions

of greatly reduced X-ray, EUV and metric radio emission; that they are regions of low-density and/or temperature; that they occur in weak, open, diverging, unipolar magnetic-field regions; that polar coronal holes cover ~ 15 percent of the Sun while low-latitude coronal holes cover from 2 to 5 percent of the Sun's surface (in 1973); that coronal holes are associated with recurrent, high-speed solar wind streams; and that polytrope-model calculations show that the expansion speed in the corona is increased well-above and density is decreased well-below the values expected from the standard solar wind model with spherical symmetry.

Davis et al. [95] (see also, Davis and Golub [96]), based on two rocket flights (16 September and 17 November 1976), have determined from solar X-ray images the number of XBP observed on the disk and have compared these results with early results obtained during the Skylab mission. They find that the number of XBP observed in 1976 is more than a factor of 2 greater than that the number observed in 1973, and, since all other indicators of activity have decreased during this time interval, the cyclical variation of the short-lifetime end of the magnetic-flux emergence spectrum is out of phase with the solar cycle as defined by active regions or sunspots. The authors note that, since XBP in 1973 contributed more to the emerging magnetic flux than did active regions, the possibility exists that the total amount of emerging magnetic flux may be maximized at sunspot minimum.

Doschek and Feldman [97] have compared the intensities and widths of several EUV forbidden-lines (e.g., Si VIII/1446 Å, Fe X/1463 Å, Fe XI/1467 Å, and Fe XII/1242, 1349 Å) observed above the limb ($\lesssim 30$ arcs) over a quiet-Sun region, a coronal hole, and two active regions. The authors note that the higher temperature ($> 10^6$ K) iron lines are not observed in the coronal hole spectra, indicating that in the coronal hole most of the plasma is at a temperature of less than 10^6 K. The authors also derive emission measures and column densities of the lines and report nonthermal velocities in the coronal hole and quiet-Sun regions to be 20 km s^{-1} , with velocities in the active regions being substantially less.

Doschek and Feldman [98] have discussed the limb-brightening curves and line profiles that originate from the first and second excited configurations in certain ions formed in the solar transition region. They show that the intensity behavior and line profiles cannot be explained under the assumption of that the lines are formed in a common plasma region, thereby supporting the view that model atmospheres must be folded into, especially the CIII (1909 Å and 1176 Å) calculations for proper interpretation of the data. In their discussion, they consider a quiet-Sun region and the north-solar, polar coronal hole.

Duggal and Pomerantz [99] have studied cosmic ray intensity variations in an attempt to identify the solar source of the modulation. They note that, while solar flares have previously been regarded as the predominant source of the modulation, their analysis indicates that the majority of transient intensity variations of galactic cosmic rays are related to the passage of active centers and cannot be assigned directly to specific solar flares. Superposed epoch analysis (Chree analysis) of the cosmic ray data with respect to the time of occurrence (zero day) of 379 solar flares of importance ($\text{Imp} \geq 2$) that occurred during solar cycle 20 (1964-74) shows that the onset of a decrease in the composite nucleonic intensity at polar stations occurs prior to the zero day, well before the arrival in the vicinity of Earth of the associated solar plasma. The authors note that the statistical significance of this result is confirmed by comparing the pooled variance determined from Chree analysis of an equal number of random epochs with that of the curve representing the flare epochs. Subdivision of the flare epoch curve into three groups, according to the heliographic longitude of the flares, shows that, whereas eastern flares might be associated with cosmic ray decreases, central ($+30^\circ$ to -30°) and western flares cannot be thus related. The authors also perform a similar analysis of all flares of $\text{Imp} \geq 2$ that occurred in a selected set of 24 extraordinary flare-rich active centers and confirm these results and show that the observed cosmic ray intensity decrease (Forbush decrease) is, in fact, associated with the central meridian passage (± 1 day) of the active regions. The specific feature associated with solar active centers that is actually the principal source of transient modulations (recently assumed to be coronal holes adjacent to active regions) remains to be identified.

Dulk [100] has examined implications on the structure of the transition region and corona from radio observations. He notes that the implication of the radio data (80 MHz, 160 MHz, and 1.42 GHz) conflict with the implications of EUV data (O VI 1032/1032 Å and Mg X/625 Å), with the radio data implying considerably lower densities and/or lower temperatures than the EUV data. Furthermore, the author finds that models incorporating thermal diffusion, mass flow, and ionization nonequilibrium indicate that thermal diffusion can be a major process, resulting in substantial increases in the abundances of heavy elements at some heights. The author suggests that a different compositional variation and lower density of the transition region and corona (by 5 to 10 times) can account for the discrepancy between the EUV and radio data.

Dulk et al. [101] have compared EUV and radio observations and results of analysis of a coronal hole (CH1) and nearby quiet regions made during July and August 1973. Attempts to derive the density and temperature distributions in the transition region and inner corona from the combined observations yield

the conclusion that no single standard model can explain both sets of observations; i. e., models based on the EUV data yield higher radio brightnesses than are observed, while models based on radio data yield lower EUV line intensities than are observed. The authors note that this discrepancy is essentially that the electron density inferred from the EUV data is about three times that inferred from the radio data. Further, they suggest that the discrepancy would disappear if the abundances of the heavier elements were increased by a factor of ~ 10 . The authors note that such increases could result from differential diffusion in the large temperature gradient of the transition region, and suggest that models which incorporate thermal diffusion, as well as mass outflow and departures from ionization equilibrium, offer the greatest hope of reconciling the EUV and radio coronal hole observations.

Feldman and Doschek [102], from the Stark broadening of hydrogen, Balmer emission lines at 2 arcs above the limb, have determined the electron densities over three active regions: McMath 12357, 12474 and 12488; and they have compared the active region results with those obtained for the quiet Sun and a coronal hole. For all three active regions, the authors find an electron density of $2 \times 10^{11} \text{ cm}^{-3}$ (error < 15 percent), and they note that the temperature of the hydrogen plasma in all of the quiet and active regions is no more than about 8000 K. The authors find that the intensity decrease of the hydrogen lines is the same as the intensity falloff of the O I intersystem lines, and they derive nonthermal velocities of the hydrogen lines over the active region (2 arcs above limb) to range from 0 km s^{-1} to about 15 km s^{-1} . Finally, they note that the lines of high members of the Balmer series are in Boltzmann equilibrium, and they compare their previous and present findings with observations of spicules.

Feldman et al. [103] have reviewed the present knowledge (as of 1977) of the interplanetary plasma and magnetic field at 1 AU. They devote a great deal of discussion to the solar wind, in particular high-speed solar wind. Concerning coronal holes, they note that high-speed streams of solar wind originate in coronal holes and that, since the polar regions are nearly always covered by coronal holes, it may be expected that on the average, the global flow pattern should converge towards, rather than diverge from, the equatorial regions. Also, they note that during 1972-73, the observed solar wind sector structure had its origin in alternate polar cap regions of the Sun.

Francis and Roussel-Dupré [104] have investigated the Si IV (1393 \AA) line emission, formed in the transition region at about $8 \times 10^4 \text{ K}$, in a coronal hole. They report that their results indicate that the line width is somewhat greater (~ 14 percent) in coronal holes compared to the quiet Sun, implying a difference in the broadening mechanism. Also, the authors note that there is no evidence that the line is Doppler shifted in coronal holes relative to the

quiet Sun implying there is no mass flow in coronal holes, at the 8×10^4 K level, greater than 4.3 km s^{-1} . They determine that the integrated line intensities are the same in a coronal hole as in the quiet Sun.

Frankenthal and Krieger [105] have investigated the nature of photospheric magnetic fields beneath large coronal holes. They consider proposed mechanisms for the formation of coronal holes and explore whether coronal holes are permeated by rigidly rotating fields. The authors suggest that the interaction between such a field and the differentially rotating, diffusive solar envelope will produce a fore-aft asymmetry in the distribution of fields which emerge to the photosphere. They conduct an initial study in the context of an illustrative example, and their results indicate that the asymmetry may be observed for a certain range of parameters involving the properties of the solar envelope and the characteristic size of the emerging-field pattern.

Harvey and Sheeley [106,107] have compared simultaneously obtained (31 January 1974) spectroheliograms of He II (304 Å) and He I (10830 Å) line emission to determine their differences. The authors note that differences between the images include that disk filaments and line darkening are strongly visible in the 10830-Å positive image, but they are weakly visible (as lightnings) in the 304-Å negative images, and that the contrast between the chromospheric network and the network cell centers is much greater in the 10830-Å than in the 304-Å negative image. Coronal holes are apparent in both 304-Å and 10830-Å spectroheliograms.

Hearn [108] has investigated differences in coronal holes as compared to quiet coronal regions. He is able to explain these main differences by a reduction of the thermal conduction coefficient by transverse components of the magnetic field in the transition region of quiet coronal regions. He shows that calculations of minimum flux coronae show that if the flux of energy heating the corona is maintained constant while the thermal conductivity in the transition region is reduced, the coronal temperature, the pressure in the transition region and the corona, and the temperature gradient in the transition region all increase, while the intensities of lines emitted from the transition region are almost unchanged. The author deduces the flux of energy heating the corona in both coronal holes and quiet coronal regions to be $3.0 \times 10^5 \text{ erg cm}^{-2} \text{ s}^{-1}$, of which $2.7 \times 10^5 \text{ erg cm}^{-2} \text{ s}^{-1}$ is removed by thermal conduction down the transition region towards the photosphere. Further, he notes that a reduction by a factor of 5.5 in the thermal conduction coefficient is required to turn a coronal hole into a quiet coronal region. Furthermore, the author shows that the calculations of minimum flux coronae show that the energy lost from coronal holes through high-speed streams in the solar wind is not sufficient to explain the observed differences between the coronal temperatures in coronal holes and

quiet coronal regions; instead, he suggests that a reduction in the density at the bottom of a conductivity maintained solar wind will increase the velocity of expansion in interplanetary space.

Hoang and Steinberg [109] have computed the meter-wavelength thermal radiation (at 169 and 80 MHz) from enhanced and depleted density sheets, corresponding to density coronal streamers and coronal holes, respectively, using a model which considers absorption, refraction, and scattering. The electron density distribution across these structures is approximated either by a Gaussian profile or by a sharp-edged profile. They find that the sharp-edged profile can reproduce correctly the enhanced emission from streamers if the temperature in the streamer is enhanced relative to the corona, thereby not requiring a special nonthermal emission mechanism to explain the slowly-varying component of the solar meter-wavelength radiation. Further, they find that, for coronal holes, a decrease in both the electron density and temperature can account for their reduced emission no matter what their electron density profiles are, a finding which is in agreement with published observations.

Hollweg [110,111] has performed a theoretical investigation of Alfvén waves in the solar atmosphere and a coronal hole. His analysis solves the full-wave equation without recourse to the small-wavelength eikonal approximation and it uses a realistic background solar atmosphere consisting of an HSRA/VAL representation of the photosphere and chromosphere, a 200-km thick transition region, an appropriate model for the upper-transition region below a coronal hole, and the Munro-Jackson model of a polar coronal hole [131]. A number of results are discussed including, in part, that the wave Poynting flux exhibits a series of strong resonant peaks at periods downwards from 1.6 h; that the Poynting flux in the resonant peaks can be large enough to strongly affect the solar wind; that near the base, nonlinear effects may be important and some density and vertical velocity fluctuations may be associated with the Alfvén waves; that below the low corona most energy is kinetic, except near the base where it becomes mostly magnetic at the resonances; and that the Alfvén wave pressure tensor will be important in the transition region only if the magnetic field diverges rapidly and it can be important in the coronal hole.

Houminer [112] has reviewed current IPS observations of corotating solar wind streams and flare-associated shock waves. Also, he discusses their dependence on solar latitude and radial distance from the Sun. The author reviews recent scintillation observations of the power spectrum of the small irregularities and he compares these to in situ measurements. While little is discussed regarding the origin of high-velocity streams (namely, coronal holes), the author does present a few findings: more than half of the observed

coronal hole passages, in one study, are found to be associated with high-velocity streams; observed streams tend to be wider in longitude than the holes and can be detected at latitudes up to about 20° from the holes; and the width of corotating streams associated with coronal holes is dependent on the latitudinal width of the holes and should be at least $20\text{--}30^\circ$ wide.

Howard [113], using Mt. Wilson magnetograph measurements for the periods 3-17 June and 29 June-20 July 1975, has investigated the true average field strength near the poles. Although a certain amount of uncertainty may still exist, the author estimates the true average field strengths to be about twice the measured values (0-2 gauss), with an absolute upper limit on the underestimation of the field strengths of about a factor of 5 (for latitudes $< 80^\circ$).

Howard and Švestka [114] have investigated the development of a complex of activity in the solar corona during its whole lifetime of seven solar rotations (during the Skylab mission period). The authors note that the basic components of the activity complex were permanently interconnected through sets of magnetic-field lines; however, the visibility of individual loops in these connections was greatly variable and typically shorter than one day. Only loops connecting active regions with remnants of old fields can be seen in about the same shape for many days. The authors describe several examples of possible reconnections of magnetic-field lines, giving rise to the onset of the visibility or, more likely, to sudden enhancements of the loop emission. They also discuss cases of loop brightening that definitely could not have resulted from reconnection of magnetic-field lines and that appear to be flare-associated. Further, they explore the birth of the interconnecting loops, their lifetime, altitude, variability in shape in relation to the photospheric magnetic field, the similarity of interconnecting and internal loops in the late stages of active regions, phases of development of an active region as manifested in the corona, the remarkably linear boundary of the X-ray emission after the flare of 25 July 1973, and a striking sudden change in the large-scale pattern of unipolar fields to the north of the activity complex. Lastly, the authors note that the final decay of the complex of activity was accompanied by the penetration of a coronal hole into the region where the complex existed before.

Hundhausen [115] has summarized information regarding plasma flow from the Sun and described additional evidence for solar wind variability given by geomagnetic activity observations over more than a century and cosmic ray data available for several decades. Concerning coronal holes, the author points out that long-lived solar wind streams and the related magnetic polarity structures (sectors) appear to have been the dominant form of solar wind variability throughout the epoch of in situ observations and that these streams seem to originate in coronal holes or the polar caps of the Sun. He presents a simple descriptive

and interpretative scheme explaining the occurrence of geomagnetic activity, coronal holes, and interplanetary changes during the declining portion solar cycle 20.

Intriligator [116,117] has investigated solar cycle variations in the solar wind for the period mid-1964 through 1973. The author notes that the present analysis confirms early results that indicate statistically significant variations in the solar wind in 1968 and 1969 (years of solar maximum), where these variations are in phase with the solar cycle. The author shows that selected high-speed streams in the solar wind in 1968 and 1969 and the total duration (in days) of high-speed streams in 1968 are considerably more than the predicted yearly average, with 1965 and 1972 being years of considerably lower numbers. Further, the author notes that histograms of solar wind speed indicate that in 1968 there was the highest percentage of elevated solar wind speeds, and in 1965 and 1972 the lowest. The author suggests that the duration of the streams, together with the histogram data for 1973, may imply a shifting in the primary stream source.

Iucci et al. [118] have studied the influence of the high-speed streams produced by coronal holes on the cosmic ray intensity in the period 1965-74. They find that when corotating fast streams connected with coronal holes envelop the Earth, small cosmic ray depressions ($\lesssim 2$ percent at the energies of high-latitude neutron monitors) are observed that last for the period of enhanced solar wind velocity and that has their amplitude correlated with the velocity increase. The authors note that two types of corotating regions can be observed in the interplanetary space in the vicinities of the ecliptic plane; regions connected to solar zones where magnetic-field loops and active regions may exist and regions connected to quiet solar zones where the magnetic-field lines are divergent (coronal holes). The authors state that in coronal hole regions the cosmic ray density is maintained depressed by the continuous outflow of enhanced solar wind and the amount of the quasi-stationary cosmic ray depression is linearly related with the increase in solar wind velocity. Also, they observe that the amount of the cosmic ray decrease observed in the presence of broad coronal holes, like those in 1973-74, may offer a rough estimate of the cosmic ray intensity level over the solar poles where extended coronal holes are present.

Jacques [119] has presented the fluid equations for the solar wind in a form which includes the momentum and energy flux of waves in a general and consistent way. He also introduces the concept of conservation of wave action and uses it to derive expressions for the wave-energy density as a function of heliocentric distance. The author gives the explicit form of the terms due to waves in both the momentum and energy equations for radially propagating acoustic, Alfvén, and fast-mode waves. He explores the effect of waves as a

source of momentum by examining the critical points of the momentum equation for isothermal spherically symmetric flow, and he finds that the principal effect of waves on the solutions is to bring the critical point closer to the Sun's surface and to increase the Mach number at the critical point. Finally, he notes that, when a simple model of dissipation is included for acoustic waves, in some cases there are multiple critical points.

Kakinuma [120] has reviewed observations of the solar wind velocity by the IPS method. He reports that detailed analyses show that the diffraction pattern is anisotropic and he derives a latitudinal distribution of the solar wind velocity (the solar wind velocity is 800 km s^{-1} for latitudes $> 45^\circ$). He notes that the observations indicate the presence of the corotating stream which extends from this high-speed region to the equator. Further, comparisons of IPS data with EUV or XUV solar observations show that there is a close relationship between holes and streams, but the association is not one-to-one. Finally, the author reports that IPS observations show that the most turbulent region of the flare-associated shock wave lies in the piston.

Koutchmy [121], using radially and tangentially polarized pictures of the solar corona obtained near 4500 \AA and EUV spectroheliograms during the 30 June 1973 solar total eclipse, has derived a model of a trans-polar coronal hole. The author notes that the line-of-sight coincides with the "privileged plane" of the hole over the north polar region. Further, the author observes extrapolated values of densities down to the surface that are lower than have ever been previously observed, although derived hydrostatic temperatures are not: electron density equal to $1.8 \times 10^7 \text{ cm}^{-3}$ and temperature equal to $2 \times 10^6 \text{ K}$. The author also discusses the morphological peculiarities of polar regions.

Levine [122] has examined the evolution of the photospheric magnetic-field pattern over eleven solar rotations preceding a minimum of the activity cycle. He finds the period to be characterized by abrupt changes of the dominant geometrical patterns of the field, where these changes are associated with the onset and end of a sudden increase in the calculated total energy of the field, which is otherwise decreasing through the period. The author notes that the calculated geometrical arrangements correspond in time to observed restructurings of the corona, the interplanetary field, and the solar rotation period. A brief discussion of CH4 and CH2* (read coronal hole two star) is given.

Levine [123], using high-resolution harmonic analysis of the measured photospheric magnetic field of the Sun, has constructed models of open magnetic structures over a period of 11 solar rotations (Carrington rotations 1601-1611). He notes that the models successfully reproduce the surface location and topology

of all coronal holes during the Skylab mission period, and that there is persistent evidence in the models that open field lines are associated with active regions in a systematic way, suggesting that open field lines are a basic feature of solar magnetism. The author gives specific examples of the evolution of coronal holes and of calculated open structures, and he reports that quantitative study of the measured field strength within and neighboring a hole confirms the fact that coronal hole regions are indistinguishable by local magnetic properties. He does note, however, that the calculated field strengths at the foot points of open field lines within coronal holes show distinct evolutionary patterns and may indicate that, at least in young coronal holes, a significant amount of magnetic flux is closed. The author also discusses problems of studying magnetic-field divergence by using his models.

Levine et al. [124] (see also Levine et al. [125]), using high-resolution harmonic analysis of the global magnetic field, have calculated the geometry of open magnetic-field lines in the solar corona for two solar rotations during the Skylab mission. The authors compare the loci of open field-line footpoints with solar X-ray photographs and show that all of the coronal holes are successfully represented, including details of their evolution. Some open field lines were observed to emanate from separatrices between close-loop systems comprising active regions. The authors note that some magnetic configurations derived in the calculation precede by up to one solar rotation the manifestation of coincident dark areas on the X-ray photographs. Further, they find that by varying the radius at which field lines are forced to be open in the calculation, it is possible to more closely reproduce the surface configuration of particular coronal holes. They note that comparison of the size of X-ray holes with the fraction of the solar surface covered by open field lines leads to the conclusion that a significant part of the area of coronal holes must contain closed magnetic fields, and that comparison of open field lines which lie in the equatorial plane of the Sun with solar wind data indicates that eventual high-speed solar wind streams are associated with those parts of open magnetic structures that diverge the least.

MacQueen and Poland [126] have explored the temporal evolution of the equatorial K-corona at 2.5 solar radii during the Skylab mission period. The authors subdivide the observations into three periods, each characterized by a different variation of the radiance pattern with time. During the initial period, (2 solar rotations), the authors report that the radiance pattern shows a more or less smooth variation with time; however, during the second period (2 solar rotations) the radiance signal is neither persistent on the short-term nor recurrent from one limb passage to the next. During the last period (5 solar rotations), the radiance signal exhibits an orderly periodic behavior of increasing intensity. Thus, the authors conclude that, during the time of the Skylab mission,

substantial, rather abrupt changes occurred in the equatorial K-coronal radiance, as the corona evolved toward a more simple configuration typical of solar minimum conditions. The authors note that late during the Skylab mission, the corona took-on the simplified alternating coronal hole-streamer pattern, which has been used in explaining the evolution of solar wind streams from coronal holes during the mission.

Marsh [127] has performed microphotometry of Ca II K-line photographs in the regions of polar coronal holes, obtained on 20 December 1973 and 2 and 15 January 1974. He reports that the chromospheric network exterior to a hole has a slightly broader intensity distribution than that inside the hole itself, a fact which can be attributed to a greater number of bright network elements outside the hole. The author presumes that these bright network elements represent the enhanced network resulting from the dispersal of magnetic flux from old active regions.

Maxson and Vaiana [128], using low photographic conversion techniques, have investigated coronal holes (associated with persistent high-speed wind streams and open magnetic-field configurations) and large-scale structures (associated with closed-field configurations). They derive irradiances, line-of-sight averaged temperatures, and total emission measures for these coronal features. The authors note that a sharp contrast (0.1) in the irradiances of the coronal hole to the large-scale structure regions is found in the X-ray corona. For the large-scale structure samples, they deduce temperatures of $2\text{--}2.2 \times 10^6$ K with corresponding emission measures of about $4 \times 10^{26} \text{ cm}^{-5}$. For coronal holes (CH1), they calculate a range of temperatures between 9×10^5 K and 3×10^6 K, with a corresponding emission measure range of $5 \times 10^{26} \text{ cm}^{-5} - 2 \times 10^{25} \text{ cm}^{-5}$, respectively. Further, they derive values for the large-scale structure samples to be 0.11 dyn cm^{-2} and for coronal holes (CH1) 0.08 dyn cm^{-2} (at 9×10^5 K). The authors also discuss atmospheric models of these features and advance suggestions about the nature of the sharp transition between these two quiet magnetic-field states of the corona.

McCabe et al. [129] have performed 10830-Å observations using a scanning aperture technique. They report that their spectroheliograms show holes in good agreement with the KPNO maps and that they can be used to locate and study holes.

Moore et al. [130] have presented observational evidence linking EUV macrospicules and flares. Based on the time-lapse H α filtergram observations of the limb in quiet regions, the authors note the existence of small surge-like eruptions, dubbed H α macrospicules, which are quite similar in size, shape,

motion, and duration to EUV macrospicules. From the similarity of $H\alpha$ and He II (304 Å) observations, the authors conclude that $H\alpha$ macrospicules are too faint in $H\alpha$ to appear on $H\alpha$ filtergrams of normal exposure. Also, from a comparison of simultaneous X-ray and $H\alpha$ observations of flares in XBP situated on the limb, the authors show that flares in XBP often produce macrospicules, suggesting that all macrospicules may be produced by similar, but usually weaker, microflares, and that spicules may be generated by still smaller microflares.

Munro and Jackson [131] (see also Jackson [132] and Munro [133]), using Skylab HAO coronagraph observations, have determined the three-dimensional density structure within the north polar coronal hole from 2 to 5 solar radii. They note that the hole is essentially axisymmetric about the north pole during the period 29 June–13 July 1973 and that the increase of the polar hole's cross-sectional area from the surface to 3 solar radii is approximately 7 times greater than if the boundary were purely radial; i.e., approximately 60 percent of the entire solar atmosphere in the northern hemisphere above 3 solar radii is connected to about 8 percent of the solar surface. The authors interpret measured radiances as due to a distribution of material within the hole whose logarithmic radial gradient is independent of position and whose magnitude increases with colatitude. The densities derived for the axis of this hole are noted to agree with published polar values at solar minimum to within a few percent. The authors determine the velocity and pressure distributions within this hole, by assuming that the outflow of polar coronal material into the solar wind is similar to high-speed streams measured at 1 AU. Although temperatures cannot be directly determined, the authors note that the derived velocities indicate that the transonic point lies between 2.2 and 3 solar radii, implying a coronal temperature between $1\text{--}2.5 \times 10^6$ K. They also remark that the analysis indicates that energy — as thermal energy and/or momentum addition — must be deposited in the solar wind at least from 2 to beyond 5 solar radii.

Munro and Mariska [134,135], have developed an empirical, self-consistent coronal hole model between ~ 1.05 and 5 solar radii, based on EUV and white-light observations. Assuming the outward flow of the polar coronal material into the solar wind is similar to high-speed streams measured at 1 AU, they determine velocity and pressure distributions within this hole. They note that, in the absence of accelerating forces other than those due to gravity and gas pressure, the derived kinetic temperature of the plasma is consistent with EUV observations and increases outward from the Sun. Also, they note the discrepancy between EUV-based model and those based on radio observations at frequencies below 100 MHz.

Nolte et al. [136,137], have examined the relationship between coronal hole evolution and solar active regions during the Skylab period. They find that there is a tendency for holes to grow or remain stable when the activity nearby, seen as calcium plages and bright regions in X-rays, is predominantly large, long-lived regions. They also find that there is a significantly higher number of small, short-lived active regions, as indicated by XBP, in the vicinity of decaying holes than there is near other holes, a finding that the authors interpret to mean that holes disappear at least in part because they become filled with many small-scale, magnetically-closed, X-ray emitting features. The authors use this interpretation, together with the previously reported observation that the number of XBP was much larger near solar minimum than it was during the Skylab period, as a possible explanation for the disappearance of the large, near-equatorial coronal holes at the time of solar minimum.

Nolte et al. [138] have examined the relationship between high-speed streams of solar wind and coronal structure during the period September–December 1976. They find that the solar wind streams during this period were generally of lower amplitude, lower maximum velocity, and shorter duration than those in the preceding Skylab period. They compare solar wind data with X-ray images of the corona taken on 16 September and 17 November 1976, and they note that, while a moderate-sized stream was seen during September, no equatorial coronal holes were observed (a small, less well-defined, north polar hole extension was observed but it is not regarded as a strong candidate for the source of the stream). Further, the authors note that the November image showed a better-defined extension from the south polar hole which may be regarded as the source of a small solar wind stream with peak velocity of $\sim 510 \text{ km s}^{-1}$. Thus, the authors conclude that either there has been a change in the solar wind coronal hole relationship or the relationship between coronal holes and solar wind streams is not as general as might be inferred from the Skylab period.

Nolte et al. [139] have investigated the high coronal structure of high-velocity solar wind stream sources. They note that when solar wind plasma in the trailing (eastern) edge of a high-speed stream is mapped back to its estimated source in the high corona using the constant radial velocity (Extrapolated Quasi-Radial Hypervelocity or EQRH) approximation, a large range of velocities appears to come from a restricted range in longitude, often only a few degrees. Using interplanetary data, the authors infer a systematic variation in "source altitude" (identified approximately with the Alfvén point), with faster solar wind attaining its interplanetary characteristics at lower altitudes, and infer a width in the high corona of $4\text{--}6^\circ$ for the source of the trailing edges of streams which appear to originate from a single longitude. Further, the authors demonstrate

that the possible systematic interplanetary effects (in at least some cases) are not large ($\lesssim 2^\circ$ in heliocentric longitude). The authors note that the relatively sharp boundaries imply that high-speed streams are well-defined structures all the way down to their low coronal sources, and that the magnetic-field structure controls the propagation of the plasma through the corona out to the vicinity of the Alfvén point ($\gtrsim 20$ solar radii).

Nolte and Roelof [140] have investigated coronal magnetic-field structures as indicated by chromospheric magnetic polarities and interplanetary polarities mapped back to the high corona using observed solar wind velocities during nine solar rotations (Carrington rotations 1489-1497) in 1965 following the minimum of solar cycle 19. The authors find in the general case that the interplanetary polarity correlated best with mid-latitude solar polarity, where this correlation was due more to large-scale magnetic fields than to the strong fields in the mid-latitude solar active regions. Performing the same correlation analysis for the same time period, but restricted only to those times when energetic particles were present in the interplanetary medium and to those times of enhanced solar wind velocity, the authors find that both energetic particles and fast solar wind exhibited a strong tendency to come from a different magnetic structure than that which was normal during the time period, as evidenced by its polarity signature. In both cases the correlation is best between interplanetary and equatorial solar polarities. Hence, the authors infer that energetic particles and fast solar wind escape preferentially from equatorial coronal magnetic structures which are open (coronal holes), while the more usual equatorial structures during the data time period are closed.

Papagiannis and Wefer [141] have obtained observations of coronal holes at 1420 and 2600 MHz using the Arecibo radiotelescope during the period 31 August to 4 September 1977. The authors construct maps obtained from those data and find a large coronal hole in the southern polar region. The authors note that the radio coronal hole is in excellent agreement with the perimeter of the coronal hole seen in the 10830-Å He-line spectroheliogram obtained by KPNO. Further, the authors note that the brightness temperature in the central region of the coronal hole appears to be 20-30 percent lower than the background temperature of the quiet solar disk.

Raghavan [142] has used medium-resolution observation to find the fractional emitting area in three transition-region lines (N V/1239 Å, O VI/1032 Å, and Ne VIII/770 Å). The author combines the fractional emitting areas at different values of the Mg X (625 Å) intensity and at different temperatures to find the variation of the areas with height.

Rosenberg et al. [143] (see also Rosenberg et al. [144]), have examined the hydrogen, Balmer emission-line spectrum (H_β /3835 Å to the series limit at 3646 Å) above the limb (2 arcs and 4 arcs) of the quiet Sun and above the north solar, polar coronal hole, based on Skylab NRL XUV spectrograph data. They deduce electron densities of $\sim 2 \times 10^{11} \text{ cm}^{-3}$, 2 arcs above the limb of both the quiet Sun and coronal hole, calculated from the Stark broadening of the higher series member lines and the related merging of the higher member lines. The authors remark that the widths of the lines with principal quantum number $m < 15$ are broadened by opacity, and the opacities are estimated from the line widths. Further, the widths of lines of $m < 15$ are not appreciably affected by either opacity or Stark broadening. They note that the combined ion temperature and nonthermal mass motion determined from the widths of these lines are consistent with previously determined values, and that the intensities of the lines indicate that the upper levels (≥ 9) are populated in statistical equilibrium with each other. The authors give absolute intensities, as well as the decrease of the intensity, of the lines as a function of height above the limb.

Saito et al. [145,146] have investigated the equatorial and polar K- and F-coronal components during the declining phase of the solar cycle near solar minimum. Based on Skylab HAO white-light coronagraph data between 2.5—5.5 solar radii during the period May 1973 to February 1974, they report that the equatorial corona is dominated by either streamers or coronal holes seen in projections on the limb approximately 50 percent and 30 percent of the time, respectively; despite the domination by streamers and holes, two periods of time were found which were free from the influences of streamers or holes (neither streamers nor holes were within 30° longitude of the limb); the derived equatorial background density model is less than 15 percent below the minimum equatorial of certain published models; a spherically symmetric density model for equatorial coronal holes yields densities of one-half those of the background density model; and the inferred brightness of the F-corona is constant to within ± 10 percent and ± 5 percent for the equatorial and polar values, respectively, over the observation period. The authors note that, while the F-corona is symmetric at 2 solar radii, it begins to show increasing asymmetry beyond this point such that at 5 solar radii the equatorial F-coronal brightness is 25 percent greater than the polar brightness.

Sandlin et al. [147] have reported new forbidden lines characteristic of plasmas at temperatures of $5 \times 10^4 - 3 \times 10^6 \text{ K}$ and densities of $10^{11} - 10^8 \text{ cm}^{-3}$, from Skylab NRL spectrograph observations. They also report new identifications, accurate wavelengths, ionization classes, intensities, and half-widths, and they note coronal blends with He II (1640 Å). The spectra used in their analysis came from 55 different solar pointings, including active and quiet Sun regions and

coronal holes. They note that the intensities of all forbidden lines of temperature greater than 5×10^4 K peaked in the range 2-4' arcs above the limbs, however, the coronal lines had the greatest scale heights. Also the authors note that the coronal intensity above quiet regions maximized in Si VIII-X and Fe IX-XI and that coronal lines characteristic of temperatures greater than 10^6 K were weak near the poles and absent in coronal holes where transition-region lines were broadened and Doppler shifted, while the coronal lines that appeared later were not. The authors see variations in nonthermal velocities with distance above limb and note that Doppler shifts in the coronal lines observed on the disk may be related to the solar wind. They also give evidence for atomic fluorine on the Sun, based on the coincidence of two lines with F IV.

Sheeley et al. [148] have combined observations of interplanetary magnetic-field polarity, solar wind speed, and geomagnetic disturbance index (C9) during the years 1962-75 in a 27-day pictorial format that emphasizes their associated variations during the sunspot cycle. The authors note that their display accentuates graphically several recently reported features of solar wind streams including the fact that the streams were faster, wider, and longer-lived during 1962-64 and 1973-75 in the declining phase of the sunspot cycle than during intervening years. Further, they report that their display reveals strikingly that these high-speed streams were associated with the major, recurrent patterns of geomagnetic activity that are characteristic of the declining phase of the sunspot cycle, and that their display shows that during 1962-75 the association between long-lived solar wind streams and recurrent geomagnetic disturbances was modulated by the annual variation of the response of the geomagnetic field to solar wind conditions. The authors also observe that the phase of this annual variation depends on the polarity of the interplanetary magnetic field in the sense that negative sectors of the interplanetary field have their greatest geomagnetic effect in northern hemisphere spring, and positive sectors have their greatest effect in the fall. During 1965-72 when the solar wind streams were relatively slow ($\lesssim 500 \text{ km s}^{-1}$), the authors report that the annual variation strongly influenced the visibility of the corresponding geomagnetic disturbance patterns.

Shibasaki et al. [149] have reported observations of a coronal hole at 8-cm wavelength radiation. The authors note that the hole was observed for 3 solar rotations in the latter part of 1975, that it was accompanied by a high-speed solar wind stream, and that it was associated with recurrent-type geomagnetic storms. The authors observe a brightness temperature in the coronal hole about 6000 K lower than in a normal region (~ 22000 K). Also, they report that the electron pressures at the base of the corona obtained by EUV and soft X-ray observations are too high to explain the present radio observations of the coronal hole and the normal quiet region.

Solodyna et al. [150] (see also Solodyna et al. [151]) have observed temporal changes in the X-ray emission structure associated with the birth of a small coronal hole (CH6). The authors note that CH6 was born near the equator in a time interval less than 9-1/2 h. By constructing a light curve for a point near the center of CH6, the authors report a sudden 40 percent decrease in X-ray emission associated with the birth of this coronal hole. Further, they note that, on a time scale of hours, the growth of CH6 in area proceeded faster than the average rate predicted by the diffusion of solar fields; however, its short-term decay did follow the diffusive rate.

Steinolfson and Tandberg-Hanssen [152] have examined thermally conductive flows in coronal holes. Their work incorporates the concepts of polytropic solar wind flows in flow tubes whose cross-sectional area increases faster with radius than for a radial expansion and includes thermal conduction. The authors compare thermally conductive and polytropic flows in the lower corona for given high-speed conditions at 1 AU and find that the thermally conductive flows do yield closer agreement with observations, although the predicted electron density is still too low and the predicted temperature is too high. They also consider modified thermal conductivity which decreases more rapidly with increasing radius and find that although results are improved, the agreement cannot be termed quantitative. The authors conclude that thermal conduction alone will not explain solar wind flows originating in coronal holes and that some other mechanism (e.g., wave pressure) is necessary.

Based on the technique of autocorrelation, Stenflo [153] has studied solar-cycle variations in the rotation rate of solar magnetic fields using Mt. Wilson photospheric magnetic-field data. He finds that there appears to be significant solar-cycle variations in the differential rotation of solar magnetic fields with a pattern in latitude-time space correlated with the pattern of solar activity. The regions of large latitudinal shear and low angular velocity drift towards the equator similar to the sunspot and prominence zones. The author notes that these results, together with earlier observations of coexisting rotation laws in the solar atmosphere (e.g., sunspots, coronal holes, etc.), can be given a consistent explanation by assuming that the observed rotation rate of a magnetic feature (tracer) indicates the rotation rate at the depth in the convection zone where the corresponding surface field is rooted. The time variations observed at the surface, then, may reflect solar-cycle variations of the depths to which the surface fields penetrate. In this picture the background fields are not mainly the remnants of old active region fields, but are more representative of new poloidal magnetic flux, which spreads from the toroidal fields by three-dimensional turbulent diffusion in the convection zone. Thus, by using the observed patterns of surface rotation rates and solar activity as boundary conditions, one may probe the solar interior.

Stix [154] has investigated the spherical harmonic coefficients of the solar magnetic field to divide the observed field into "normal modes," the independent solutions of the turbulent solar dynamo theory. Using Mt. Wilson magnetograms, the author computes the coefficients and finds that the S1 and S3 modes, which are symmetric with respect to the equator and have 2 and 6 magnetic sectors, respectively, were dominant in 1973. The analysis indicates that, at least in some cases (e.g., CH1, CH2 and CH4), the occurrence and position of coronal holes appear to be governed by the behavior of the normal modes.

Suess et al. [155], using a quasi-radial approximation to the full-MHD equations for axisymmetric, polytropic solar wind flow, have simulated the north polar coronal hole (July 1973). The authors report that, from 2 out to 5 solar radii, the temperature varies only slightly with radius, but is larger near the center of the polar hole than at the edge. They also find that the magnetic-field intensity at 2 solar radii could be about 1 gauss at the center of the hole, decreasing toward the edge of the hole. Extrapolating this field intensity to the surface implies a field as high as 20 gauss. The authors note that these results lead to further meridional motion of the solar wind in the interplanetary medium, with a total of perhaps 50° of north to south migration in the mid-latitudes of the northern hemisphere between the photosphere and 1 AU during July 1973.

Švestka et al. [156,157] have explored open magnetic fields in active regions. They report that dark X-ray gaps are sometimes located between the loops that interconnect active regions and between the active region cores. They note that, although some of these gaps are simply due to decreased temperature in the low-lying portions of the interconnecting loops or are the roots of high and less dense or cooler loops, large dark X-ray corridors extending over active regions have been found in positions predicted by global potential-field model computations, correctly extending over the expected polarities. The authors observe that, in one case, a corridor had been a part of a coronal hole (CH3) and, in two other cases, the dark X-ray corridors preceded the formation of coronal holes (CH4 and CH6) by one to three rotations. Finally, the authors note that all the active regions in which the existence of open fields can be suspected have been regions two or more rotations, indicating that the field lines open only in a later state of the active region development.

Timothy [158] has reviewed the current state of knowledge (as of 1977) on the solar spectral irradiance at EUV wavelengths between 300 and 1200 Å and the techniques for photometric measurements at EUV wavelengths. He also presents some observational data, discusses current ideas about the effects of specific solar features on the variability of the spectral irradiance, and suggests

future measurements. Concerning coronal holes, he notes that they are regions of very low intensity at coronal wavelengths which have lifetimes of several solar rotations and they have a negligible effect on the irradiance of chromospheric and transition-region lines but contribute to the variability of coronal lines.

Tyler et al. [159], using Viking orbiter radio transmissions at the time of Martian solar conjunction in 1976, have studied the K corona very near solar minimum. During the conjunction period, coherent 3.5- and 13-cm wavelength radio waves from the Viking orbiters passed through the solar corona, including both equatorial and south polar solar (coronal hole) latitudes, and were received on Earth. Data were obtained within at least 0.3 solar radii for the 3.5-cm radio waves and 0.8 solar radii for the 13-cm radio waves. The authors have used these data to determine (in preliminary form) the plasma density integrated along the radio path (~ 60 solar radii), the velocity of density irregularities in the coronal plasma, and the spectrum of the density fluctuations in the plasma. The authors report that observations of integrated plasma density near the south solar pole generally agree with a model of the corona which has an 8:1 decrease in plasma density from the equator to the pole. Further, power spectra of the 3.5- and 13-cm signals at a heliocentric radial distance of about 2 solar radii have a one-half power width of several hundred hertz and vary sharply with proximate geometric miss distance. Spectral broadening indicates a marked progressive increase in plasma irregularities with decreasing altitude at scales between about 1 and 100 km.

Wefer and Papagiannis [160] have studied a coronal hole radio structure on 2 and 3 September 1977 at 7.88, 15.3, 15.5, and 35 GHz. The authors report that the radio coronal hole appeared barely detectable as an enhancement at 35 GHz, as a small but detectable enhancement at 15.3 GHz, as a clearly detectable enhancement at 15.5 GHz, and as a small depression at 7.88 GHz.

Withbroe [161] has discussed empirical and theoretical models for the transition layer. Concerning coronal holes, the author notes that line-ratio data indicate that the electron pressure in the transition layer of coronal holes is approximately equal to that in quiet regions, suggesting that the temperature gradient in the transition layer of coronal holes is approximately the same as in quiet regions. Further, he points out that empirical data indicate that the electron pressure in the coronal layers of coronal holes is lower by a factor of 2 to 3 than in quiet regions, implying a temperature gradient a factor of 5 to 10 shallower in coronal holes than in quiet regions, for a plane-parallel model in hydrostatic equilibrium. Also, the author notes that differences in the physical condition above various areas of the solar surface appear to be intimately related to the configuration and strength of the magnetic fields in these areas; thus, open-field configuration areas become coronal holes.

Yoshimura [162] has examined a theoretical solar-cycle model driven by the dynamo action of the global convection. He finds that this concept appears to be valid when compared to the evolution of the coronal general magnetic field calculated from the observed surface general magnetic field of 1959-74. He uses this concept to explain the variation and phasing of the high-speed solar wind streams and the modulation of the galactic cosmic rays, as well as a variety of other topics (including coronal holes).

Results from 1978

Ahmad and Webb [163] have detected polar plumes at X-ray wavelengths. They present observations and analysis results of one well-observed plume and deduce the plasma pressure. They propose a hydrodynamic model which is consistent with earlier white-light and EUV observations, and they note that their calculations indicate that the total outward mass flux in polar plumes is comparable to that in high-speed solar wind streams expected from a polar coronal hole.

Bohlin and Sheeley [164], based on XUV Skylab observations and KPNO magnetic-field data, have studied the origin and evolution of coronal holes. They show that holes exist only within the large-scale unipolar magnetic cells into which the solar surface is divided at any given time. The authors observe a well-defined boundary zone to usually exist between the edge of a hole and the neutral line which marks the edge of its magnetic cell, where this boundary zone is the region across which a cell is connected by magnetic arcades with adjacent cells of opposite polarity. The authors offer three pieces of observational evidence to support the hypothesis that the magnetic lines of force from a hole are open: (1) plumes in polar coronal holes, (2) the coronal hole of the 7 March 1970 eclipse, and (3) XUV observations of CH2*. Further, the authors use Kitt Peak magnetograms to show that, at least on a relative scale, the average field strengths within holes are quiet variable, but indistinguishable from the field strengths in other quiet parts of the Sun's surface. The authors also show that the large equatorial holes, characteristic of the declining phase of the last solar cycle during Skylab (1973-74), were all formed as a result of the mergence of bipolar magnetic regions, a hypothesis is dubbed the "unbalanced" flux model for coronal holes. The authors note that systematic application of this model to the different aspects of the solar cycle correctly predicts the occurrence of both large, equatorial coronal holes and the polar cap holes.

Broussard et al. [165] (see also Broussard et al. [166]), based on an analysis primarily of rocket-obtained X-ray and XUV solar images during the period 1963-74 corresponding to approximately sunspot cycle 20, have investigated the relationships between solar activity, the occurrence and variability of coronal holes, and the association of such holes with solar wind features, such as high-velocity streams. They find that the polar coronal holes, prominent at solar minimum, decreased in area as solar activity increased and were small or absent at maximum phase, and they note that this evolution exhibited the same phase difference between the two hemispheres that was observed in other indicators of activity. Further, they find that, during solar maximum, coronal holes occurred poleward of the sunspot belts and in the equatorial region between them, where the observed equatorial holes were small and persisted for one or two solar rotations only and some high-latitude holes had lifetimes exceeding two solar rotations. The authors note that during 1963-74, whenever XUV and X-ray images were available, nearly all recurrent solar wind streams of speed $\geq 500 \text{ km s}^{-1}$ were found associated with coronal holes at less than 40° latitude; however, some holes appeared to have no associated wind streams at the Earth.

Chambe [167] has shown that analysis of both the UV and radio emission, by inversion of the flux equations, lead to the differential emission measure of the solar atmosphere. He notes that, while the physical mechanisms for the UV emission are more complex, the inversion process appears safe; however, in the radio case, the simpler equation is unsuited for inversion. Yet, the radio data provide a proper test involved in the UV equation by comparison with the radio spectrum inferred from the UV emission measure. He finds the calculated spectrum to be systematically higher than the observed, from centimetric to metric wavelengths, but to a lesser extent for coronal holes than for the quiet Sun. Apart from the lower frequency end of the spectrum, this result is quite independent of the model. Substantially increasing the elemental abundances brings agreement in the middle part of the spectrum; however, accounting for the network and cell inhomogeneities does not help resolve the remaining higher frequency discrepancy which the author suggests is likely due to over-simplified physics in the writing of the EUV-line intensity equation. The author further notes that, while the model independence of the result is based on the 'no-reflection' assumption for radio waves, even if reflection occurs it alters only marginally his conclusions.

Cuperman and Dryer [168] have investigated the long-term correlation between the latitude-dependent $5303\text{-}\text{\AA}$, coronal green-line intensity and the solar wind streams measured at 1 AU heliocentric distance during the period 1962-70. Using half-year averages of the daily green-line intensities obtained at Kislovodsk Station together with published solar wind data, they find that the

intensity of the light radiation is anticorrelated with the high-speed solar wind streams (i.e., that high-speed streams are associated with reduced green-line-emitting regions) and that the magnitude of the anticorrelation coefficient increases with heliographic latitude to a value of ~ 0.6 at about 30° , after which it changes only slightly. Further, the authors note that their results suggest the association of high-speed, solar wind flows observed in the ecliptic plane at 1 AU with coronal holes, whose main emitting regions were located at medium to high heliographic latitudes during 1962-70, a suggestion consistent with the idea that the relative contribution of high-latitude (polar cap) holes and low-latitude holes may change with the solar cycle.

Cuperman et al. [169], using the Helios 1 space-dependent measurements between 0.3 and 1 AU heliocentric distance in conjunction with two-fluid model equations, have investigated the spatial structure of the interplanetary medium. The authors note that their results indicate that (1) the normalized particle flux $\bar{J} \equiv J/J_E$ (where E indicates Earth or 1 AU heliocentric distance) varies by a factor of 10 (between ~ 0.5 and 5) over the interplanetary range explored by Helios 1; (2) the strong deviations from the value 1 are found only for states with streaming velocities below about 500 km s^{-1} , while for the high-speed states $\bar{J} \approx 1$; (3) the deviations found for low-speed states are strongly correlated with particle density fluctuations and moderately anticorrelated with streaming velocity fluctuations; and (4) time-dependent and/or additional processes could play a significant role. Using observational data representative of the high-speed flows ($v \geq 600 \text{ km s}^{-1}$, where v is the solar wind speed) in conjunction with the fluid equations for a two-component plasma (protons and electrons), they estimate some properties of the solar wind. In particular, using best fits to the observed proton density, velocity, and temperature profile values, they deduce the electron temperature profile.

Cushman and Rense [170] have presented additional results of a 30 August 1973 rocket experiment. They discuss line profiles of He II (304 \AA) and Si XI (303 \AA) emission. They note that the profile of the He II line is everywhere clearly non-Gaussian across the solar disk, except in bright active areas; near the limb, the profile is reversed. The authors also report that the profile of the Si XI line is essentially Gaussian for all regions across the solar disk. The authors note that measurements of the He II/Si XI intensity ratio indicate that the average value of this ratio across the disk depends markedly on solar activity, being about 10:1 for a moderate level of activity and 30:1 for a quiet Sun. Some discussion of coronal holes also occurs.

Dittmer et al. [171] have performed an observational search for large-scale organization of five-minute oscillations on the Sun. They measure the

large-scale solar velocity field over an aperture of radius 0.8 solar radius on 121 days between April and September 1976, based on the Fe I (5123.730 Å) line. They compare the amplitude and frequency of the five-minute resonant oscillation with the geomagnetic C9 index and magnetic sector boundaries and find no evidence of any relationship between the oscillations and coronal holes or sector structure.

Doschek and Feldman [172] have investigated the profiles and electron densities of EUV lines emitted in regions of significant mass motion activity in the solar atmosphere. They define regions of significant mass motion activity as those regions which emit allowed spectral lines that are significantly broader than those emitted in quiet Sun regions (including coronal holes). The data are those recorded by the NRL spectrograph aboard Skylab. The authors show that the line profiles result from the superposed emission of a number of physically distinct regions at different electron densities and with different mass motions. Although high densities ($>10^{12} \text{ cm}^{-3}$) are found for some surge-like phenomena at transition-region temperatures, the densities can also be comparable to normal active region densities ($\sim 10^{11} \text{ cm}^{-3}$). The surge-like events addressed in this paper are those of 1 September 1973/1404 UT, 2 December 1973/2152 UT, 11 January 1974/2028 UT, 13 January 1974/1622 UT, and 16 January 1974/1355 UT. The authors conclude that line profiles, as well as spectral line intensities, must be considered if meaningful theoretical models of dynamic activity in the transition region are to be constructed.

Doschek et al. [173] have described a method for determining densities in quiet Sun areas and coronal holes that is not strongly sensitive to temperature variations and is independent of instrumental efficiency as a function of wavelength. They show that the EUV-line intensity ratios C III (1909 Å)/O III (1666 Å), O III (1666 Å)/Si IV (1403 Å), and C III (1909 Å)/Si IV (1403 Å) are sensitive to variations in the electron density at densities typical of the quiet Sun ($\sim 10^{10} \text{ cm}^{-3}$ at $6 \times 10^4 \text{ K}$). Using the O III line, the authors note that the aforementioned ratios can be normalized to observational data, and densities in quiet-Sun regions and coronal holes can be determined. They deduce the average value of the density determined for these quiet-Sun regions is $1.9 \times 10^{10} \text{ cm}^{-3}$, and note that, while five coronal hole observations gave densities comparable to the quiet-Sun value, the density in the north polar coronal hole was found to be about $9.4 \times 10^9 \text{ cm}^{-3}$, a factor of 2 less than in the quiet Sun.

Eadon and Billings [174,175] have measured areas of emission features in C II (1135 Å), C III (997 Å), O IV (544 Å), and O VI (1032 Å) both in and out of coronal holes. In the quiet Sun, the authors note that, on the average, these areas showed a 20 percent increase between C II and O VI; however, in coronal holes, they find no significant average variation, although a number of the features showed an interesting decrease in area at intermediate temperatures.

Feldman and Doschek [176], using the so-called "O-IV technique," have derived emission measures, densities and volumes for a typical solar active region and several selected flares (i.e., the flares of 2 December 1973/2024 UT; 17 December 1973/0033 UT; and 21 January 1974/2318 UT) from EUV spectral lines of O IV (1401 Å), N V (1242 Å), C IV (1550 Å), and Si IV (1402 Å) recorded by the NRL spectrograph aboard Skylab. The densities are determined for a temperature of about 1.3×10^5 K. The authors deduce typical densities for active regions of $\sim 10^{11} - 10^{13} \text{ cm}^{-3}$, where the $\sim 10^{13} \text{ cm}^{-3}$ is deduced for the rather complicated 15 June 1973/1420 UT flare. Further, they find volumes of high-density emitting plasma in active regions and flares to be quite small, with values ranging from $1.5 \times 10^{23} \text{ cm}^3$ to less than $2.2 \times 10^{20} \text{ cm}^3$. The authors also determine the relative difference in electron density between typical quiet-Sun regions and a polar coronal hole, using the diagnostic lines of C III (1909 Å) and Si IV (1402 Å). They report that while the C III line has approximately the same intensity in the quiet-Sun and coronal hole regions, the Si IV line is about two times more intense in the quiet-Sun region, suggesting that the density in a polar coronal hole is about one-half of the density in a typical quiet-Sun region, at a temperature near 6×10^4 K.

Feldman et al. [177] have extended past investigations of long-term solar wind variability to include the minimum of solar cycle 20. In particular, the authors present variations in solar wind characteristics (e.g., He abundance; relative He-H velocity difference; He-H temperature ratio; and proton density, speed, rms-velocity variation, temperature, and number flux) observed between 18 March 1971 and 6 January 1977, data obtained from IMP 6, 7, and 8. The authors note the salient features observed during this period to be: (1) the existence of large-amplitude, broad, corotating high-speed streams between January 1973 and mid-1976, resulting in enhanced average flow speeds during this epoch of solar cycle 20; (2) both proton number and total energy fluxes were generally larger after September 1972 than before August 1972, where this increase is believed to result from an areal expansion of both polar coronal holes in response to the increasing disk-like region postulated to surround the Sun in interplanetary space; (3) the occurrence frequency of density enhancements, not obviously produced by interplanetary compressions, did not decrease with decreasing solar activity, thereby suggesting that it is unlikely that all such enhancements are caused by coronal transients; and (4) the average solar wind He abundance varied from about 3 to 5 percent, then back to 3 percent during solar cycle 20, where this variation lagged by about 1-2 years behind that of the smoothed sunspot number. The authors also note that He-abundance variations, like all other known systematic solar wind ion variations, occurred preferentially during low-speed and/or high-density flow conditions, suggesting that this result may be caused by a systematic time

variation in the mixture of coronal flow types leading to low-speed conditions at 1 AU. Finally, the authors emphasize that near solar maximum, energetic transient disturbances may dominate, while near solar minimum, spatially-structured high-density expansions may dominate.

Feldman et al. [178] have investigated electron variations across simple high-speed streams. In particular, from the data set extending from March 1971 through August 1974, they fully document two streams and present hourly-averaged parameter plots. Based on comprehensive scans of the shape of electron distributions measured at the very highest bulk speeds, they confirm the description that electron velocity distributions are composed of two parts: a low-energy nearly isotropic component and a high-energy strongly beamed component. They note that, at 174 eV, the high-energy beam typically has a FWHM of $\sim 18^\circ$, where this width decreases with increasing energy. Further, the authors note that the fact that high-energy electrons are strongly beamed is consistent with the suggestion made previously that for them, pitch-angle-scattering collisions are rare beyond some base radius, denoted R_0 . Their angular widths as a function of energy can be reproduced if it is assumed that their velocity distribution is isotropic below R_0 and evolves with heliocentric distance according to Liouville's theorem. The authors report that their data are consistent with a base radius between 10 and 30 solar radii. The near isotropy and low temperature of low-energy electrons suggest that binary Coulomb interactions and waves couple them efficiently to one another as well as to the solar wind ions. Beyond the speed maxima but within the constant high-speed portions of simple streams, systematic trends in most electron parameters are small, a fact that reinforces the conclusion that high-speed flows represent a special structure-free state of the solar wind at 1 AU.

Fenimore et al. [179], using more than 11 years of solar wind speed data as recorded by Vela 2-6 and IMP 6-8, have employed a power spectrum analysis to such a time series to investigate the frequency range near the solar rotational period. The authors note that, while year-by-year power spectra show such large differences that the solar wind time series is nonstationary, the spectrum of the entire 11-year time series shows broad bands of power near periods of 27 days (corresponding to the rotational period of the Sun), 13.5 days, and higher harmonics. At 27 days, periods differing by as little as 0.1 day can be resolved. The band power near 27 days extends from about 25 to about 31.5 days and contains a number of sharply defined peaks. Further, the authors note that, while the geomagnetic index aa has similar groups of peaks near a period of 27 days which has been explained as a solar latitude effect caused by differential rotation, they suggest that the individual peaks in both

the geomagnetic and solar wind spectra are probably not due to differential rotation, owing to recent observations which indicate that the source regions of the solar wind during solar cycle 20 did not rotate differentially but instead occurred at a preferred range of longitudes (being associated with coronal holes). They thus explain the multipeak nature of the power spectra by a wave-packet concept in which recurring high-speed streams are described as a series of pulses (separated by a constant period) that last for a varying number of solar rotations. Subsequent wave packets have the same period but are shifted in phase to mimic the range of possible longitudes for sources of solar wind streams. The authors find that power spectra obtained for such idealized wave packets closely resemble the measured spectra of the solar wind speed and geomagnetic activity. Furthermore, the authors remark that they do not find the frequencies predicted by a theory concerning the nonradial oscillation of the Sun.

Fisher [180] has observed the distribution of the Fe XIV (5303 Å) green-line brightness as a function of position angle, height above the limb, and time. He uses these data to construct models of the volume emissivity as a function of solar latitude and longitude, and then uses these models to estimate the distribution of electron density in the lower solar corona as a function of latitude and longitude for several specific periods in 1973 and 1975. He notes that an observational upper-limit for the inferred electron density in a coronal hole region is set at $\log N_e = 7.4$ (where N_e is the electron density) for an altitude of 1.15 solar radii. Secondly, he finds that density models from late 1973 demonstrate an evolutionary trend toward a rather regular four-lobbed appearance of coronal material and that models from 1975 suggest that this characterization persisted for 27 solar rotations. Finally, he infers a decrease in the total integrated 5303-Å intensity of a factor of 2.9 to have taken place between 1973 and 1975.

Glackin et al. [181], from Skylab NRL spectroheliograph observations, have shown that the He II (256 Å) line intensity is very nearly uncorrelated with He II (304 Å) at the same location on the Sun and that the 256-Å line is formed mainly by the photoionization-recombination process. The authors derive center-to-limb variations of He II (304, 256 Å) and He I (584, 537 Å) for network and cell regions separately and find that, in both network and cells, the 304-Å and 584-Å lines each limb-brighten in the quiet Sun and each limb-darken in coronal holes and, for both the 304-Å and 584-Å lines, network and cell regions are each brighter in the quiet Sun than in coronal holes. Thus, the authors note that the appearance of dark coronal holes in the helium lines is not a geometrical effect involving the chromospheric network, but is rather an intrinsic property of the atmosphere in both network and cell regions. The authors suggest that the network and cells can be treated as isolated atmospheres in the solution of the transfer equation in the helium lines.

Jacques [182] has studied the effects of wave pressure and wave heating on one-fluid models of the solar wind. He gives solutions to the MHD equations for the solar wind which include fluxes of Alfvén waves ranging from 0 to $\sim 10^5$ ergs $\text{cm}^{-2} \text{s}^{-1}$ at the base of corona. Damping of the waves is simulated by limiting the wave magnetic-field amplitude to that of the background magnetic field, and two states of the solar wind are considered: high-speed or fast streams (speeds $\sim 700 \text{ km s}^{-1}$) and low-speed or slow streams (speeds $\sim 300 \text{ km s}^{-1}$). The author notes that his model is successful in reproducing observed densities both at the Sun and at 1 AU and in producing flows with speeds of $\sim 750 \text{ km s}^{-1}$ at 1 AU, simply by including an Alfvén wave flux at the Sun of $\sim 10^5$ ergs $\text{cm}^{-2} \text{s}^{-1}$. Further, the author notes that the inclusion of waves steepens the density profile near the Sun, making it possible to construct models with electron densities near the Sun of several times 10^8 cm^{-3} which also match density and velocity observations at 1 AU.

Joselyn and Holzer [183] have investigated the effects of rapid flow tube divergence on multifluid models of the solar wind. In particular, they have developed, for nonspherically symmetric flow geometries of the general sort thought to be characteristic of coronal holes, a steady three-fluid model of the solar coronal expansion, in which alpha particles ($^4\text{He}^{++}$ ions) are treated as a major species. They find that the very high-mass fluxes in the low corona, which are associated with rapidly diverging flow geometries, lead to a locally enhanced frictional coupling between protons and alphas and consequently to a significant reduction of the He/H abundance ratio in the lower corona from that normally predicted by multifluid models. The authors note that, in the models considered, the frictional drag on the protons by the alphas is found to play an important role near the Sun. Heavy ions (other than alphas) are treated as minor species and are seen to exhibit varying responses to the rapidly diverging flow geometries, depending on the ion and charge. For protons, the frictional effect of the alphas on the heavier ions is found to be significant.

Lantos [184], based on a two-component structured corona (i.e., one which contains coronal holes and arches, in addition to active regions and streamers), has re-interpreted the classical characteristics of the centimetric quiet Sun. The author invokes the irregular presence of coronal holes in order to explain both the center-to-limb effects and the cycle variation of the central brightness temperature of the radio quiet Sun. The author, using a number of radio observations at 3-, 6-, 9.1-, 11- and 21-cm wavelength, derives an average emission measure in the arches of $3.8 \pm 1 \times 10^6 \text{ cm}^{-5}$ for an assumed electron temperature of $1.5 \times 10^6 \text{ K}$ in the arches, and he infers that the lowest K-corona mean models during solar minimum correspond, at low altitudes, to the arch structures.

Levine [185,186], using high-resolution harmonic analysis (potential-field modeling) of the solar magnetic field, has studied the connection between the solar surface and solar wind flow observed at 1 AU over 11 solar rotations to determine whether systematic features in the evolution of open magnetic configurations in the corona can be associated with distinct solar wind flow phenomena. The author notes that, although such associations are strongly suggested by the models, the study pinpoints the problems of associating significant portions of the observed solar wind with sources outside coronal holes. Further, the author examines the phenomenological relationship between observed high solar wind speed at 1 AU and small coronal field divergence near the Sun and he finds it to be well-established but causally inconclusive in light of models of the outer heliosphere.

Levine [185], using high-resolution, spherical harmonic analysis, has performed potential-field modeling of the solar magnetic field and confirmed the association of high-speed, solar wind streams with established coronal holes during the Skylab period, approximately June 1973 to February 1974 (Carrington rotations 1601-1611). His analysis also suggests possible sources of other parts of the solar wind at 1 AU. He lists several specific properties which are suggested as being applicable to at least the declining phase of the solar cycle; namely, (1) the loci of solar surface points corresponding via magnetic connection to a continuous path near the solar equator at 1 AU can be discontinuous and can vary greatly in latitude; (2) all new open magnetic structures first appear in the models in association with strong surface flux (active regions), and most remain associated with active regions or coronal holes for their entire life; (3) when an open structure becomes manifest at 1 AU is not clear, but if this occurs early in its development (i.e., before a large coronal hole can be distinguished), the systematic solar wind signature might be locally low solar wind speed; otherwise, low-speed solar wind at 1 AU most likely is controlled by the edges of the same large structures whose centers contain high-speed solar wind streams; (4) a smoothly evolving solar wind structure may be associated with different active regions during its lifetime; (5) some solar wind structures may have surface connections which extend beyond the major features with which they are associated (e.g., beyond the defined boundary of a small coronal hole); and (6) there is probably a quantitative relationship between solar wind speed at 1 AU and magnetic-field divergence along a connecting path in the heliosphere.

Mango et al. [187] (see also, Mango et al. [188]), based on the Skylab NRL spectroheliograph observations of 17 December 1973 and 21 January 1974, have derived the center-to-limb variation of the He II (304, 256 Å) and He I (584, 537 Å) lines in quiet-Sun, coronal hole, and nonhole unipolar magnetic

region structures. The authors report that the general trend is for limb brightening in quiet-Sun regions, limb neutrality in unipolar magnetic regions, and limb darkening in polar coronal holes. Also, they note that the center-to-limb behavior in these optically-thick emission lines indicates collisional excitation and decreasing transition-region temperature gradients with respect to optical depth in the sequence quiet Sun, unipolar magnetic region, and coronal hole.

Mariska [189] (see also, Mariska [190]), has investigated a temperature and density model for the upper-transition region and inner corona of the north polar coronal hole observed on 14 August 1973. Using Skylab HCO EUV spectroheliometer observations of the resonance lines of lithium-like ions (O VI/1032 Å, Ne VIII/770 Å, Mg X/625 Å, Al XI/550 Å, and Si XII/521 Å), he constructs emission gradient curves. His analysis indicates both reduced density and coronal temperature in the coronal hole. The author determines the boundary geometry of the coronal hole and constructs a temperature-density model that is consistent with the observed intensities. The author notes that the best agreement for all the data was found to be with an electron density of $1.7 \times 10^8 \text{ cm}^{-3}$ at 1.03 solar radii, a conductive flux of $6 \times 10^4 \text{ ergs cm}^{-2} \text{ s}^{-1}$, and a coronal temperature of $7.63 \times 10^5 \text{ K}$ which increased to $1.1 \times 10^6 \text{ K}$ at 1.08 solar radii. Further, he notes that the boundary geometry and density distribution are combined with typical solar wind parameters at the earth to determine an outflow velocity of 15 km s^{-1} at 1.08 solar radii.

Mariska and Withbroe [191] have constructed emission gradient curves for EUV resonance lines of O VI (1032 Å) and Mg X (625 Å) from spectroheliograms of quiet-limb regions observed from Skylab. The authors note that their analysis suggests that the coronal temperature rises throughout the height range 1.03 to 1.3 solar radii, a result that implies that in quiet regions there is significant coronal heating beyond 1.3 solar radii.

Marsh [192], using high-resolution filtergrams of the solar limb in D_3 (5876 Å) and off-band $H\alpha$, has investigated the spatial structure of the D_3 chromosphere. He finds that spicules provide the major contribution to the intensity of the D_3 -emission band observed above the limb, with the remainder of the emission coming from a semi-homogeneous background component at low heights. He notes that the observations can be understood on the basis of the photoionization model, whereby it is found that helium is only slightly ionized at the height of peak intensity in the D_3 -emission band, and that spicules are at least 3 times denser than their surroundings at this height. The author also notes that, in coronal holes, the D_3 emission is confined to isolated patches and that these patches contain fine structure resembling normal chromospheric spicules.

McIntosh [193], using $H\alpha$ synoptic charts for Carrington rotations 1487-1616, has compiled an atlas of large-scale solar magnetism patterns for an entire solar cycle (1964-1974). He presents evidence for large-scale convergence and divergence among these patterns, for significant variations in rates of solar rotations throughout the solar cycle, and for the presence of a semi-permanent feature in the polar latitudes that corresponds to the location of large, long-lived coronal holes. He notes that displays of these patterns by latitude zones in sequences of 20 solar rotations reveal long-lived patterns resembling the solar sector structure in interplanetary magnetic fields and suggests that the $H\alpha$ patterns reveal the source of the interplanetary patterns.

Mihalov and Wolfe [194] have studied the solar wind isotropic proton temperature as measured out to 12.2 AU heliocentric distance by instrumentation aboard Pioneer 10. They present and discuss these temperatures as consecutive averages over three Carrington solar rotations. The authors note that the weighted least-squares fit of average temperature to heliocentric radial distance, denoted R , yields the power law $R^{-0.52}$ and that the average proton temperatures are not correlated as well with Pioneer 10's heliocentric radial distance as are the corresponding average Zürich sunspot numbers.

Musman and Altrock [195] (see also, Altrock and Musman [196]), utilizing green-line, coronal photometer Fe XIV (5303 Å) data for the period 3 October to 22 December 1976, have inferred the positions of coronal holes. During this period, the authors report that there was a pattern of three coronal holes and three emissions regions near the solar equator. They note that two of the three holes were associated with recurrent geomagnetic disturbances (based on the geomagnetic index A_p). A simple model is proposed that allows for predicting recurrent geomagnetic disturbances at times of low solar activity, based on coronal brightness, and the method is found to give correct results 72 percent of the time, as compared to 64 percent of the time for 27-day recurrence.

Niedner et al. [197, 198], using IMP 8 data, have investigated the large-scale disturbance in the tail of comet Kohoutek 1973f, apparent on photographs taken on late 19 January and early 20 January 1974, to ascertain whether an event in the interplanetary medium was responsible for the disturbance. Their analysis indicates that, at the time of formation of the perturbed tail structure (the comet was only 3° north of the ecliptic plane), the comet was entering the compression region of the strong high-speed solar wind stream which produced a geomagnetic storm on 24-27 January, the stream being associated with the large equatorward extension of the south polar coronal hole which underwent central meridian passage on 22 January. The authors use the

"wind sock" theory of ionic comet-tail orientations in conjunction with the corotated IMP 8 observations to generate a theoretical time history of the position angle made by the comet tail on the plane of the sky. They note that comparison of the observed and predicted position angles show that the complex tail morphology on 20 January is the signature of a large, rapid change in the polar component of the solar wind bulk velocity on the forward edge of the density buildup.

Nolte et al. [199] have compared average values of solar wind stream amplitude, maximum velocity and half-width for periods shortly after the preceding solar cycles 20 and 21. They note that, while high maximum velocities (associated with large, equatorial coronal holes) were observed for streams during the early part of cycle 21, the differences between cycles 20 and 21 in their average amplitudes and half-widths, were not significant. The authors conclude that, except for the large streams seen late in the solar cycle, the variation of these stream parameters is nearly as large from cycle to cycle as it is within a solar cycle.

Nolte et al. [200] (see also, Nolte et al. [201]), based on Skylab X-ray observations between May and November 1973, within 1 day of central meridian passage of coronal holes, have investigated sudden large-scale shifts in coronal hole boundaries. They find that large-scale changes in boundary locations can account for most if not all of the evolution of coronal holes and that the temporal and spatial scales of the large-scale changes imply that they are the results of a physical process occurring in the corona. The authors conclude that coronal holes evolve by magnetic-field lines opening when the holes are growing, and by fields closing as the holes shrink.

Nolte et al. [202] have examined the evolution of coronal hole boundaries on a scale of ~ 1 day. They find that 38 percent of all boundaries of coronal holes observed near central meridian passage during the Skylab mission period shifted in location by $>1^\circ$ heliocentric in ~ 1 day. Further, they note that, of these boundary changes, 70 percent occurred on a scale ≤ 3 times the average supergranulation cell size. The authors observe large-scale shifts in the boundary locations to occur, which involved changes in the X-ray emission from these areas of the Sun. Also, they note that X-ray emitting structures on the borders of isolated and evolving holes were less clearly defined than those on the boundaries of well-established, elongated holes, and that there were generally more changes in the boundaries of the most rapidly evolving holes, but no simple relationship between the amount of change and the rate of hole growth or decay.

Pneuman et al. [203] have performed global magnetic-field calculations, using potential-field theory, for Carrington rotations 1601-1610 during the Skylab period to quantitatively test the spatial correspondence between calculated open- (coronal holes) and closed-field distributions in the solar corona with observed brightness structures. The authors observe that the comparison between computed open-field line locations and coronal holes show a generally good correspondence in spatial location on the Sun; however, the areas occupied by the open field seem to be somewhat smaller than the corresponding areas of X-ray holes. The authors discuss possible explanations for this discrepancy and note that the locations of open-field lines and coronal holes coincide with the locations of maximum field strength in the higher corona with the closed regions consisting of relatively weaker fields. The authors also note the general correspondence between bright regions in the K-corona and computed closed-field regions is good, with the computed neutral lines lying at the top of the closed loops following the same general "warped" path around the Sun as the maxima in the brightness. They observe that the neutral lines at a given longitude tend systematically to lie somewhat closer to the poles than the brightness maxima for all rotations considered, with the discrepancy in latitude increasing as the poles are approached. The authors report that, by artificially increasing the line-of-sight photospheric-field strengths above 70° latitude, the discrepancy correspondingly decreased, with the best agreement between neutral-line locations and brightness maxima being obtained for a polar field of about 30 gauss.

Poland [204] has investigated motions and mass changes of a persistent (5 successive limb passages between 1 June and 6 August 1973) coronal streamer which defined the southern boundary of the north polar coronal hole and a region on the south having a brightness similar to equatorial coronal holes. The author notes that the streamer's visual appearance changed slightly between successive limb passages indicating that it was not a steady-state feature. Further, the author observes (1) the streamer's axis to migrate southward from 25° N at first east limb passage to 11° N at second east limb passage to 8° N latitude at third east limb passage; (2) the streamer's mass (and mass gradient with height) varied by between 20 and 50 percent from one east limb passage to the next; (3) the streamer's longitudinal extent was also observed to be less on successive east limb passages; and (4) mass changes occurring over hours were detected during at least two limb passages. The author concludes that the streamer was associated with a complex of solar activity consisting of active regions and filaments, and notes that positional changes of the regions and filaments brought corresponding changes to the streamer.

Rabin and Moore [205] have investigated polar coronal holes and the variation with latitude of the chromosphere. They find that there is a steady increase in average height of about 25 percent from equator to pole but that there is no discontinuity at hole boundaries nor any increase under holes beyond that expected from the latitude trend. The authors conclude that spicules are not generated by heat conduction or other energy transfer from the corona and are therefore driven from below. Further, they note that the observed increase in height with latitude suggests that the chromosphere magnetic field becomes, on average, more vertical as the poles are approached, thereby, allowing spicules to attain greater heights.

Schwenn et al. [206] have presented results of a study of solar wind speeds measured from the Helios 1 solar probe between 0.31 and 1.0 AU and the earth-orbiting IMP 7 and 8 satellites correlated with coronal holes as determined from K-coronal brightness measurements. The authors report that, in March 1975 during perihelion passage, Helios 1 traversed the range of heliographic latitudes from -6° to $+6^\circ$ in a period of 20 days. During that time, Helios 1 crossed the northern boundary of the high-speed stream associated with an equatorward extension of the south-polar coronal hole. While this stream continued to be observed by IMP satellites at -5° latitude, it was no longer observable from the solar probe at $+5^\circ$ latitude. The authors note that the data supports the view that sharp boundaries separate high-speed flows from the surrounding solar wind, where the thickness of the boundary in latitude appears to be narrower than about 10° . They state that the local gradient in flow speed is at least $30 \text{ km s}^{-1} \text{ deg}^{-1}$ and may actually exceed $100 \text{ km s}^{-1} \text{ deg}^{-1}$ at 0.31 AU.

Shah et al. [207] have performed a study of the 112 recurrent Forbush decreases (with decreases ≥ 2 percent) recorded at Deep River for the period 1966-75 to examine any possible relationship between M regions with solar active regions. They show that at the onset of the recurrent Forbush decreases at the Earth there is a high probability of encountering a class of active regions at the central meridian of the Sun, which gives rise to flares of importance $\geq 2B/3N$. The authors note that these active regions are found to be long lasting and to have large areas, as well as high $H\alpha$ intensities. Other active regions, producing flares of lower importance, are distributed randomly on the Sun with respect to the onset of a recurrent Forbush decrease. By using the quasi-radial hypervelocity approximation, the authors trace the base of the leading edge of the high-velocity stream at the onset of a recurrent Forbush decrease at the Earth to the solar longitude about 40° west of the central meridian. Hence, they deduce that M regions are located preferentially to the west of long-lasting, magnetically-complex active regions. The authors conclude with a discussion of a possible mechanism of the development of an M region to the west of a long-lasting, magnetically-complex active region, and the relation of M regions and coronal holes.

Sheeley [208], based on U.S. Air Force Defense Meteorological Satellite Program auroral imagery, has investigated the equatorward boundary of auroral activity during 1973-74. The author notes that, on a time scale of days, the equatorward position of the northern auroral oval varied in phase with the average level of geomagnetic activity. Further, he notes that, in general, this variation was associated with the occurrence of solar flares and coronal holes. On a time scale of hours, the author observes the equatorward position of the oval to be correlated with the AE index of substorm activity and with the strength of the southward component of the interplanetary magnetic field.

Sheeley and Harvey [209, 210], using daily He I (10830 Å) spectroheliograms and photospheric magnetograms, have extended their previous study of coronal holes, solar wind streams, and geomagnetic disturbances (based on the C9 index) from the declining phase (1973-75) of sunspot cycle through sunspot minimum (1976) into the rising phase (1977) of sunspot cycle 21. They report that, as the magnetic-field patterns changed, the solar atmosphere evolved from a structure having a few, large, long-lived, low-latitude coronal holes to one having numerous small, short-lived, high-latitude holes, in addition to the persistent polar holes. Also, the authors note that the high-latitude holes recurred with a synodic rotation period of 28-29 days instead of the 27-day period characteristic of low-latitude holes. Furthermore, during 1976-77, the authors observed many coronal holes that were intrinsically 'weak' in the sense that their average intensities did not differ greatly from the intensity of their surroundings, a find that was very rare during 1973-75. The authors present an updated Bartels display of the occurrence of holes, wind speed, and geomagnetic activity and they note that although long-lived, low-latitude holes have become rare, they are still terrestrially effective. Finally, the authors observe that the more common, high-latitude holes are effective only when the Earth lies at a relatively high-heliographic latitude in the same solar hemisphere.

Speich et al. [211] have examined solar activity regions observed during the period of Skylab observations (May 1973-February 1974) for properties that varied systematically with location on the Sun, particularly with respect to the location of coronal holes. The authors note that approximately 90 percent of the optical and X-ray flare activity occurred in one solar hemisphere (136-315 heliographic degrees longitude) and that active regions within 20 heliographic degrees of coronal holes were below average in lifetimes, flare production, and magnetic complexity.

Svalgaard et al. [212] have investigated the field strengths of the polar caps. Using Fe I (5250 Å) data, the authors find that the average flux density poleward of 55° latitude is about 0.6 mT peaking to more than 1 mT at the pole.

and decreasing to 0.2 mT at the polar cap boundary. They compute that the total open flux through either polar cap is about 3×10^{14} Wb. Within coronal holes outside of the polar cap, the authors find the magnetic-field strength at sunspot minimum to be rather small (0.15 mT). The authors also show that observed magnetic-field strengths vary as the line-of-sight component of nearly radial fields.

Trottet and Lantos [213] have examined the problem of the compatibility of radio and UV observational interpretations in the corona by means of homogeneous empirical models. The radio observations are one-dimensional measurements taken with the Nançay interferometers at 408 and 169 MHz; the UV observations are Fe XV (284 Å) measurements taken with OSO 7. The authors show that a simple model exists which is compatible with the UV-line intensities, with the altitudes of the UV-line emissions on the limb, and with radio observations from the decimeter to the decameter range. Further, they find that the obtained densities are in agreement with the mean K-corona measurements at the pole during the solar cycle minimum, and they derive some parameters of coronal arches. For coronal holes, they deduce a density of $\sim 10^8 \text{ cm}^{-3}$ and a temperature of $\sim 8 \times 10^5 \text{ K}$. For the arches, they obtain a temperature of $1.25 \times 10^6 \text{ K}$ and a density of $5 \times 10^9 \text{ cm}^{-3}$ (at 10^5 K). Also, they note that the temperature decreases with altitude above arches.

Vernazza and Mason [214] have investigated the level populations and the EUV-line emission arising from ions of the boron isoelectronic sequence from N III, O IV, Ne VI, Mg VIII, and Si X. They find that, under conditions present in the solar corona, some of these ions have pairs of emission lines having intensity ratios which are density sensitive. They derive densities for a number of features, including quiet and active regions, coronal holes, sunspots, and flares, and they discuss some aspects of the differences in the behavior of the emission from the lithium and boron sequences. The authors note that, from the Mg VIII results, the coronal hole electron density is 50 percent of the values in quiet areas (at 10^6 K), and they confirm that, in the low-transition region ($8 \times 10^4 \text{ K}$), the electron density in coronal holes is the same as in quiet areas.

Vorpahl and Broussard [215] (see also, Broussard and Vorpahl [216]), using Skylab X-ray image data, have determined significant quantitative values for physical parameters defining the changing structure of a coronal hole. They note that a new active region (McMath 12363) developed near a large coronal hole (CH1) late on 1 June 1973, and that as the new bipolar region developed, a distinct decrease occurred (in the formation of a channel) in a nearby X-ray emission source, thereby allowing the large central coronal hole to extend all

the way to the large active region. The authors give quantitative values for the change in X-ray flux, average electron density, and temperature in the channel, as well as relate these variations to the corresponding photospheric and coronal magnetic fields in the region. The authors show that the decrease in X-ray flux (by 40 percent) resulted from a reduction in electron density (by 60 percent from a value of about $9 \times 10^8 \text{ cm}^{-3}$) rather than from cooling (temperature remained essentially constant) and that their study suggests that changes in a coronal hole may be explained by the loss of material along weakened, less-confining magnetic-field lines in the corona.

Webb et al. [217] have explored the possible relationship linking coronal transients to the evolution of coronal holes. By superposition of the positions of X-ray coronal transients outside of active regions observed during Skylab on $H\alpha$ synoptic charts and coronal hole boundaries, the authors confirm a detailed spatial association between the transients and neutral lines. They find that most of the transients were related to large-scale changes in coronal hole area and tended to occur on the borders of evolving equatorial holes.

Wefer et al. [218] have constructed radio synoptic charts of coronal holes at 9.1-cm wavelength for Carrington rotations 1601-1605 (May-August 1973). They note the presence of CH1 as a distinct depression in radio emission in Carrington rotations 1602 and 1603, but not in 1601 or 1604, apparently due to being wiped out either by adjacent active regions or side-lobe effects of other active regions during these rotations. Also, they clearly see CH5 as a depression only in rotation 1602. CH2 and CH3 were not seen.

Whang and Chien [219] have investigated the expansion of the solar wind in streamtubes with rapid divergence in their supersonic section and have shown that the wind can be accelerated to a speed $\gtrsim 600 \text{ km s}^{-1}$ at 1 AU. The authors note that, in a streamtube with a cross-sectional area in the supersonic section which increases more rapidly than the square of the heliocentric distance, the extra area expansion produces a solar wind at a high Mach number at 1 AU than does normal spherical expansion. Also, the energy needed for the kinetic energy of a high-speed solar wind must be deposited at the base of the corona mainly in the form of convective thermal energy and conductive heat, thus, requiring a very high temperature ($\sim 2.5 - 4.5 \times 10^6 \text{ K}$) at the source region of the Sun's surface for these high-speed streams. The authors note that the increase in the solar wind due to Alfvén waves which propagate according to the WKB solution is one order of magnitude less than that of the rapidly diverging streamtubes.

Woo [220], using Helios 1 and 2 and Pioneer 10 and 11 spacecraft data, has investigated radio scattering at 2.3 GHz over an extensive heliocentric distance range (1.7-180 solar radii) of the solar wind. The author deduces a solar wind velocity of 24 km s^{-1} at 1.7 solar radii, based on spectral and angular broadening of the spacecraft signal. By assuming that the rms-density fluctuation σ_{ne} is proportional to the mean density n_e , and using an appropriate density model, he obtains the velocity profile of the acceleration region of the solar wind. The author notes that phase or Doppler scintillations, which are shown to be proportional to $\sigma_{ne} v^{5/6}$, where v is the solar wind velocity, have been measured out at 180 solar radii, and that beyond 10 solar radii the radial dependence of the phase scintillations is roughly $R^{-1.3}$ where R is the distance from the Sun in solar radii. (The author notes that this latter relationship is true within the assumptions that $\sigma_{ne} \propto n_e$ and $v^{5/6} \sim v$.) This suggests that the solar wind is slightly converging in the equatorial region between approximately 20 and 180 solar radii.

Zombeck et al. [221] have compiled an atlas of soft X-ray images of the solar corona obtained by the AS&E X-ray telescope experiment aboard Skylab. Daily photographs of the full-Sun taken through two broadband filters during the period 29 May-27 November 1973 are given. The images readily show the presence of coronal holes.

Miscellaneous

In addition to the aforementioned articles, a number has appeared which either give brief discussions concerning coronal holes or show coronal hole imagery or boundary positions. Also, some have appeared in journals other than those primarily used in this review. Thus, these articles [222-253] are contained in the reference listing purely for completeness.

REFERENCES

1. Wilson, R. M.: Results of Coronal Hole Research: An Overview. NASA TM X-73317, Marshall Space Flight Center, AL, July 1976.
2. Zirker, J. B. (ed.): Coronal Holes and High Speed Wind Streams. Colorado Associated University Press, Boulder, CO, 1977.
3. Orrall, F. Q.: Coronal Holes. Proceedings of the November 7-10, 1977 OSO-8 Workshop (eds.: E. Hansen and S. Schaffner), University of Colorado, Boulder, CO, 1977, pp. 58-74.
4. Zirker, J. B.: Recent Progress in the Study of Coronal Holes. B.A.A.S. 8, 1976, p. 376.
5. Zirker, J. B.: Coronal Holes and High-Speed Wind Streams. Rev. Geophys. & Space Phys. 15, August 1977, pp. 257-269.
6. Bumba, V. and Šýkora, J.: Large-Scale Magnetic Structures Responsible for Coronal Disturbances. Coronal Disturbances (ed. G. Newkirk, Jr.), IAU Symp. No. 57, D. Reidel Publ. Co., Dordrecht, Holland, 1974, pp. 73-83.
7. Tousey, R., Bartoe, J.-D. F., Bohlin, J. D., Brueckner, G. E., Purcell, J. D., Scherrer, V. E., Schumacher, R. J., Sheeley, N. R., and VanHoosier, M. E.: Preliminary Results from the NRL/ATM Instruments from Skylab SL/2. Coronal Disturbances (ed. G. Newkirk, Jr.), IAU Symp. No. 57, D. Reidel Publ. Co., Dordrecht, Holland, 1974, pp. 491-495.
8. Pneuman, G. W.: Magnetic Structure Responsible for Coronal Disturbances: Theory. Coronal Disturbances (ed. G. Newkirk, Jr.), IAU Symp. No. 57, D. Reidel Publ. Co., Dordrecht, Holland, 1974, pp. 35-68.
9. Altschuler, M. D.: Magnetic Structure Responsible for Coronal Disturbances: Observations. Coronal Disturbances (ed. G. Newkirk, Jr.), IAU Symp. No. 57, D. Reidel Publ. Co.; Dordrecht, Holland, 1974, pp. 3-33.

REFERENCES (Continued)

10. Culhane, J. L. and Acton, L. W.: The Solar X-Ray Spectrum. Annual Review of Astronomy and Astrophysics (eds., G. R. Burbidge, D. Layzer, and J. G. Phillips), Vol. 12, Annual Rev. Inc., Palo Alto, CA, 1974, pp. 359-381.
11. Parker, E. N.: The Origin of Solar Activity. Annual Review of Astronomy and Astrophysics (eds., G. Burbidge, D. Layzer and J. G. Phillips), Vol. 15, Annual Rev. Inc., Palo Alto, CA, 1977, pp. 45-68.
12. Withbroe, G. L. and Noyes, R. W.: Mass and Energy Flow in the Solar Chromosphere and Corona. Annual Review of Astronomy and Astrophysics (eds., G. Burbidge, D. Layzer, and J. G. Phillips), Vol. 15, Annual Rev. Inc., Palo Alto, CA, 1977, pp. 363-387.
13. Howard, R.: Large-Scale Solar Magnetic Fields. Annual Review of Astronomy and Astrophysics (eds., G. Burbidge, D. Layzer, and J. G. Phillips), Vol. 15, Annual Rev. Inc., Palo Alto, CA, 1977, pp. 153-173.
14. Noyes, R. W., Foukal, P. V., Huber, M. C. E., Reeves, E. M., Schmahl, E. J., Timothy, J. G., Vernazza, J. E., and Withbroe, G. L.: EUV Observations of the Active Sun from the Harvard Experiment on ATM. Solar Gamma-, X-, and EUV Radiation (ed. S. R. Kane), IAU Symp. No. 68, D. Reidel Publ. Co., Dordrecht, Holland, 1975, pp. 3-17.
15. Golub, L., Krieger, A. S., Silk, J. K., Timothy, A. F., and Vaiana, G. S.: Time Variations of Solar X-Ray Bright Points. Solar Gamma-, X-, and EUV Radiation (ed. S. R. Kane), IAU Symp. No. 68, D. Reidel Publ. Co., Dordrecht, Holland, 1975, pp. 23-24.
16. Glencross, W. M.: Holes in the Solar Corona. Solar Gamma-, X-, and EUV Radiation (ed. S. R. Kane), IAU Symp. No. 68, D. Reidel Publ. Co., Dordrecht, Holland, 1975, pp. 19-21.
17. Cavallini, F. and Righini, A.: H and K (Ca II) Emissions as Observed in Coronal Spectrum in the July 20, 1963 Solar Eclipse. Solar Phys. 45, 1975, pp. 291-299.

REFERENCES (Continued)

18. Kanno, M. and Tanaka, R. : The Geometry of the Chromosphere-Corona Transition Region Inferred from the Center-to-Limb Variation of the Radio Emission. *Solar Phys.* 43, 1975, pp. 63-77.
19. Kopp, R. A., White, O. R., and Baur, T. G. : The Koobi Fora Experiment: Continuum Observations of Solar Spicules During the 30 June 1973 Eclipse. *Astron. Astrophys.* 44, 1975, pp. 299-304.
20. Liebenberg, D. H., Bessey, R. J. and Watson, B. : Coronal Emission Line Profile Observations at Total Solar Eclipse. *Solar Phys.* 44, 1975, pp. 345-359.
21. Straka, R. M., Papagiannis, M. D., and Kogut, J. A. : Study of a Filament with a Circularly Polarized Beam at 3.8 cm. *Solar Phys.* 45, 1975, pp. 131-139.
22. Svalgaard, L., Wilcox, J. M., Scherrer, P. H., and Howard R. : The Sun's Magnetic Sector Structure. *Solar Phys.* 45, 1975, pp. 83-91.
23. Adams, W. M. : Differential Rotation of Photospheric Magnetic Fields Associated with Coronal Holes. *B.A.A.S.* 8, 1976, p. 338.
24. Adams, W. M. : Differential Rotation of Photospheric Magnetic Fields Associated with Coronal Holes. *Solar Phys.* 47, 1976, pp. 601-605.
25. Akasofu, S.-I. : Solar Cycle Review (General Aspects). *Physics of Solar Planetary Environments* (ed. D. J. Williams), Vol. I, Am. Geophys. Union, Boulder, CO., 1976, pp. 1-33.
26. Axford, W. I. : Flow of Mass and Energy in the Solar System. *Physics of Solar Planetary Environments* (ed. D. J. Williams), Vol. I, Am. Geophys. Union, Boulder, CO, 1976, pp. 270-285.
27. Bame, S. J., Asbridge, J. R., Feldman, W. C., and Gosling, J. T. : Solar Cycle Evolution of High-Speed Solar Wind Streams. *Astrophys. J.* 207, 1976, pp. 977-980.

REFERENCES (Continued)

28. Beckers, J. M.: Magnetic Fields in the Solar Atmosphere. Physics of Solar Planetary Environments (ed. D. J. Williams), Vol. I, Am. Geophys. Union, Boulder, CO, 1976, pp. 89-113.
29. Behannon, K. W.: Mariner 10 Interplanetary Magnetic Field Results. Physics of Solar Planetary Environments (ed. D. J. Williams), Vol. I, Am. Geophys. Union, Boulder, CO, 1976, pp. 332-345.
30. Bell, B. and Noci, G.: Intensity of the FeXV Emission Line Corona, the Level of Geomagnetic Activity, and the Velocity of the Solar Wind. J. Geophys. Res. 81, 1976, pp. 4508-4516.
31. Bohlin, J. D.: The Physical Properties of Coronal Holes. Physics of Solar Planetary Environments (ed. D. J. Williams), Vol. I, Am. Geophys. Union, Boulder, CO, 1976, pp. 114-128.
32. Bridge, H. S.: Solar Cycle Manifestations in the Interplanetary Medium. Physics of Solar Planetary Environments (ed. D. J. Williams), Vol. I, Am. Geophys. Union, Boulder, CO, 1976, pp. 47-62.
33. Chiuderi-Drago, F. and Noci, G.: A Model of the Solar Transition Region and Corona for the Minimum of Activity. Astron. Astrophys. 48, 1976, pp. 367-371.
34. Cushman, G. W. and Rense, W. A.: Evidence of Outward Flow of Plasma in a Coronal Hole. Astrophys. J. (Letters) 207, 1976, pp. L61-L62.
35. Cushman, G. W. and Rense, W. A.: Evidence of Outward Flow of Plasma in a Coronal Hole. Erratum. Astrophys. J. (Letters) 211, 1976, p. L57.
36. Cushman, G. W., Kint, W. A., and Rense, W. A.: Profiles of Solar Lines in the Range 200-700 Å. B.A.A.S. 8, 1976, pp. 501-502.
37. Doschek, G. A., Feldman, U., VanHoosier, M. E., and Bartoe, J.-D.F.: The Emission-Line Spectrum Above the Limb of the Quiet Sun: 1175-1940 Å. Astrophys. J. Suppl. Ser. 31, 1976, pp. 417-443.

REFERENCES (Continued)

38. Dürst, J.: Observations of Coronal Polarization at the Solar Eclipse of 7 March, 1970. *Solar Phys.* 50, 1976, pp. 457-464.
39. Feldman, U., Dorschek, G. A., VanHoosier, M. E., and Purcell, J. D.: The Emission-Line Spectrum Above the Limb of a Solar Coronal Hole: 1175-1940 Å. *Astrophys. J. Suppl. Ser.* 31, pp. 445-466.
40. Feldman, U., Doschek, G. A., and Patterson, N. P.: The Quiet Sun Chromospheric Network Observed from Skylab. *Astrophys. J.* 209, 1976, pp. 270-281.
41. Flower, D. R. and Pineau des Forêts, G.: Shock Wave Heating of the Outer Solar Atmosphere. *Astron. Astrophys.* 52, 1976, pp. 191-198.
42. Golub, L., Krieger, A. S., and Vaiana, G. S.: Observation of Spatial and Temporal Variations in X-Ray Bright Point Emergence Patterns. *Solar Phys.* 50, 1976, pp. 311-327.
43. Golub, L., Krieger, A. S., and Vaiana, G. S.: Distribution of Lifetimes for Coronal Soft X-Ray Bright Points. *Solar Phys.* 49, 1976, pp. 79-90.
44. Holzer, T. E.: Our Quantitative Understanding of the Coronal Expansion. *Physics of Solar Planetary Environments* (ed. D. J. Williams), Vol. I, Am. Geophys. Union, Boulder, CO, 1976, pp. 366-412.
45. Kopp, K. A. and Holzer, T. E.: Dynamics of Coronal Hole Regions. I. Steady Polytopic Flows with Multiple Critical Points. *Solar Phys.* 49, 1976, pp. 43-56.
46. Kopp, R. A. and Orrall, F. Q.: Temperature and Density Structure of the Corona and Inner Solar Wind. *Astron. Astrophys.* 53, 1976, pp. 363-375.
47. Koutchmy, S. and Stellmacher, G.: Photometric Study of Chromospheric and Coronal Spikes Observed During the Total Eclipse of 30 June, 1973. *Solar Phys.* 49, 1976, pp. 253-265.

REFERENCES (Continued)

48. Kundu, M. R. and Liu, S.-Y.: Observation of a Coronal Hole at 85 GHz. *Solar Phys. (Res. Notes)* 49, 1976, pp. 267-269.
49. Levy, E. H.: Theory of the Solar Magnetic Cycle Wave in the Diurnal Variation of Energetic Cosmic Rays: Physical Basis of the Anisotropy. *J. Geophys. Res.* 81, 1976, pp. 2082-2088.
50. Liu, S.-Y. and Kundu, M. R.: Differential Rotation of the Solar Atmosphere as Determined from Millimeter Data. *Solar Phys.* 46, 1976, pp. 15-22.
51. McIntosh, P. S.: An Empirical Model for the Origin and Evolution of Coronal Holes. *B.A.A.S.* 8, 1976, p. 325.
52. McIntosh, P. S., Krieger, A. S., Nolte, J. T., and Vaiana, G.: Association of X-Ray Arches with Chromospheric Neutral Lines. *Solar Phys.* 49, 1976, pp. 57-77.
53. Montgomery, M. D.: Solar Wind Observations Throughout the Solar System. *Physics of Solar Planetary Environments* (ed. D. J. Williams), Vol. I, Am. Geophys. Union, Boulder, CO, 1976, pp. 304-318.
54. Neupert, W. M.: Evolution of Coronal Holes as Observed in Synoptic Observations of Fe XV Emission from OSO-7. *B.A.A.S.* 8, 1976, pp. 324-325.
55. Nolte, J. T., Krieger, A. S., Timothy, A. F., Vaiana, G. S., and Zombeck, M. V.: An Atlas of Coronal Hole Boundary Positions May 28 to November 21, 1973. *Solar Phys.* 46, 1976, pp. 291-301.
56. Nolte, J. T., Krieger, A. S., Timothy, A. F., Gold, R. E., Roelof, E. C., Vaiana, G., Lazarus, A. J., Sullivan, J. D., and McIntosh, P. S.: Coronal Holes as Sources of Solar Wind. *Solar Phys.* 46, 1976, pp. 303-322.
57. Ohman, Y.: Some Aspects on Solar Submicron Particles. *Astron. Astrophys. (Res. Note)* 52, 1976, pp. 461-464.

REFERENCES (Continued)

58. Parker, E. N.: The Enigma of Solar Activity. Basic Mechanisms of Solar Activity (eds., V. Bumba and J. Kleczek), IAU Symp. No. 71, D. Reidel Publ. Co., Dordrecht, Holland, 1976, pp. 3-16.
59. Pneuman, G. W.: The Influence of Coronal Magnetic Fields on the Solar Wind. Physics of Solar Planetary Environments (ed. D. J. Williams), Vol. I, Am. Geophys. Union, Boulder, CO, 1976, pp. 428-442.
60. Reeves, E. M.: The EUV Chromosphere Network in the Quiet Sun. Solar Phys. 46, 1976, pp. 53-72.
61. Rhodes, E. J. Jr. and Smith, E. J.: Further Evidence of a Latitude Gradient in the Solar Wind Velocity. J. Geophys. Res. 81, 1976, pp. 5833-5840.
62. Rickett, B. J., Sime, D. G., Sheeley, N. R. Jr., Crockett, W. R., and Tousey, R.: High-Latitude Observations of Solar Wind Streams and Coronal Holes. J. Geophys. Res. 81, 1976, pp. 3845-3850.
63. Roelof, E. C.: Solar Particle Emission. Physics of Solar Planetary Environments (ed. D. J. Williams), Vol. I, Am. Geophys. Union, Boulder, CO, 1976, pp. 214-231.
64. Rosenbauer, H., Miggenrieder, H., Montgomery, M., and Schwenn, R.: Preliminary Results of the Helios Plasma Measurements. Physics of Solar Planetary Environments (ed. D. J. Williams), Vol. I, Am. Geophys. Union, Boulder, CO, 1976, pp. 319-331.
65. Sheeley, N. R. Jr.: Polar Faculae During the Interval 1906-1975. J. Geophys. Res. 81, 1976, pp. 3462-3464.
66. Sheeley, N. R. Jr., Harvey, J. W., and Feldman, W. C.: Coronal Holes, Solar Wind Streams, and Recurrent Geomagnetic Disturbances: 1973-1976. Solar Phys. 49, 1976, pp. 271-278.
67. Smerd, S. F.: Radio Observations of Coronal Phenomena and Solar Flares. Physics of Solar Planetary Environments (ed. D. J. Williams), Vol. I, Am. Geophys. Union, Boulder, CO, 1976, pp. 193-213.

REFERENCES (Continued)

68. Sofue, Y., Kawabata, K., Takahashi, F., and Kawajiri, N.: Coronal Faraday Rotation of the Crab Nebula, 1971-1975. *Solar Phys.* 50, 1976, pp. 465-480.
69. Stenflo, J. O.: Small-Scale Solar Magnetic Fields. *Basic Mechanisms of Solar Activity* (eds., V. Bumba and J. Kleczek), IAU Symp. No. 71, D. Reidel Publ. Co., Dordrecht, Holland, 1976, pp. 69-99.
70. Stix, M.: Dynamo Theory and the Solar Cycle. *Basic Mechanisms of Solar Activity* (eds., V. Bumba and V. Kleczek), IAU Symp. No. 71, D. Reidel Publ. Co., Dordrecht, Holland, 1976, pp. 367-388.
71. Suess, S. T.: Latitudinal Variations in the Solar Wind. *Physics of Solar Planetary Environments* (ed. D. J. Williams), Vol. I, Am. Geophys. Union, Boulder, CO, 1976, pp. 443-458.
72. Svalgaard, L. and Wilcox, J. M.: The Hale Solar Sector Boundary. *Solar Phys.* 49, 1976, pp. 177-185.
73. Tousey, R.: The XUV Sun as Observed by ATM S082. *Scientific Investigations on the Skylab Satellite* (eds., M. I. Kent, E. Stuhlinger, and S.-T. Wu), *Progress in Astronautics and Aeronautics* (Ser. ed. M. Summerfield), Vol. 48, Am. Inst. Aeron. Astron., New York, NY, 1976, pp. 47-72.
74. Reeves, E. M., Timothy, J. G., Foukal, P. V., Huber, M. C. E., Noyes, R. W., Schmahl, E. J., Vernazza, J. E., and Withbroe, G. L.: Initial Results from the EUV Spectroheliometer on ATM. *Scientific Investigations on the Skylab Satellite* (eds., M. I. Kent, E. Stuhlinger, and S.-T. Wu), *Progress in Astronautics and Aeronautics* (Ser. Ed. M. Summerfield), Vol. 48, Am. Inst. Aeron. Astron., New York, NY, 1976, pp. 73-103.
75. Van Tend, W. and Zwaan, C.: On Differences in Differential Rotation. *Basic Mechanisms of Solar Activity* (eds., V. Bumba and J. Kleczek), IAU Symp. No. 71, D. Reidel Publ. Co., Dordrecht, Holland, 1976, pp. 45-46.

REFERENCES (Continued)

76. Wagner, W. J.: Rotational Characteristics of Coronal Holes. Basic Mechanisms of Solar Activity (eds., V. Bumba and J. Kleczek), IAU Symp. No. 71, D. Reidel Publ. Co., Dordrecht, Holland, 1976, pp. 41-43.
77. Wefer, F. L. and Bleiweiss, M. P.: Observations of Coronal Hole Associated Features at Wavelengths of 2.0 cm and 8.6 mm. B.A.A.S. 8, 1976, pp. 338-339.
78. Weisberg, J. M., Rankin, J. M., Payne, R. R., and Counselman, C. C. III: Further Changes in the Distribution of Density and Radio Scattering in the Solar Corona in 1973. Astrophys. J. 209, 1976, pp. 252-258.
79. Wibberenz, G.: Energetic Particles Throughout Solar System. Physics of Solar Planetary Environments (ed. D. J. Williams), Vol. I, Am. Geophys. Union, Boulder, CO, 1976, pp. 346-365.
80. Wilcox, J. M.: History of Solar-Terrestrial Relations as Deduced from Spacecraft and Geomagnetic Data: Solar M Regions. Physics of Solar Planetary Environments (ed. D. J. Williams), Vol. II, Am. Geophys. Union, Boulder, CO, 1976, pp. 947-957.
81. Ahmad, I. A.: Fourier Analysis of the EUV Chromospheric Network. B.A.A.S. 9, 1977, p. 337.
82. Ahmad, I. A. and Withbroe, G. L.: EUV Analysis of Polar Plumes. Solar Phys. 53, 1977, pp. 397-408.
83. Ahmad, I. A.: Extreme Ultraviolet Observations of Polar Plumes. B.A.A.S. 8, 1976, p. 325.
84. Altschuler, M. D., Levine, R. H., Stix, M., and Harvey, J.: High Resolution Mapping of the Magnetic Field of the Solar Corona. Solar Phys. 51, 1977, pp. 345-375.
85. Antonucci, E., Azzarelli, L., Casalini, P., and Cerri, S.: Chromospheric Rotation During 1972-73, Years of Declining Activity. Solar Phys. 53, 1977, pp. 519-529.

REFERENCES (Continued)

86. Antonucci, E., and Dodero, M. A.: Coronal Rotation Dependence on the Solar Cycle Phase. *Solar Phys.* 53, 1977, pp. 179-188.
87. Axford, W. I.: The Three-Dimensional Structure of the Interplanetary Medium. *Study of Travelling Interplanetary Phenomena 1977* (eds., M. A. Shea, D. F. Smart, and S. T. Wu), *Astrophysics and Space Science Library*, Vol. 71, D. Reidel Publ. Co., Dordrecht, Holland, 1977, pp. 145-164.
88. Benz, A. O. and Gold, T.: On the Kinetics of Solar Wind Acceleration. *Astron. Astrophys.* 55, 1977, pp. 229-237.
89. Bohlin, J. D.: Extreme-Ultraviolet Observations of Coronal Holes I: Locations, Sizes, and Evolution of Coronal Holes, June 1973-January 1974. *Solar Phys.* 51, 1977, pp. 377-398.
90. Chiuderi-Drago, F., Avignon, Y., and Thomas, R. J.: Structure of Coronal Holes from UV and Radio Observations. *Solar Phys.* 51, 1977, pp. 143-158.
91. Chiuderi-Drago, F. and Poletto, G.: A Dynamical Model of Coronal Holes Based on Radio Observations. *Astron. Astrophys.* 60, 1977, pp. 227-231.
92. Covington, A. E.: Coronal X-Ray Holes and the Quiet Radio Sun at 2800 MHz. *Solar Phys.* 54, 1977, pp. 393-402.
93. Covington, A. E.: Coronal Holes and the Quiet Radio Sun at 2800 MHz. *B.A.A.S.* 8, 1976, p. 339.
94. Cuperman, S.: Theoretical Contributions of Solar Wind Research-A Review. *Study of Travelling Interplanetary Phenomena 1977* (eds., M. A. Shea, D. F. Smart, and S. T. Wu), *Astrophysics and Space Science Library*, Vol. 71, D. Reidel Publ. Co., Dordrecht, Holland, 1977, pp. 165-194.
95. Davis, J. M., Golub, L., and Krieger, A. S.: Solar Cycle Variation of Magnetic Flux Emergence. *Astrophys. J. (Letters)* 214, 1977, pp. L141-L144.

REFERENCES (Continued)

96. Davis, J. M. and Golub, L.: Evolutionary Trends in the Development of Coronal Holes and Their Relationship to the Sub Photospheric Magnetic Field. *B.A.A.S.* 8, 1976, p. 326.
97. Doschek, G. A. and Feldman, U.: The Coronal Temperature and Nonthermal Motions in a Coronal Hole Compared with Other Solar Regions. *Astrophys. J. (Letters)* 212, 1977, pp. L143-L146.
98. Doschek, G. A. and Feldman, U.: On the Problem of Density Diagnostics for the EUV Spectrum of the Solar Transition Zone. *Astron. Astrophys. (Letters)* 58, 1977, pp. L13-L15.
99. Duggal, S. P. and Pomerantz, M. A.: The Origin of Transient Cosmic Ray Intensity Variations. *J. Geophys. Res.* 82, 1977, pp. 2170-2174.
100. Dulk, G. A.: Implications on the Structure of the Transition Region and Corona from Radio Observations. *Proceedings of the November 7-10, 1977 OSO-8 Workshop* (eds., E. Hansen and S. Schaffner), University of Colorado, Boulder, CO, 1977, pp. 77-82.
101. Dulk, G. A., Sheridan, K. V., Smerd, S. F., and Withbroe, G. L.: Radio and EUV Observations of a Coronal Hole. *Solar Phys.* 52, 1977, pp. 349-367.
102. Feldman, U. and Doschek, G. A.: The Emission Spectrum of the Hydrogen Balmer Series Observed Above the Solar Limb from Skylab II. Active Regions. *Astrophys. J.* 212, 1977, pp. 913-922.
103. Feldman, W. C., Asbridge, J. R., Bame, S. J., and Gosling, J. T.: Plasma and Magnetic Fields from the Sun. *The Solar Output and Its Variation* (ed. O. R. White), Colorado Associated University Press, Boulder, CO, 1977, pp. 351-382.
104. Francis, M. H. and Roussel-Dupré, R.: The Si IV $\lambda 1393$ Line in a Coronal Hole Compared to the Quiet Sun from OSO-8 Observations. *Solar Phys.* 53, 1977, pp. 465-470.

REFERENCES (Continued)

105. Frankenthal, S. and Krieger, A. S.: On the Nature of Photospheric Magnetic Fields Beneath Large Coronal Holes. *Solar Phys.* 55, 1977, pp. 83-97.
106. Harvey, J. W. and Sheeley, N. R. Jr.: A Comparison of He II 304 Å and He I 10830 Å Spectroheliograms. *Solar Phys.* 54, 1977, pp. 343-351.
107. Harvey, J. W. and Sheeley, N. R. Jr.: A Comparison of He II 304 Å and He I 10830 Å Spectroheliograms. *B.A.A.S.* 9, 1977, p. 325.
108. Hearn, A. G.: An Exploration of the Observed Differences Between Coronal Holes and Quiet Coronal Regions. *Solar Phys.* 51, 1977, pp. 159-168.
109. Hoang, S. and Steinberg, J. L.: About the Computed Meter-Wavelength Thermal Radiation from Coronal Streamers and Coronal Holes. *Astron. Astrophys. (Res. Notes)* 58, 1977, pp. 287-290.
110. Hollweg, J. V.: Alfvén and Compressive Waves in the Solar Atmosphere. *Proceedings of the November 7-10, 1977 OSO-8 Workshop* (eds., E. Hansen and S. Scaffner), University of Colorado, Boulder, CO, 1977, pp. 424-425.
111. Hollweg, J. V.: Alfvén Waves in the Solar Atmosphere. *Solar Phys.* 56, 1978, pp. 305-333.
112. Houminer, Z.: Scintillation Observations of the Interplanetary Plasma. *Study of Travelling Interplanetary Phenomena 1977* (eds., M. A. Shea, D. F. Smart, and S. T. Wu), *Astrophysics and Space Science Library*, Vol. 71, D. Reidel Publ. Co., Dordrecht, Holland, 1977, pp. 119-141.
113. Howard, R.: Studies of Solar Magnetic Fields. V: The True Average Field Strengths near the Poles. *Solar Phys.* 52, 1977, pp. 243-248.
114. Howard, R. and Švestka, Z.: Development of a Complex of Activity in the Solar Corona. *Solar Phys.* 54, 1977, pp. 65-105.

REFERENCES (Continued)

115. Hundhausen, A.: Plasma Flow from the Sun. The Solar Output and Its Variation. (ed. O. R. White); Colorado Associated University Press, Boulder, CO, 1977, pp. 36-39.
116. Intriligator, D. S.: The Large-Scale and Long Term Evolution of the Solar Wind Speed Distribution and High Speed Streams. Study of Travelling Interplanetary Phenomena 1977 (eds., M. A. Shea, D. F. Smart, and S. T. Wu), Astrophysics and Space Science Library, Vol. 71, D. Reidel Publ. Co., Dordrecht, Holland, 1977, pp. 195-225.
117. Intriligator, D. S.: Additional Evidence Consistent with Solar Cycle Variations in the Solar Wind. *Astrophys. J.* 221, 1978, pp. 1009-1013.
118. Iucci, N., Orsini, S., Parisi, M., Storini, M., and Villoresi, G.: Cosmic Ray Perturbations Produced by Fast Streams Coming from Quiet Solar Regions — Coronal Holes. Contributed Papers to the Study of Travelling Interplanetary Phenomena/1977 (eds., M. A. Shea, D. F. Smart, and S. T. Wu), AFGL-TR-77-0309, Special Report No. 209, Air Force Geophysics Laboratory, Hanscom AFB, MA, 29 December 1977, pp. 209-220.
119. Jacques, S. A.: Momentum and Energy Transport by Waves in the Solar Atmosphere and Solar Wind. *Astrophys. J.* 215, 1977, pp. 942-951.
120. Kakinuma, T.: Observations of Interplanetary Scintillation: Solar Wind Velocity Measurements. Study of Travelling Interplanetary Phenomena 1977 (eds., M. A. Shea, D. F. Smart, and S. T. Wu), Vol. 71, D. Reidel Publ. Co., Dordrecht, Holland, 1977, pp. 101-118.
121. Koutchmy, S.: Study of the June 30, 1973 Trans-Polar Coronal Hole. *Solar Phys.* 51, 1977, pp. 399-407.
122. Levine, R. H.: Evolution of Photospheric Magnetic Field Patterns During Skylab. *Solar Phys.* 54, 1977, pp. 327-341.
123. Levine, R. H.: Evolution of Open Magnetic Structures on the Sun: The Skylab Period. *Astrophys. J.* 218, 1977, pp. 291-305.

REFERENCES (Continued)

124. Levine, R. H., Altschuler, M. D., Harvey, J. W., and Jackson, B. V.: Open Magnetic Structures on the Sun. *Astrophys. J.* 215, 1977, pp. 636-651.
125. Levine, R. H., Altschuler, M. D., and Harvey, J. W.: Open Magnetic Structures on the Sun. *B.A.A.S.* 8, 1976, p. 326.
126. MacQueen, R. M. and Poland, A. I.: Temporal Evolution of the Equatorial K-Corona. *Solar Phys.* 55, 1977, pp. 143-159.
127. Marsh, K. A.: The Calcium K-Line Network in Coronal Holes. *Solar Phys.* 52, 1977, pp. 343-348.
128. Maxson, C. W. and Vaiana, G. S.: Determination of Plasma Parameters from Soft X-Ray Images for Coronal Holes (Open Magnetic Field Configurations) and Coronal Large-Scale Structures (Extended Closed-Field Configurations). *Astrophys. J.* 215, 1977, pp. 919-941.
129. McCabe, M. K., Mickey, D. L., and Chesley, S. E.: Coronal Holes in $\lambda 10830$ He I. *B.A.A.S.* 9, 1977, pp. 371-372.
130. Moore, R. L., Tang, F., Bohlin, J. D., and Golub, L.: $H\alpha$ Macrospicules: Identification with EUV Macrospicules and with Flares in X-Ray Bright Points. *Astrophys. J.* 218, 1977, pp. 286-290.
131. Munro, R. H. and Jackson, B. V.: Physical Properties of a Polar Coronal Hole from 2 to 5 R_{\odot} . *Astrophys. J.* 213, 1977, pp. 874-886.
132. Jackson, B. V.: A Polar Coronal Hole: I. The Three-Dimensional Boundary. *B.A.A.S.* 8, 1976, p. 325.
133. Munro, R. H.: A Polar Coronal Hole: II. Three-Dimensional Density Distribution. *B.A.A.S.* 8, 1976, p. 325.
134. Munro, R. H. and Mariska, J. T.: A Composite Coronal Hole Model. *Proceedings of the November 7-10, 1977 OSO-8 Workshop* (eds., E. Hansen and S. Schaffner), University of Colorado, Boulder, CO, 1977, p. 76.

REFERENCES (Continued)

135. Munro, R. H. and Mariska, J. T.: A Composite Coronal Hole Model. B.A.A.S. 9, 1977, pp. 370-371.
136. Nolte, J. T., Davis, J. M., Gerassimenko, M., Krieger, A. S., and Solodyna, C. V.: Variation of Coronal Holes and Associated Solar Wind Streams with the Scale Size of Emerging Magnetic Flux. B.A.A.S. 9, 1977, p. 346.
137. Nolte, J. T., Davis, J. M., Gerassimenko, M., Krieger, A. S., Solodyna, C. V., and Golub, L.: The Relationship Between Solar Activity and Coronal Hole Evolution. Solar Phys. 60, 1978, pp. 143-153.
138. Nolte, J. T., Davis, J. M., Gerassimenko, M., Lazarus, A. J., and Sullivan, J. D.: A Comparison of Solar Wind Streams and Coronal Structure near Solar Minimum. Geophys. Res. Letters 4, 1977, pp. 291-294.
139. Nolte, J. T., Krieger, A. S., Roelof, E. C., and Gold, R. E.: High Coronal Structure of High Velocity Solar Wind Stream Sources. Solar Phys. 51, 1977, pp. 459-471.
140. Nolte, J. T. and Roelof, E. C.: Solar Wind, Energetic Particles, and Coronal Magnetic Structure: The First Year of Solar Cycle 20. J. Geophys. Res. 82, 1977, pp. 2175-2186.
141. Papagiannis, M. D. and Wefer, F. L.: Coronal Hole Observations at 1420 and 2600 MHz with the Arecibo Radiotelescope. B.A.A.S. 9, 1977, p. 617.
142. Raghavan, N.: Medium Resolution EUV Observations and Network Structure. Solar Phys. 54, 1977, pp. 363-370.
143. Rosenberg, F. D., Feldman, U. and Doschek, G. A.: The Emission Spectrum of the Hydrogen Balmer Series Observed Above the Solar Limb from Skylab. I. A Quiet Sun and a Polar Coronal Hole. Astrophys. J. 212, 1977, pp. 905-912.

REFERENCES (Continued)

144. Rosenberg, F. D., Feldman, U., and Doschek, G. A.: Densities in the Solar Chromosphere Above the Quiet Sun and a Coronal Hole Derived from the Hydrogen Balmer Lines. *B.A.A.S.* 8, 1976, p. 338.
145. Saito, K., Polans, A. I., and Munro, R. H.: A Study of the Background Corona near Solar Minimum. *Solar Phys.* 55, 1977, pp. 121-134.
146. Saito, K., Poland, A., Munro, R., and MacQueen, R.: The Background Corona near Solar Minimum. *B. A. A. S.* 9, 1977, p. 371.
147. Sandlin, G. D., Brueckner, G. E., and Tousey, R.: Forbidden Lines of the Solar Corona and Transition Zone: 975-3000 Å. *Astrophys. J.* 214, 1977, pp. 898-904.
148. Sheeley, N. R. Jr., Asbridge, J. R., Bame, S. J., and Harvey, J. W.: A Pictorial Comparison of Interplanetary Magnetic Field Polarity, Solar Wind Speed, and Geomagnetic Disturbance Index During the Sunspot Cycle. *Solar Phys.* 52, 1977, pp. 485-495.
149. Shibasaki, K., Ishiguro, M., Enome, S., and Tanaka, H.: A Coronal Hole Observed by $\lambda 8$ -cm Radioheliograph. Contributed Papers to the Study of Travelling Interplanetary Phenomena/1977 (eds., M. A. Shea, D. F. Smart, and S. T. Wu), AFGL-TR-77-0309, Special Report No. 209, Air Force Geophysics Laboratory, Hanscom AFB, MA, 29 December, 1977, pp. 263-274.
150. Solodyna, C. V., Krieger, A. S., and Nolte, J. T.: Observations of the Birth of a Small Coronal Hole. *Solar Phys.* 54, 1977, pp. 123-124.
151. Solodyna, C. V., Nolte, J. T., and Krieger, A. S.: Soft X-Ray Emission near Coronal Hole Boundaries. *B. A. A. S.* 8, 1976, p. 338.
152. Steinolfson, R. S. and Tandberg-Hanssen, E.: Thermally Conductive Flows in Coronal Holes. *Solar Phys.* 55, 1977, pp. 99-109.
153. Stenflo, J. O.: Solar-Cycle Variations in the Differential Rotation of Solar Magnetic Fields. *Astron. Astrophys.* 61, 1977, pp. 797-804.

REFERENCES (Continued)

154. Stix, M.: Coronal Holes and the Large-Scale Magnetic Field. *Astron. Astrophys.* 59, 1977, pp. 73-78.
155. Suess, S. T., Richter, A. K., Winge, C. R., and Nerney, S. F.: Solar Polar Coronal Hole—A Mathematical Simulation. *Astrophys. J.* 217, 1977, pp. 296-305.
156. ^VSvestka, Z., Solodyna, C. V., Howard, R., and Levine, R. H.: Open Magnetic Fields in Active Regions. *Solar Phys.* 55, 1977, pp. 359-369.
157. ^VSvestka, Z., Solodyna, C. V., Howard, R., and Levine, R. H.: Open Magnetic Fields in Active Regions. *B.A.A.S.* 9, 1977, p. 344.
158. Timothy, J. G.: The Solar Spectrum Between 300 and 1200 Å. *The Solar Output and Its Variation* (ed. O. R. White), Colorado Associated University Press, Boulder, CO, 1977, pp. 237-259.
159. Tyler, G. L., Brenkle, J. P., Komarek, T. A., and Zygielbaum, A. I.: The Viking Solar Corona Experiment. *J. Geophys. Res.* 82, 1977, pp. 4335-4340.
160. Wefer, F. L. and Papagiannis, M. D.: Observations of Enhanced Radio Emission at 15 GHz from a Coronal Hole Region. *B.A.A.S.* 9, 1977, pp. 617-618.
161. Withbroe, G. L.: Models for the Solar Transition Layer. *Proceedings of the November 7-10, 1977 OSO-8 Workshop* (eds., E. Hansen and S. Schaffner), University of Colorado, Boulder, CO, 1977, pp. 2-27.
162. Yoshimura, H.: Solar-Cycle Evolution of the Coronal General Magnetic Field of 1959-1974 and the Synchronous Variation of High-Speed Solar Wind Streams and Galactic Cosmic Rays. *Solar Phys.* 54, 1977, pp. 229-258.
163. Ahmad, I. A. and Webb, D. F.: X-Ray Analysis of a Polar Plume. *Solar Phys.* 58, 1978, pp. 323-336.

REFERENCES (Continued)

164. Bohlin, J. D. and Sheeley, N. R. Jr.: Extreme Ultraviolet Observations of Coronal Holes. II. Association of Holes with Solar Magnetic Fields and a Model for Their Formation During the Solar Cycle. *Solar Phys.* 56, 1978, pp. 125-151.
165. Broussard, R. M., Sheeley, N. R. Jr., Tousey, R., and Underwood, J. H.: A Survey of Coronal Holes and Their Solar Wind Associations Throughout Sunspot Cycle 20. *Solar Phys.* 56, 1978, pp. 161-183.
166. Broussard, R. M., Underwood, J. H., Tousey, R., and Sheeley, N. R. Jr.: Observations of Coronal Holes Throughout Sunspot Cycle 20. *B.A.A.S.* 8, 1976, p. 557.
167. Chambe, G.: Comparison of the EUV and Radioelectric Diagnostics of the Solar Chromosphere-Corona Transition Region. *Astron. Astrophys.* 70, 1978, pp. 225-263.
168. Cuperman, S. and Dryer, M.: Long-Term Correlation Between Latitude-Dependent Solar Activity and Solar Wind Streams. *Astrophys. J.* 223, 1978, pp. 601-604.
169. Cuperman, S., Levush, B., Dryer, M., Rosenbauer, H., and Schwenn, R.: On the Radial Expansion of the Solar Wind Plasma Between 0.3 and 1.0 Astronomical Units. *Astrophys. J.* 226, 1978, pp. 1120-1128.
170. Cushman, G. W. and Rense, W. A.: Solar He II (304 \AA) and Si XI (303 \AA) Line Profiles. *Solar Phys.* 58, 1978, pp. 299-305.
171. Dittmer, P. H., Scherrer, P. H., and Wilcox, J. M.: An Observational Search for Large-Scale Organization of Five-Minute Oscillations on the Sun. *Solar Phys.* 57, 1978, pp. 3-11.
172. Doschek, G. A., and Feldman, U.: EUV Spectra from Skylab (1175-1940 \AA): Mass Motions in the Transition Zone in Regions of Solar Activity. *Astron. Astrophys.* 69, 1978, pp. 11-21.

REFERENCES (Continued)

173. Doschek, G. A., Feldman, U., Bhatia, A. K., and Mason, H. E.: Densities in the Quiet Sun and Polar Coronal Holes from EUV Line Ratios Involving O III (1666.15 Å). *Astrophys. J.* 226, 1978, pp. 1129-1134.
174. Eadon, E. J., and Billings, D. E.: Area Variation with Temperature of Supergranule Network Features in the Solar Transition Zone. *Solar Phys.* 58, 1978, pp. 31-36.
175. Eadon, E. J., and Billings, D. E.: The Shape of Network Elements in the Solar Transition Zone. *B.A.A.S.* 9, 1977, p. 569.
176. Feldman, U. and Doschek, G. A.: The Electron Density at 10^5 K in Different Regions of the Solar Atmosphere Derived from an Intersystem Line of O IV. *Astron. Astrophys.* 65, 1978, pp. 215-222.
177. Feldman, W. C., Asbridge, J. R., Bame, S. J., and Gosling, J. T.: Long-Term Variations of Selected Solar Wind Properties: IMP 6, 7, and 8 Results. *J. Geophys. Res.* 83, 1978, pp. 2177-2189.
178. Feldman, W. C., Asbridge, J. R., Bame, S. J., Gosling, J. T., Lemons, D. S.: Characteristic Electron Variations Across Simple High-Speed Solar Wind Streams. *J. Geophys. Res.* 83, 1978, pp. 5285-5295.
179. Fenimore, E. E., Asbridge, J. R., Bame, S. J., Feldman, W. C., and Gosling, J. T.: The Power Spectrum of the Solar Wind Speed for Periods Greater than 10 Days. *J. Geophys. Res.* 83, 1978, pp. 4353-4357.
180. Fisher, R. R.: $\lambda 5303$ Fe XIV Density Models of the Inner Solar Corona. *Solar Phys.* 57, 1978, pp. 119-128.
181. Glackin, D. L., Linsky, J. L., Mango, S. A. and Bohlin, J. D.: The Solar XUV He I and He II Emission Lines. II. Intensity Ratios and Distribution Functions. *Astrophys. J.* 222, 1978, pp. 707-715.

REFERENCES (Continued)

182. Jacques, S. A.: Solar Wind Models with Alfvén Waves. *Astrophys. J.* 226, 1978, pp. 632-649.
183. Joselyn, J. and Holzer, T. E.: A Steady Three-Fluid Coronal Expansion for Nonspherical Geometries. *J. Geophys. Res.* 83, 1978, pp. 1019-1026.
184. Lantos, P.: A Reinterpretation of the Centimetric Quiet Sun and the Density in the Long Distance Arches. *Astron. Astrophys.* 62, 1978, pp. 69-74.
185. Levine, R. H.: The Relation of Open Magnetic Structures to Solar Wind Flow. *J. Geophys. Res.* 83, 1978, pp. 4193-4199.
186. Levine, R. H., Altschuler, M. D., Harvey, J. W.: Solar Sources of the Interplanetary Magnetic Field and Solar Wind. *J. Geophys. Res.* 82, 1977, pp. 1061-1065.
187. Mango, S. A., Bohlin, J. D., Glackin, D. L., and Linsky, J. L.: The Solar XUV He I and He II Emission Lines. I. Intensities and Gross Center-to-Limb Behavior. *Astrophys. J.* 220, 1978, pp. 683-691.
188. Mango, S., Bohlin, D., Glackin, D., and Linsky, J.: Preliminary Analysis of NRL Skylab Spectroheliograms in Lines of He I and He II. *B.A.A.S.* 8, 1976, p. 332.
189. Mariska, J. T.: Analysis of Extreme-Ultraviolet Observations of a Polar Coronal Hole. *Astrophys. J.* 225, 1978, pp. 252-258.
190. Mariska, J. T.: Extreme Ultraviolet Observations of a Polar Coronal Hole. *B.A.A.S.* 8, 1976, p. 338.
191. Mariska, J. T. and Withbroe, G. L.: Temperature Gradients in the Inner Corona. *Solar Phys.* 60, 1978, pp. 67-82.
192. Marsh, K. A.: D₃ Spicules and the Lower Chromosphere. *Solar Phys.* 57, 1978, pp. 37-48.

REFERENCES (Continued)

193. McIntosh, P. S.: Atlas of Large-Scale Solar Magnetic Patterns. B.A.A.S. 10, 1978, p. 730.
194. Mihalov, J. D., and Wolfe, J. H.: Pioneer-10 Observation of the Solar Wind Proton Temperature Heliocentric Gradient. Solar Phys. 60, 1978, pp. 399-406.
195. Musman, S. and Altrock, R. C.: Recurrent Geomagnetic Disturbances and Coronal Holes as Observed in Fe XIV $\lambda 5303 \text{ \AA}$. J. Geophys. Res. 83, 1978, pp. 4817-4822.
196. Altrock, R. C. and Musman, S. A.: Coronal Holes as Observed in Fe XIV 5303 \AA . B.A.A.S. 9, 1977, p. 432.
197. Niedner, M. B. Jr., Rothe, E. D., and Brandt, J. C.: Interplanetary Gas. XXII. Interaction of Comet Kohoutek's Ion Tail with the Compression Region of a Solar-Wind Corotating Stream. Astrophys. J. 221, 1978, pp. 1014-1025.
198. Niedner, M. B., Rothe, E. D., and Brandt, J. C.: A Solar-Wind Produced Structure in the Plasma Tail of Comet Kohoutek. B.A.A.S. 9, 1977, p. 344.
199. Nolte, J. T., Davis, J. M., and Sullivan, J. D.: Solar Wind Stream Structure During the Early Phase of Solar Cycles 20 and 21. Solar Phys. (Res. Notes) 60, 1978, pp. 207-210.
200. Nolte, J. T., Gerassimenko, M., Krieger, A. S., and Solodyna, C. V.: Coronal Hole Evolution by Sudden Large Scale Changes. Solar Phys. 56, 1978, pp. 153-159.
201. Nolte, J. T., Gerassimenko, M., Krieger, A. S., and Solodyna, C. V.: Large-Scale Changes in Coronal Hole Boundaries. B.A.A.S. 8, 1976, p. 557.
202. Nolte, J. T., Krieger, A. S., and Solodyna, C. V.: Short Term Evolution of Coronal Hole Boundaries. Solar Phys. 57, 1978, pp. 129-139.

REFERENCES (Continued)

203. Pneuman, G. W., Hansen, S. F., and Hansen, R. T.: On the Reality of Potential Magnetic Fields in the Solar Corona. *Solar Phys.* 59, 1978, pp. 313-330.
204. Poland, A. I.: Motions and Mass Changes of a Persistent Coronal Streamer. *Solar Phys.* 57, 1978, pp. 141-153.
205. Rabin, D. M. and Moore, R. L.: Polar Coronal Holes and the Variation with Latitude of the Height of the H α Chromosphere. *B.A.A.S.* 10, 1978, pp. 430-431.
206. Schwenn, R., Montgomery, M. D., Rosenbauer, H., Miggenrieder, H., Mühlhäuser, K. H., Bame, S. J., Feldman, W. C., and Hansen, R. T.: Direct Observation of the Latitudinal Extent of a High-Speed Stream in the Solar Wind. *J. Geophys. Res.* 83, 1978, pp. 1011-1017.
207. Shah, G. N., Kaul, C. L., Razdan, H., and Bemalkhedkar, M. M.: Recurrent Forbush Decreases and the Relationship Between Active Regions and M Regions. *J. Geophys. Res.* 83, 1978, pp. 3740-3744.
208. Sheeley, N. R. Jr.: The Equatorward Extent of Auroral Activity During 1973-1974. *Solar Phys.* 58, 1978, pp. 405-422.
209. Sheeley, N. R. Jr., and Harvey, J. W.: Coronal Holes, Solar Wind Streams, and Geomagnetic Activity During the New Sunspot Cycle. *Solar Phys.* 59, 1978, pp. 159-173.
210. Sheeley, N. R. and Harvey, J. W.: Coronal Holes, Solar Wind Streams and Geomagnetic Activity During the New Solar Cycle. *B.A.A.S.* 10, 1978, p. 461.
211. Speich, D. M., Smith, J. B. Jr., Wilson, R. M., and McIntosh, P. S.: Solar Activity During Skylab — Its Distribution and Relation to Coronal Holes. NASA TM-78166, Marshall Space Flight Center, AL, April 1978.
212. Svalgaard, L., Duvall, T. L. Jr., and Scherrer, P. H.: The Strength of the Sun's Polar Fields. *Solar Phys.* 58, 1978, pp. 225-240.

REFERENCES (Continued)

213. Trottet, G. and Lantos, P.: Brightness Temperatures of Solar Coronal Holes and Arches at Metric Wavelengths and the Coherency Between Radio and UV Observations. *Astron. Astrophys.* 70, 1978, pp. 245-253.
214. Vernazza, J. E. and Mason, H. E.: Density Sensitivity of the Solar EUV Emission from Boron-Like Ions. *Astrophys. J.* 226, 1978, pp. 720-728.
215. Vorpahl, J. A. and Broussard, R. M.: Physical Parameters Defining the Changing Structures of a Coronal Hole. *Astrophys. J.* 219, 1978, pp. 300-303.
216. Broussard, R. M. and Vorpahl, J. A.: Changes in Coronal Holes and the Accompanying Magnetic Fields. *B.A.A.S.* 8, 1976, p. 326.
217. Webb, D. F., McIntosh, P. S., Nolte, J. T., and Solodyna, C. V.: Evidence Linking Coronal Transients to the Evolution of Coronal Holes. *Solar Phys.* 58, 1978, pp. 389-396.
218. Wefer, F. L., Papagiannis, M. D., Van Steenberg, M., and Varner, T. M.: Synoptic Charts of Coronal Holes and 9.1 cm Solar Data, May through August 1973, *B.A.A.S.* 10, 1978, p. 684.
219. Whang, Y. C. and Chien, T. H.: Expansion of the Solar Wind in High-Speed Streams. *Astrophys. J.* 221, 1978, pp. 350-361.
220. Woo, R.: Radial Dependence of Solar Wind Properties Deduced from Helios 1/2 and Pioneer 10/11 Radio Scattering Observations. *Astrophys. J.* 219, 1978, pp. 727-739.
221. Zombeck, M. V., Vaiana, G. S., Haggerty, R., Krieger, A. S., Silk, J. K., and Timothy, A.: An Atlas of Soft X-Ray Images of the Solar Corona from Skylab. *Astrophys. J. Suppl. Ser.* 38, 1978, pp. 69-85.
222. Athay, R. G.: The Solar Chromosphere and Corona: Quiet Sun. *Astrophysics and Space Science Library*, Vol. 53, D. Reidel Publ. Co., Dordrecht, Holland, 1976.

REFERENCES (Continued)

223. Belew, L. E. (ed.): Skylab, Our First Space Station. NASA SP-400, Washington, D. C., 1977.
224. Bohlin, J. D. and Rubenstein, D. M.: Synoptic Maps of Solar Coronal Hole Boundaries Derived from He II Å Spectroheliograms from the Manned Skylab Missions. World Data Center A for Solar-Terrestrial Physics, Report UAG-51, NOAA, Boulder, CO, November 1975.
225. Bonnet, R. M., Lemaire, P., Vial, J. C., Artzner, G., Gouttebroze, P., Jouchoux, A., Leibacher, J. W., Skumanich, A., and Vidal-Madjar, A.: The LPSP Instrument on OSO 8. II. In-Flight Performance and Preliminary Results. *Astrophys. J.* 211, 1978, pp. 1032-1061.
226. Cook, J. W. and Nicolas, K. R.: Solar C III Line Ratios Observed from Skylab. *B.A.A.S.* 10, 1978, p. 439.
227. Dulk, G. A. and McLean, D. J.: Coronal Magnetic Fields. *Solar Phys.* 57, 1978, pp. 279-295.
228. Dupree, A. K., Foukal, P. V., and Jordan, C.: Plasma Diagnostic Techniques in the Ultraviolet: The C III Density-Sensitive Lines in the Sun. *Astrophys. J.* 209, 1976, pp. 621-632.
229. Eddy, J. A.: A New Sun: The Solar Results from Skylab (ed. R. Ise). NASA SP-402, Washington, D. C., 1979.
230. Erickson, W. C., Gergely, T. E., Kundu, M. R., and Mahoney, M. J.: Determination of the Decameter Wavelength Spectrum of the Quiet Sun. *Solar Phys.* 54, 1977, pp. 57-63.
231. Feldman, U. and Doschek, G. A.: A Search for a Turbulent-Free Region in the Solar Transition Zone. *Astrophys. J. (Letters)* 216, 1977, pp. L119-L121.
232. Feldman, W. C., Abraham-Shrauner, B., Asbridge, J. R., and Bame, S. J.: The Internal Plasma State of the High Speed Solar Wind at 1 AU. *Physics of Solar Planetary Environments* (ed. D. J. Williams), Vol. I, Am. Geophys. Union, Boulder, CO, 1976, pp. 413-427.

REFERENCES (Continued)

233. Friedman, H.: Sun and Earth: A New View of Climate (Part Two).
Astron. Aeron. 17, 1979, pp. 58-63.
234. Gilman, P. A.: Theory of Convection in a Deep Rotating Spherical Shell,
and Its Application to the Sun. Basic Mechanisms of Solar Activity (eds.,
V. Bumba and J. Kleczek), IAU Symp. No. 71, D. Reidel Publ. Co.,
Dordrecht, Holland, 1976, pp. 207-228.
235. Hachenberg, O., Steffen, P., and Harth, W.: The Sun at 8.5 mm
Wavelength-Results of Observations with High Angular Resolution. Solar
Phys. 60, 1978, pp. 105-118.
236. Herman, J.R. and Goldberg, R.A.: Sun, Weather, and Climate. NASA
SP-426, Washington, D. C., 1978.
237. Hundhausen, A. J.: Streams, Sectors and Solar Magnetism. The New
Solar Physics (ed. J. A. Eddy), AAS Selected Symp. No. 17, Westview
Press, Boulder, CO, 1978, pp. 59-133.
238. Kumar, S. and Broadfoot, A. L.: Signatures of Solar Wind Latitudinal
Structure in Interplanetary Lyman- α Emissions: Mariner 10 Observa-
tions. Astrophys. J. 228, 1979, pp. 302-311.
239. McGuire, J. P., Tandberg-Hanssen, E.; Krall, K. R., Wu, S. T., Smith,
J. B., and Speich, D. M.: A Long-Lived Coronal Arch System Observed
in X-Rays. Solar Phys. 52, 1977, pp. 91-100.
240. McKenzie, D. L., Rugge, H. R., Underwood, J. H., and Young, R. M.:
The Quiet Coronal X-Ray Spectrum of Highly Ionized Oxygen and Nitrogen.
Astrophys. J. 221, 1978, pp. 342-349.
241. Mihalov, J. D., and Wolfe, J. H.: Pioneer 10 Observation of the Solar
Wind Proton Temperature Heliocentric Gradient. Solar Phys. 60, 1978,
pp. 399-406.
242. Pasachoff, J. M.: Our Sun. Astronomy 6, 1978, pp. 6-24.

REFERENCES (Concluded)

- 243. Rosner, R., Golub, L., Coppi, B., Vaiana, G. S.: Heating of Coronal Plasma by Anomalous Current Dissipation. *Astrophys. J.* 222, 1978, pp. 317-332.
- 244. Rosner, R., Tucker, W. H., and Vaiana, G. S.: Dynamics of the Quiescent Solar Corona. *Astrophys. J.* 220, 1978, pp. 643-665.
- 245. Rust, D. M.: An Active Role for Magnetic Fields in Solar Flares. *Solar Phys.* 47, 1976, pp. 21-40.
- 246. Serio, S., Vaiana, G. S., Godoli, G., Motta, S., Pirronello, V., and Zappala, R. A.: Configuration and Gradual Dynamics of Prominence-Related X-Ray Coronal Cavities. *Solar Phys.* 59, 1978, pp. 65-86.
- 247. Siscoe, G. L., Crooker, N. U., and Christopher, L.: A Solar Cycle Variation of the Interplanetary Magnetic Field. *Solar Phys.* 56, 1978, pp. 449-461.
- 248. Spruit, H.: Magnetic Flux Tube Models. Proceedings of the November 7-10, 1977 OSO-8 Workshop (eds., E. Hansen and S. Schaffner), University of Colorado, Boulder, CO, 1977, pp. 83-97.
- 249. Underwood, J. H.: X-Ray Optics. *Am. Sci.* 66, 1978, pp. 476-486.
- 250. Vorpahl, J. and Underwood, J. H.: (X-Ray photograph of Sun) *Solar Phys.* 49, 1976, p. 2.
- 251. Wagner, W. J. and Gilliam, L. B.: A Possible Example of Giant Convective Cells Delineated by Magnetic Fields. *Solar Phys. (Res. Notes)* 50, 1976, pp. 265-268.
- 252. Wefer, F. L.: Observations of Coronal Hole Associated Features at Wavelengths of 2.0 cm and 8.6 mm. Megatek Corporation, Final Report No. R2005-031-F-1, Contract No. N00123-75-C-0328, Naval Electronics Laboratory Center, San Diego, CA, July 1976.
- 253. Wilson, R. M., Teuber, D. L., Watkins, J. R., Thomas, D. T., and Cooper, C. M.: Image Data-Processing System for Solar Astronomy. *Appl. Optics* 16, 1977, pp. 944-949.

APPENDIX A

REFERENCED ARTICLES FROM WILSON [1]

Adams, W. M. and Sturrock, P. A.: A Model of Coronal Holes. *Astrophys. J.* 202, 1975, pp. 259-264.

Adams, W. M. and Sturrock, P. A.: A Model of Coronal Holes. *B.A.A.S.* 7, 1975, p. 358.

Altschuler, M. D. and Newkirk, G.: Magnetic Fields and the Structure of the Solar Corona. *Solar Phys.* 9, 1969, pp. 131-149.

Altschuler, M. D. and Perry, R. M.: On Determining the Electron Density Distribution of the Solar Corona from K-Coronameter Data. *Solar Phys.* 23, 1972, pp. 410-428.

Altschuler, M. D. Trotter, D. E., and Orrall, F. Q.: Coronal Holes. *Solar Phys.* 26, 1972, pp. 354-365.

Antonucci, E. and Svalgaard, L.: Rigid and Differential Rotation of the Solar Corona. *Solar Phys.* 34, 1974, pp. 3-10.

Athay, R. G. and Menzel, D. H.: A Model of the Chromosphere from the Helium and Continuum Emissions. *Astrophys. J.* 123, 1956, pp. 285-298.

Avignon, Y., Lantos, P., Palagi, F., and Patriarchi, P.: The Quiet Sun Brightness at 408 MHz. *Solar Phys.* 45, 1975, pp. 141-145.

Bartels, J.: Twenty-Seven Day Recurrences in Terrestrial-Magnetic and Solar Activity, 1923-1933, *J. Geophys. Res.* 39, 1934, p. 201.

Beckers, J. M.: Solar Spicules. *Annual Review of Astronomy and Astrophysics* (eds., L. Goldberg, D. Layzer, and J. G. Phillips), Vol. 10, Annual Rev. Inc., Palo Alto, CA, 1972, pp. 73-100.

Beckers, J. M.: Solar Spicules. *Solar Phys.* 3, 1968, pp. 367-433.

Bell, B. and Noci, G.: Are Coronal Holes M Regions? B.A.A.S. 5, 1973, p. 269.

Bell, B., and Noci, G.: Coronal Holes as M Regions: Correlation Between Solar Features and Solar Wind Disturbances. Skylab Solar Workshop (ed. G. Righini), Osservazioni e Memorie, Arcetri Astrophysical Observatory, Fascicolo 104, Baccini and Chiappi, Florence, Italy, 1974, pp. 111-119.

Bohlin, J. D.: Letter to Participants of the Skylab Solar Workshop on Coronal Holes (December), 1975.

Bohlin, J. D., Rubenstein, D. M., and Sheeley, N. R. Jr.: The Sun's Polar Caps as Coronal Holes: Their Sizes, Evolution, and Phenomenology During the Skylab Mission. B.A.A.S. 7, 1975, p. 457.

Bohlin, J. D., Vogel, S. N., Purcell, J. D., Sheeley, N. R. Jr., Tousey, R., and VanHoosier, M. E.: A Newly Observed Solar Feature: Macrospicules in He II 304 Å. Astrophys. J. (Letters) 197, 1975, pp. L133-L135.

Bohlin, J. D., Vogel, S. N., Purcell, J. D., Sheeley, N. R. Jr., Tousey, R., and VanHoosier, M. E.: Macrospicules in He II 304 Å Over the Sun's Polar Cap. B.A.A.S. 7, 1975, p. 354.

Brueckner, G. E. and Bartoe, J.-D.F.: The Fine Structure of the Solar Atmosphere in the Far Ultraviolet. Solar Phys. 38, 1974, pp. 133-156.

Burton, W. M.: Extreme Ultraviolet Observations of Active Regions in the Solar Corona. Structure and Development of Solar Active Regions (ed. K. Kiepenheuer), IAU Symp. No. 35, D. Reidel Publ. Co., Dordrecht, Holland, 1968, pp. 395-402.

Burton, W. M.: Solar Photography in the Extreme Ultraviolet. Solar Phys. 8, 1969, pp. 53-71.

Chapman, S.: The Absorption and Dissociative or Ionizing Effect of Monochromatic Radiation in an Atmosphere on a Rotating Earth. Proc. Phys. Soc. 43, 1931, pp. 26-45.

Chiuderi, F., Fürst, E., Hirth, W., and Lantos, W.: Limb Brightening and Dark Features Observed at 6 cm Wavelength. Astron. Astrophys. 39, 1975, pp. 429-434.

Doschek, G. A., Feldman, U., and Tousey, R.: Limb-Brightening Curves of XUV Transition Zone Lines in the Quiet Sun and in a Polar Coronal Hole Observed from Skylab. *Astrophys. J. (Letters)* 202, 1975, pp. L151-L154.

Drago, F.: A Coronal Hole Observed at X, UV, and Radio Wavelengths. *Skylab Solar Workshop* (ed. G. Righini), Osservazioni e Memorie, Arcetri Astrophysical Observatory, Fascicolo 104, Baccini and Chiappi, Florence, Italy, 1974, pp. 120-124.

Dulk, G. A. and Sheridan, K. V.: The Structure of the Middle Corona from Observations at 80 and 160 MHz. *Solar Phys.* 36, 1974, pp. 191-202.

Feldman, U., Doschek, G. A., and Tousey, R.: The Intensities and Profiles of XUV Transition Zone Lines in a Quiet Sun Region Compared to a Polar Coronal Hole. *Astrophys. J. (Letters)* 202, 1975, pp. L147-L150.

Feldman, U., Doschek, G. A., VanHoosier, M. E., and Tousey, R.: The 1640.4 H α Line of He II Observed from Skylab. *Astrophys. J. (Letters)* 199, 1975, pp. L67-L70.

Fisher, R. and Musman, S.: Detection of Coronal Holes from $\lambda 5303$ FeXIV Observations. *Astrophys. J.* 195, 1975, pp. 801-803.

Foukal, P.: Spectroscopic Evidence for a Higher Rotation Rate of Magnetized Plasma at the Photosphere. *Astrophys. J. (Letters)* 203, 1976, pp. L145-L148.

Fürst, E. and Hirth, W.: A Coronal Hole Observed at 10.7 GHz with a Large Single Dish. *Solar Phys.* 42, 1975, pp. 157-161.

Garcia, J. D. and Mack, J. E.: Energy Level and Line Tables for One-Electron Atomic Spectra. *J. Opt. Soc. Am.* 55, 1965, pp. 654-685.

Gold, R. E., Krimigis, S. M., Roelof, E. C., Krieger, A. S., and Nolte, J. T.: Enhanced ~ 3 MeV Helium and Medium Fluxes Associated with Coronal Holes. *B.A.A.S.* 7, 1975, pp. 458.

Goldberg, L.: Research with Solar Satellites. *Astrophys. J.* 191, 1974, pp. 1-37.

Goldberg, L., Noyes, R. W., Parkinson, W. H., Reeves, E. M., and Withbroe, G. L.: Ultraviolet Solar Images from Space. *Science* 162, 1968, pp. 95-99.

Gurman, J. B., Withbroe, G. L., and Harvey, J. W.: A Comparison of EUV Spectroheliograms and Photospheric Magnetograms. *Solar Phys.* 34, 1974, pp. 105-111.

Harvey, J. W., Krieger, A. S., Davis, J. M., Timothy, A. F., and Vaiana, G. S.: Comparison of Skylab X-Ray and Ground-Based Helium Observations. *B.A.A.S.* 7, 1975, p. 358.

Harvey, J., Krieger, A. S., Timothy, A. F., and Vaiana, G. S.: Comparison of Skylab X-Ray and Ground-Based Helium Observations. *Skylab Solar Workshop* (ed. G. Righini), *Osservazioni e Memorie, Arcetri Astrophysical Observatory, Fascicolo 104*, Baccini and Chiappi, Florence, Italy, 1974, pp. 50-58.

Henze, W., Wefer, F., Bleiweiss, M., and Baugher, C.: Solar Chromospheric Radio Observation of a Coronal Hole. *B.A.A.S.* 6, 1974, p. 428.

Hirayama, T.: Spectral Analysis of Four Quiescent Prominences Observed at the Peruvian Eclipse. *Solar Phys.* 17, 1971, pp. 50-75.

Howard, R. and Harvey, J.: Spectroscopic Determinations of Solar Rotation. *Solar Phys.* 12, 1970, pp. 23-51.

Huber, M. C. E., Foukal, P. V., Noyes, R. E., Reeves, E. M., Schmahl, E. J., Timothy, J. G., Vernazza, J. E., and Withbroe, G. L.: Extreme-Ultraviolet Observations of Coronal Holes: Initial Results from Skylab. *Astrophys. J. (Letters)* 194, 1974, pp. L115-L118.

Jordan, C.: The Intensities of Helium Lines in the Solar EUV Spectrum. *Mon. Not. Roy. Astron. Soc.* 170, 1975, pp. 429-440.

Krieger, A., Barrett, T., Timothy, A. F., Vaiana, G. S., and Van Speybroeck, L.: Large Scale Coronal X-Ray Structures. *B.A.A.S.* 4, 1972, p. 386.

Krieger, A. S., Timothy, A. F., and Roelof, E. C.: A Coronal Hole and Its Identification as the Source of a High Velocity Solar Wind Stream. *Solar Phys.* 29, 1973, pp. 505-525.

Krieger, A. S., Timothy, A. F., Vaiana, G. S., Lazarus, A. J., and Sullivan, J. D.: X-Ray Observations of Coronal Holes and Their Relation to High Velocity Solar Wind Streams. *Solar Wind Three* (ed. C. T. Russell), *Institute of Geophysics and Planetary Physics, University of California, Los Angeles, CA*, 1974, pp. 132-139.

Krieger, A. S., Vaiana, G. S., and Van Speybroeck, L. P.: The X-Ray Corona and the Photospheric Magnetic Field. *Solar Magnetic Fields* (ed. R. Howard), IAU Symp. No. 43, D. Reidel Publ. Co., Dordrecht, Holland, 1971, pp. 397-412.

Kuperus, M. and Athay, R. G.: On the Origin of Spicules in the Chromosphere-Corona Transition Region. *Solar Phys.* 1, 167, pp. 361-370.

Lantos, P. and Avignon, Y.: The Metric Quiet Sun During Two Cycles of Activity and the Nature of the Coronal Holes. *Astron. Astrophys.* 41, 1975, pp. 137-142.

Liebenberg, D. H., Bessey, R., and Watson, B.: Solar Wind Development in the Middle Corona. *B.A.A.S.* 7, 1975, p. 358.

Livingston, W. C., Harvey, J., Pierce, A. K., Schrage, D., Gillespie, B., Simmons, J., and Slaughter, C.: Kitt Peak 60-cm Vacuum Telescope. *Appl. Opt.* 15, 1976, pp. 33-39.

Lundquist, C. A.: Conclusions from Skylab. AIAA Paper No. 75-260, Paper presented AIAA 11th Annual Meeting and Technical Display, Washington, D. C., 25-27 February 1975.

Mariska, J. T. and Withbroe, G. L.: Analysis of EUV Limb-Brightening Observations from ATM. *Solar Phys.* 44, 1975, pp. 55-68.

Mariska, J. T. and Withbroe, G. L.: Extreme Ultraviolet Solar Limb Brightening Observations. *B.A.A.S.* 7, 1975, p. 460.

Munro, R. H. and Withbroe, G. L.: Properties of a Coronal Hole Derived from Extreme-Ultraviolet Observations. *Astrophys. J.* 176, 1972, pp. 511-520.

Neupert, W. M. and Pizzo, V.: Solar Coronal Holes as Sources of Recurrent Geomagnetic Disturbances. *J. Geophys. Res.* 79, 1974, pp. 3701-3709.

Newkirk, G., Jr.: The Solar Corona in Active Regions and the Thermal Origin of the Slowly Varying Component of Solar Radio Radiation. *Astrophys. J.* 133, 1961, pp. 983-1013.

- Newton, H. W. and Nunn, M. L.: The Sun's Rotation Derived from Sunspots 1934-1944 and Additional Results. *Mon. Not. Roy. Astron. Soc.* 111, 1951, pp. 413-421.
- Noci, G.: Energy Budget in Coronal Holes. *Solar Phys.* 28, 1973, pp. 403-407.
- Nolte, J. T., Krieger, A. S., Timothy, A. F., Vaiana, G. S., and Zombeck, M. V.: An Atlas of Coronal Hole Boundary Positions May 28 to November 21, 1973. ASE-3787, 1976.
- Nolte, J., Krieger, A. S., Webb, D., Vaiana, G. S., Lazarus, A. J., Sullivan, J., and Timothy, A. F.: The Coronal Source of Recurrent High Speed Solar Wind Streams. *B.A.A.S.* 7, 1975, p. 358.
- Palagi, F., Patriarchi, P., and Speroni, N.: Observations of the Sun at 408 MHz. *Skylab Solar Workshop* (ed. G. Righini), *Osservazioni e Memorie*, Arcetri Astrophysical Observatory, Fascicolo 104, Baccini and Chiappi, Florence, Italy, 1974, pp. 125-128.
- Parker, E. N.: A Mechanism for Magnetic Enhancement of Sound-Wave Generation and the Dynamical Origin of Spicules. *Astrophys. J.* 140, 1964, pp. 1170-1181.
- Pneuman, G. W.: The Solar Wind and the Temperature-Density Structure of the Solar Corona. *Solar Phys.* 28, 1973, pp. 247-262.
- Pope, T. and Schoolman, S. A.: Height of Helium Emission in the Chromosphere. *Solar Phys.* 42, 1975, pp. 47-51.
- Reeves, E. M. and Dupree, A. K.: EUV Solar Spectroscopy from Skylab and Some Implications for Atomic Physics. Center for Astrophysics, Preprint Series No. 424, submitted to Proceedings of the Fourth International Conference on Beam-Foil Spectroscopy, 12 November 1975.
- Reeves, E. M., Noyes, R. W., and Withbroe, G. L.: Observing Programs in Solar Physics During the 1973 ATM Skylab Program. *Solar Phys.* 27, 1972, pp. 251-270.
- Reeves, E. M. and Parkinson, W. H.: An Atlas of Extreme-Ultraviolet Spectroheliograms from OSO-IV. *Astrophys. J. Suppl. Ser.* 21, 1970, pp. 1-30.

Roelof, E. C.: Coronal Structure and the Solar Wind. Solar Wind Three (ed. C. T. Russell), Institute of Geophysics and Planetary Physics, University of California, Los Angeles, CA, 1974, pp. 98-131.

Roelof, E. C., Cupperman, S., and Sternlieb, A.: On the Correlation of Coronal Green-Line Intensity and Solar Wind Velocity. Solar Phys. 41, 1975, pp. 349-366.

Schneider, W. C. and Green, W. D. Jr.: The Skylab Experiment Program. Advances in Space Sciences and Technology (ed. F. I. Ordway III), Vol. 11, Academic Press, New York, NY, 1972, pp. 329-436.

Schneider, W. C. and Green, W. D. Jr.: The Skylab Orbital Laboratory. Advances in Space Sciences and Technology (ed. F. I. Ordway III), Vol. 11, Academic Press, New York, NY, 1972, pp. 267-328.

Snyder, C. W. and Neugebauer, M.: The Relation of Mariner-2 Plasma Data to Solar Phenomena. The Solar Wind (eds., R. J. MacKin Jr. and M. Neugebauer), Pergamon Press, London, England, 1966, pp. 25-34.

Timothy, A. F., Gerassimenko, M., Golub, L., Krieger, A. S., Petrasso, R., and Vaiana, G. S.: The Long Term Development of the Large Scale Corona and the Evolution of Coronal Holes. Skylab Solar Workshop (ed. G. Righini), Osservazioni e Memorie, Arcetri Astrophysical Observatory, Fascicolo 104, Baccini and Chiappi, Florence, Italy, 1974, pp. 93-110.

Timothy, A. F., Krieger, A. S., and Vaiana, G. S.: The Structure and Evolution of Coronal Holes. Solar Phys. 42, 1975, pp. 135-156.

Tousey, R.: Some Results of Twenty Years of Extreme Ultraviolet Solar Research. Astrophys. J. 149, 1967, pp. 239-252.

Tousey, R., Austin, W. E., Purcell, J. D., and Widing, K. G.: The Extreme Ultraviolet Emission from the Sun Between the Lyman-Alpha Lines of H I and C VI. Ann. D' Astrophys. 28, 1965, pp. 755-773.

Tousey, R., Bartoe, J.-D. F., Bohlin, J. D., Brueckner, G. E., Purcell, J. D., Scherrer, V. E., Sheeley, N. R. Jr., Schumacher, R. J., and VanHoosier, M. E.: A Preliminary Study of the Extreme Ultraviolet Spectro-heliograms from Skylab. Solar Phys. 33, 1973, pp. 265-280.

Tousey, R., Sandlin, G. D., and Purcell, J. D.: On Some Aspects of XUV Spectroheliograms. Structure and Development of Solar Active Regions (ed. K. Kiepenheuer), IAU Symp. No. 35, D. Reidel Publ. Co., Dordrecht, Holland, 1968, pp. 411-419.

Underwood, J. H.: Glancing Incidence Optics in X-Ray Astronomy: A Short Review. Space Sci. Instr. 1, 1975, pp. 289-304.

Underwood, J. H. and Broussard, R. M.: Atlas of Coronal Hole Boundaries from Observations Made Prior to the Skylab Mission. Contribution to the Skylab Solar Workshop on Coronal Holes (February), 1976.

Underwood, J. H. and Muney, W. S.: A Glancing Incidence Solar Telescope for the Soft X-Ray Region. Solar Phys. 1, 1967, pp. 129-144.

Vaiana, G. S., Chase, R., Davis, J., Gerassimenko, M., Golub, L., Kahler, S., Krieger, A. S., Petrasso, R., Silk, J. K., Simon, R., Timothy, A. F., Zombeck, M., and Webb, D.: Skylab and the ASE X-Ray Telescope Experiment: A New View of the X-Ray Corona. Skylab Solar Workshop (ed. G. Righini), Osservazioni e Memorie, Arcetri Astrophysical Observatory, Fascicolo 104, Baccini and Chiappi, Florence, Italy, 1974, pp. 3-47.

Vaiana, G. S., Davis, J. M., Giacconi, R., Krieger, A. S., Silk, J. K., Timothy, A. F., and Zombeck, M.: X-Ray Observations of Characteristic Structures and Time Variations from the Solar Corona: Preliminary Results from Skylab. Astrophys. J. (Letters) 185, 1973, pp. L47-L51.

Vaiana, G. S., Krieger, A. S., and Timothy, A. F.: Identification and Analysis of Structures in the Corona from X-Ray Photography. Solar Phys. 32, 1973, pp. 81-116.

Vernazza, J. E. and Noyes, R. W.: Equator-Pole Differences in the Solar Chromosphere from Lyman-Continuum Data. Solar Phys. 26, 1972, pp. 335-342.

Wagner, W. J.: Solar Rotation as Marked by Extreme-Ultraviolet Coronal Holes. Astrophys. J. (Letters) 198, 1975, pp. L141-L144.

Wagner, W. J.: The Rigid Rotation of Coronal Holes. B.A.A.S. 7, 1975, p. 457.

Waldmeier, M.: The Coronal Hole at the 7 March 1970 Solar Eclipse. *Solar Phys.* 40, 1975, pp. 351-358.

Wetherbee, P. K. and Reeves, E. M.: Preliminary Atlas of Coronal Hole Observations with the HCO Spectrometer on Skylab. (Unpublished data).

Wilcox, J. M. and Howard, R.: Differential Rotation of the Photospheric Magnetic Field. *Solar Phys.* 13, 1970, pp. 251-260.

Wilson, R. M.: Atlas of Skylab ATM/S056 Coronal Hole Observations. NASA TM X-64994, Marshall Space Flight Center, AL, March 1976.

Withbroe, G. L., Dupree, A. K., Goldberg, L., Huber, M. C. E., Noyes, R. W., Parkinson, W. H., and Reeves, E. M.: Coronal Electron Density Maps for 7 March 1970, Derived from Mg X λ 625 Spectroheliograms. *Solar Phys.* 21, 1971, pp. 272-280.

Withbroe, G. L. and Gurman, J. B.: Model of the Chromospheric-Coronal Transition Layer and Lower Corona Derived from Extreme-Ultraviolet Observations. *Astrophys. J.* 183, 1973, pp. 279-289.

Withbroe, G. L. and Jaffe, D.: Polar Transients Observed in the EUV. *B.A.A.S.* 7, 1975, p. 354.

Withbroe, G. L., Jaffe, D. T., Foukal, P. V., Huber, M. C. E., Noyes, R. W., Reeves, E. M., Schmahl, E. J., Timothy, J. G., and Vernazza, J. E.: Extreme-Ultraviolet Transients Observed at the Solar Pole. *Astrophys. J.* 203, 1976, pp. 528-532.

Withbroe, G. L. and Wang, Y.-M.: A Model for the Polar Transition Layer and Corona for November 1967. *Solar Phys.* 27, 1972, pp. 394-401.

Zirin, H.: The D₃ Chromosphere, Coronal Holes, and Stellar X-Rays. *B.A.A.S.* 7, 1975, p. 359.

Zirin, H.: The Helium Chromosphere, Coronal Holes, and Stellar X-Rays. *Astrophys. J. (Letters)* 199, 1975, pp. L63-L66.

APPROVAL


RESULTS OF CORONAL HOLE RESEARCH: AN UPDATE

By Robert M. Wilson


The information in this report has been reviewed for technical content. Review of any information concerning Department of Defense or nuclear energy activities or programs has been made by the MSFC Security Classification Officer. This report, in its entirety, has been determined to be unclassified.



ANTHONY C. DeLOACH
Chief, Solar Sciences Branch



WILLIAM C. SNODDY
Chief, Solar-Terrestrial Physics Division



CHARLES A. LUNDQUIST
Director, Space Sciences Laboratory

END
DATE
FILMED
NOV. 14, 1979